

This PDF was created from the British Library's microfilm copy of the original thesis. As such the images are greyscale and no colour was captured.

Due to the scanning process, an area greater than the page area is recorded and extraneous details can be captured.

This is the best available copy

D57626'85

Attention is drawn to the fact that the copyright of this thesis rests with its author.

This copy of the thesis has been supplied on condition that anyone who consults it is understood to recognise that its copyright rests with its author and that no quotation from the thesis and no information derived from it may be published without the author's prior written consent.

168

D 5762618

HAQ, R.U.

C. of L. P.

THE HYDRODYNAMIC MODELLING OF AN EVOLVING SEA

by

RAFIQ UL HAQ, B.Sc., M.Sc.

A thesis submitted to the Council for National
Academic Awards for the Degree of Doctor of
Philosophy.

MATHEMATICS DEPARTMENT
CITY OF LONDON POLYTECHNIC

JUNE 1985

ABSTRACT.

A model of a changing tidal regime in an evolving shallow sea such as the ancient North Sea is developed and solved analytically as a generalization of Taylor's problem. Characteristic scales and coefficients are treated as functions of historical time. The z dependency, dissipative and non-linear terms are effectively separated from the governing equations by the use of a Latta expansion. A composite solution is found which takes account of each of these features. A Green's function technique is used to calculate the effects of friction. A sloping bed topography is simulated by a horizontally varying eddy viscosity.

ACKNOWLEDGEMENTS

I should like to thank the staff of the City of London Polytechnic for their support which has enabled me to complete this thesis.

I am greatly indebted to my supervisor Dr U.T. Ehrenmark for his involvement at every stage of my work. In addition, I am extremely grateful to Dr B. D'Olier for the geological information, R. McLachlan for programming advice, Dr M.G. Smith for his general encouragement, Dr B. Spain for the funding of expenses, J. Venn for numerous discussions and Dr P.S. Williams for his help with the numerical analysis.

Finally, I wish to thank my mother Mrs B. Haq who typed the script.

CONTENTS

	Page
CHAPTER 1	
Introduction	1
CHAPTER 2	
The governing equations	10
CHAPTER 3	
Existing hydrodynamic models	22
CHAPTER 4	
An analytic three dimensional model	58
CHAPTER 5	
Analysis of results	95
CHAPTER 6	
Concluding remarks	108
APPENDIX 1	
An infinite channel boundary layer model	114
APPENDIX 2	
An adaptation of the method of Green's functions	119
APPENDIX 3	
Programs	127
BIBLIOGRAPHY	159

CHAPTER 1

INTRODUCTION

A modelling of the flow regime that prevailed within the region of the southern North Sea during the Boreal and Atlantic periods is of interest to geologists. At that time marine transgressions, which followed the Last Cold Stage, caused extensive flooding of the basin and there was an active formation and upbuilding of mobile bed forms, (Nio, 1976).

11. Geological background

The ice sheet that covered Scandinavia and most of Britain during the Last Cold Stage had reached its maximum extent by about 18000 BP (before present). It had receded to the north of Iceland by time of the early Holocene, c. 9300 BP (see figure 1.1; Bowen, 1978).

The North Sea underwent several transgressive periods in the course of its Holocene evolution. Radiocarbon dating of different peat layers by Jelgersma (1961) and Hageman (1969) has established that major flooding of the basin started at c.9300 BP. The North Sea then was about 30m shallower than at present and the northern section was separated from the Southern Bight by a land bridge. By c. 8600 BP the two sections had become connected by a strait that was some 30 km wide. From c. 8300 BP to 7000 BP there was a strong sea level rise which was followed by a gradual levelling off (see figures 1.2 and 1.3; Nio, 1976).

Evans (1979) is of the opinion that the Holocene marine transgressions of the North Sea shoreline were due to the rise which resulted from the increase in the volume of the ocean as the glaciers receded. Other factors that contributed to the rise

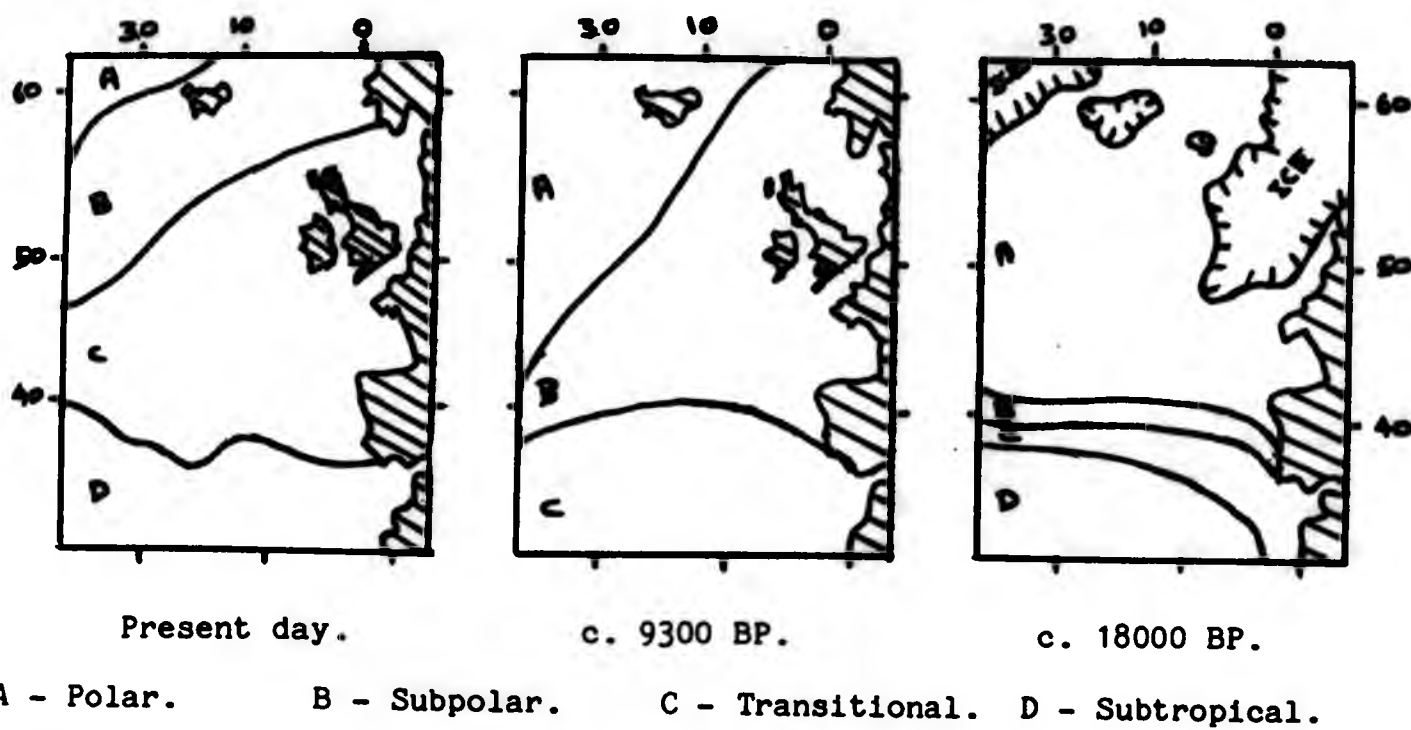


Figure 1.1

Maps of the North Atlantic Ocean showing ecologic water masses at three time levels during the Late Quaternary, (Bowen, 1978).

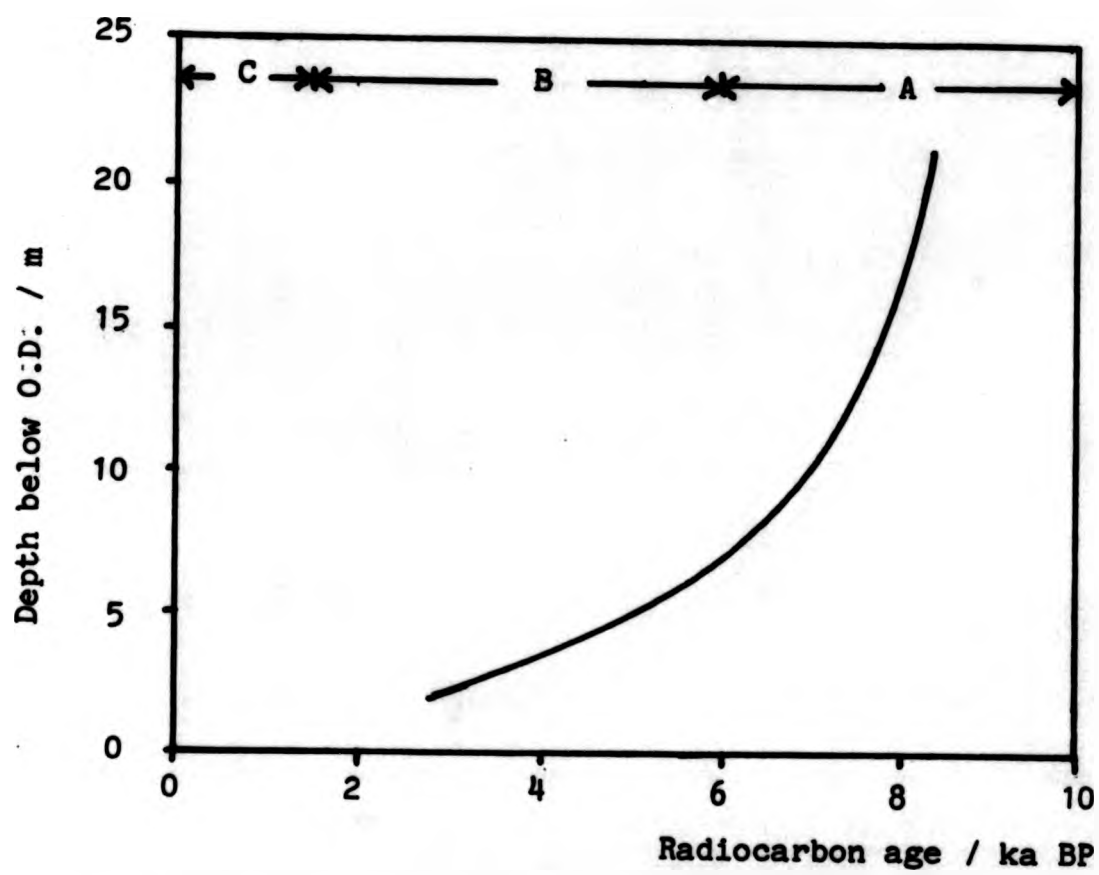


Figure 1.2

Time-depth graph showing the relative change in sea-level and the relation to different stages of sandwave formation during the Holocene of the North Sea basin, (Nio, 1976).

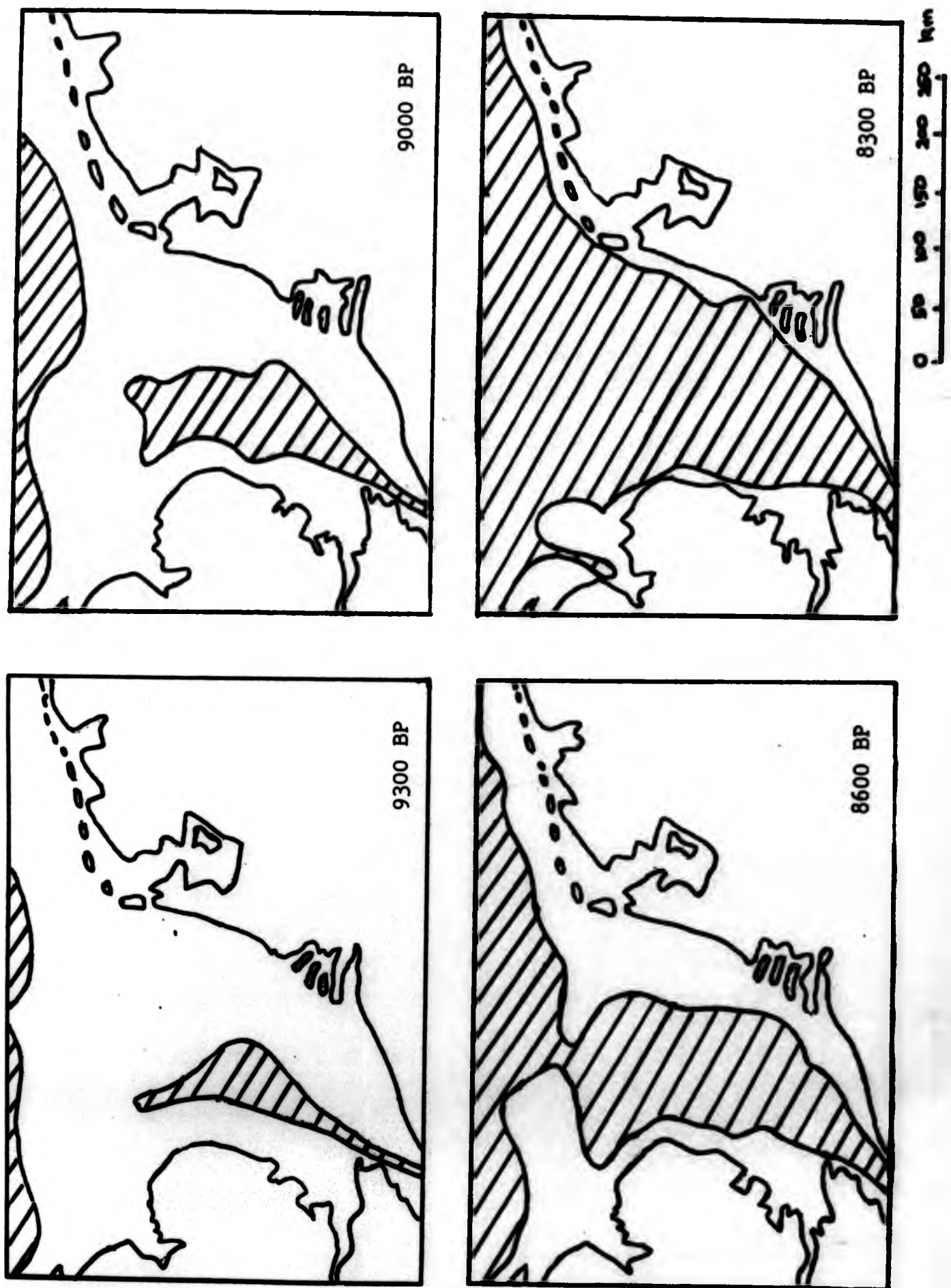


Figure 1.3

Hypothetical maps showing the extension of the southern North Sea during the different transgressive periods of the early Holocene, (Nio, 1976).

in sea level may have been the isostatic rebound of the earth which followed the lessening of the glacial load, the local compaction and deformation of the sea bed which was produced by the increased weight of water and the tectonic tilting and shifting of land masses. This latter effect is thought to cause the east coast of England to rise by an estimated 1 mm per year. The rate of migration of the shoreline depends upon the rate of change of the land-sea levels, the slope of the surface and the rate of introduction and redistribution of sediments. It is of interest to note that whilst the rate of coastal retreat for the North Sea was as much as 60 km in the period 9300 BP to 8300 BP, the coast of Texas remained virtually static owing to the supply of sediment.

The Southern Bight of the contemporary North Sea is characterised by the presence of tidal current ridges and sandwaves, which are oriented parallel and perpendicular to the tidal current, respectively. The crest heights of sandwaves are commonly in the 10-20 foot range. Sandwaves are present on the tops of many of the ridges, (Off, 1963).

Yalin (1977) defines sandwaves as statistically periodic irregularities in the surface of a mobile bed. He classifies them in accordance with their physical origin, as opposed to their geometrical appearance (c.f. Allen, 1968).

In the case of tranquil flow, for which the Froude number is less than one, two kinds of sandwaves, namely, ripples and dunes, are possible. Both are asymmetrical with gently sloping upstream surfaces and abrupt downstream surfaces. They migrate in the direction of the flow at a rate that is small compared to the mainstream velocity.

The size of dunes is strongly dependent upon the size of the flow and hence the depth. The size of ripples is very much smaller than that of dunes and is independent of the flow size.

The sandwaves that exist in a shooting flow regime, for which the Froude number is greater than one, are referred to as antidunes. Their shape is more symmetrical. They may migrate in the direction of the flow, in the opposite direction or remain stationary. Antidunes form a wavelike bed surface which is in phase with the wavy free surface.

The origins of these bed features are thought by Yalin to be caused by different effects which arise from the flow over a discontinuity plane. Antidunes originate from a discontinuity in the mobile bed, e.g. a change in bed roughness, in conjunction with waves on a free surface. Dunes are formed when a discontinuity produces a disturbance in the structure of the flow turbulence. Ripples form when a discontinuity, e.g. any slight incidental ridge of a height of more than a few grain diameters, causes a deformation of an unstable bed surface to occur.

Nio (1976) concludes that marine transgressions in association with strong tidal currents are the genetic factor for ancient sandwave complexes. The deposition of the sandwave sequence occurs during a slow uniform rise in sea-level and the gradual decrease in current velocities as the basin deepens. He postulates that:

- 1) At the beginning of the marine transgression depressions of the existing topography (e.g. river valleys and gullies) are drowned. Estuarine and tidal-flat sedimentation is prevalent.

- 2) Smaller sandwaves may be formed within these existing depressions as the sea level rises.
- 3) Larger sandwaves may be formed during a protracted transgression. Bedload transport on the stoss-side of earlier formed sandwaves causes a lateral migration and vertical accretion of the sandwaves. Fluctuations and changes of current directions produce several forms of discontinuity plane. The current directions are restricted to a narrow spread within the sandwave facies (i.e. the general appearance, composition and environment).
- 4) The confined flow conditions diminish during an advanced stage of the transgression. Lateral migration of sandwaves occurs only during periods of high energy such as arise from storm induced currents. Sedimentation on the flanks and in the troughs of sandwaves is of increased importance.
- 5) Following a further deepening of the basin, the lower energy conditions cause sedimentation on the slope and troughs to become dominant. Very slight lateral migration of the sandwaves is caused by migration of megaripples, the heights of which are less than 2 m on the slopes. Vertical accretion may be considerable. Multi-directional currents now prevail.
- 6) Once the maximum transgressive stage is reached there is a flattening of the topography. No further upbuilding of the sandwave occurs except during high energy conditions.

Evidence in support of the view that the sandwave field is localised by the basin topography is provided by Caston and Stride (1973). They find that sandwaves off the west coast of Holland, the steep slopes of which are north facing, are

confined to areas of more ancient relief, namely, Pleistocene ridges and troughs which have a northerly trend.

12. Mathematical Modelling

The scope of the present work is confined to an analytic modelling of the flow field in the Southern Bight of the North Sea for the period 8300 BP onwards. A boundary value problem approach is adopted in which the flow within the basin is determined from equations of conservation of mass, momentum and energy subject to the specification of the basin topography and the driving forces at the open sea boundaries (Shih-Zao, 1977).

The problem is considerably simplified by idealising the sea of interest as a well mixed sea, for which the effects of temperature, salinity and density stratifications may be neglected, in a basin of simple geometry such as a rectangular channel of constant depth (e.g. see Taylor, 1921; Godin, 1965(a) and 1965(b); Hendershott and Speranza, 1971; Brown, 1978; Reinecker and Teubner, 1980). Such a modelling provides useful qualitative information about the actual flow field, gives an insight into the physical mechanisms that are involved and may form the basis of a more precise numerical model (Kriess, 1957; Krauss, 1973; Nihoul and Roday, 1976).

Brown (1978), for example, obtained a good agreement with the positions of the amphidromes of the contemporary North Sea from a first order, two dimensional, linearised and frictionless model in which the flow was modified by an oscillating boundary

at the Straits of Dover and co-oscillated with the dominant lunar semi-diurnal (M_2) tidal component of the North Atlantic Ocean.

The high energy regime of the very shallow water of the ancient southern North Sea requires that the effects of non-linear wave interactions and frictional dissipation of energy at the boundaries are taken into account. The obtaining of information about the vertical current structure necessitates that a three dimensional model be utilised. Analytic models that incorporate these features appear to be rare (Nihoul and Runday, 1976; Shih-Zao, 1977).

The equations that govern the flow in such an idealised sea are justified in chapter 2. Established hydrodynamic models are reviewed in chapter 3. In chapter 4 an analytic, three dimensional model of an evolving sea is developed. The results are analysed and conclusions drawn in chapters 5 and 6.

CHAPTER 2.

EQUATIONS OF MOTION AND BOUNDARY CONDITIONS

The evolving North Sea is idealised as a rotating homogeneous sea of slowly increasing depth, in a basin of simple geometry, which co-oscillates with the tidal motion of the North Atlantic Ocean. A general analysis of the appropriate governing equations and the terms therein follows.

21. The momentum equations

The Navier-Stokes equation governs the flow in an isotropic Newtonian viscous fluid. It expresses the condition that for each fluid particle there is an equilibrium between the body forces, surface forces and inertia forces. The equation of motion is derived from Newton's second law, in accordance with which the rate of change of momentum is equated to the sum of the external forces per unit mass acting on each portion of the fluid.

Thus we may express the momentum balance in cartesian tensor notation (i.e. a repeated subscript i, j or k indicates summation over three terms) as

$$\int_V \frac{Du_i}{Dt} \rho \Delta V = \int_V F_i \Delta V + \int_V \frac{\partial \sigma_{ij}}{\partial x_j} \Delta V, \quad (1)$$

where we denote by $\frac{D}{Dt}$ the total differential operator $\frac{\partial}{\partial t} + u_i \frac{\partial}{\partial x_i}$, u_i , $i = 1, 2, 3$, the velocity components, t the time, V the volume, ρ the density, F_i the body forces per unit volume and σ_{ij} the stress tensor.

Equation (1) holds for all choices of material volume V . This is possible only if

$$\frac{Du_i}{Dt} = \frac{1}{\rho} F_i + \frac{1}{\rho} \frac{\partial \sigma_{ij}}{\partial x_j}. \quad (2)$$

The stress tensor, σ_{ij} , is conveniently regarded as the sum of an isotropic part, $-p\delta_{ij}$, and a non-isotropic part, d_{ij} , termed the deviatoric stress tensor, which contributes the tangential stresses and diagonal elements whose sum is zero. Thus we may write

$$\sigma_{ij} = -p\delta_{ij} + d_{ij} \quad (3)$$

where p is the pressure at a point in a moving liquid (it is not necessarily equal to the thermodynamic pressure $p(\rho)$) and δ_{ij} is the Kronecker delta tensor.

For a Newtonian fluid, it is assumed that there is a linear relation between the non-isotropic parts of the stress and rate of strain tensor e_{ij} . The most general relationship is of the form

$$d_{ij} = 2\mu e_{ij} + \mu' \delta_{ij} e_{kk} \quad (4)$$

where $e_{ij} = \frac{1}{2}(\frac{\partial u_i}{\partial x_j} + \frac{\partial u_j}{\partial x_i})$, μ and μ' are the temperature dependent first and second coefficients of viscosity respectively and $e_{kk} = \frac{\partial u_k}{\partial x_k}$ is the fluid dilatation.

The Navier-Stokes equation for a homogeneous viscous Newtonian fluid may be written as

$$\rho \frac{Du_i}{Dt} = F_i - \frac{\partial p}{\partial x_i} + \frac{\partial}{\partial x_j} \left[\mu \left(\frac{\partial u_i}{\partial x_j} + \frac{\partial u_j}{\partial x_i} \right) \right], \quad (5)$$

(Batchelor, 1967). The components of equation (5) are given by $i = 1, 2, 3$ and may be referred to as the momentum equations.

22. The continuity equation

In the case of an incompressible fluid, it follows from the principle of conservation of mass that the net outflow of material from any control volume is zero. Analytically this may be expressed as the equation of continuity

$$\frac{\partial u_k}{\partial x_k} = 0 \quad (1a)$$

or, in vector notation,

$$\nabla \cdot \underline{u} = 0 \quad (1b)$$

where $\underline{u} = (u, v, w) = (u_1, u_2, u_3)$.

23. The Coriolis force and body forces

It is convenient to choose a frame of reference relative to which the boundary is at rest. We transform from an absolute frame x_a, y_a, z_a , the origin O_a of which is at the centre of the earth, to an accelerating frame x, y, z , the origin O of which is situated on the earth's surface at distance R from O_a . The radius vector \underline{R} rotates about O_a with an angular velocity $\underline{\Omega}$.

The expression for the inertial force in the absolute frame, $\rho \frac{D\underline{u}_a}{Dt}$, becomes $\rho [D\underline{u}/Dt + 2\underline{\Omega} \wedge \underline{u} + \underline{\Omega} \wedge (\underline{\Omega} \wedge \underline{R})]$ in the relative frame, (Krauss, 1973). The terms $2\rho \underline{\Omega} \wedge \underline{u}$ and $\rho \underline{\Omega} \wedge (\underline{\Omega} \wedge \underline{R})$ may be regarded as apparent body forces, namely, the Coriolis force and centripetal forces respectively. They may be incorporated into the Navier-Stokes equation (21.5) by replacing the term for the body forces \underline{F} with \underline{X} where

$$\underline{X} = \underline{F} - 2\rho \underline{\Omega} \wedge \underline{u} - \rho \underline{\Omega} \wedge (\underline{\Omega} \wedge \underline{R}). \quad (1)$$

When the relative frame is such that the x-axis is at an inclination γ to the west of north, the y-axis is directed at an angle γ to the south of west and the z-axis is directed vertically upwards, the Coriolis force may be represented by

$$2\rho \underline{\Omega} \wedge \underline{u} = \rho \underline{f} \wedge \underline{u}$$

where

$$\underline{f} = (f' \cos \theta, -f' \sin \theta, f),$$

$$f = 2\Omega \sin \theta,$$

$$f' = 2\Omega \cos \theta$$

and θ is the latitude, (Johns, 1965).

For small scale motions the curvature of the earth and the latitudinal dependence of the Coriolis parameters f and f' may be ignored. Such a flat-earth approximation allows us to specify an xy -plane which is tangential to an equipotential sea surface (i.e. $z = 0$ denotes a sea at rest) and Coriolis parameters which are constant.

The expression $\underline{F} = \rho \underline{\omega} \wedge (\underline{\omega} \wedge \underline{R})$ may be reduced to $\rho \underline{g}$, where \underline{g} is the acceleration due to gravity, if the gravitational force of the earth \underline{g}_e is the only actual body force that is taken into account. The astronomical tide producing forces are usually neglected in marginal seas such as the North Sea since the internal tides are small in comparison to the incoming waves, (Nihoul and Runday, 1976).

The variation of \underline{g} with geographical position is such that it is a maximum at the poles (where the centripetal force vanishes and the polar radius being less than the equatorial radius \underline{g}_e is a maximum) and a minimum at the equator (where the centripetal force is a maximum and \underline{g}_e is a minimum). This variation may be neglected, (Pond and Pickard, 1978).

Thus for a rotating sea we may replace the term for the body forces in the Navier-Stokes equation (21.5) by

$$\underline{X} = \rho (\underline{g} - \underline{f} \wedge \underline{u}) \quad (2a)$$

where the components are

$$X_1 = \rho f v - \rho f' w \cos \theta \quad (2b)$$

$$X_2 = -\rho f u - \rho f' w \sin \theta \quad (2c)$$

and

$$X_3 = -\rho g + \rho f' v \sin \theta + \rho f' u \cos \theta. \quad (2d)$$

The Navier-Stokes equation may now be written as

$$\rho \frac{Du_i}{Dt} = X_i - \frac{\partial p}{\partial x_i} + \mu \frac{\partial^2 u_i}{\partial x_j \partial x_j} \quad (3)$$

A further simplification occurs when terms in f' are neglected. This would correspond to the f -plane approximation in which the horizontal xy -plane rotates with angular velocity $\frac{1}{2}f$ about the z -axis, (Hendershott and Munk, 1970).

When the time scale of the fluid motion is much less than half a pendulum day $\frac{1}{2}T_f$, where $T_f = 1 \text{ sidereal day}/\sin \Theta$, the effects of the Coriolis terms become negligible, (Pond and Pickard, 1978). However, this is not the situation for mid-latitudinal tidal motions in which the principal lunar semi-diurnal period is dominant since the M_2 period is of the same order of magnitude as $\frac{1}{2}T_f$.

24. Boundary conditions

The equations of motion and continuity are solved subject to the following boundary conditions:

- 1) The surface elevation $\eta(x,y,t)$ and current velocity $\underline{u}(x,y,z,t)$ are specified at open sea boundaries.
- 2) There is continuity of velocity at rigid boundaries. This condition, referred to as the no-slip condition, is based on the observed behaviour of real fluids. It may be explained in terms of the interactions between the surface molecules at the interface of the fluid and the solid.

The no-slip condition may be relaxed and replaced by a less stringent kinematic boundary condition of zero flow through the solid boundary in cases when the relative velocity decreases to zero within a relatively thin boundary layer (i.e. a region adjacent to the

boundary which is characterised by large velocity gradients and higher order derivatives). This may be permissible at the shoreline if the effects of the boundary do not penetrate far into the interior, but is less appropriate at the sea bed where the frictional influence may well extend to the surface of a very shallow sea, (Kraav, 1969).

3) The applied stress is specified at the free surface $z = \eta(x, y, t)$. A simplified momentum transfer process will be supposed to apply at the air-sea interface and wind stresses, pressure fluctuations and surface tension effects will be neglected. The dynamic surface condition that the normal stress equals the atmospheric pressure and the condition that the surface shear stresses are negligible will be assumed.

4) Water does not pass through the free surface, i.e. there is a kinematic surface condition $w = \frac{D\eta}{Dt}$ at $z = \eta$.

25. Averaged equations of motion.

The fluid motions in real seas are generally turbulent, i.e. highly irregular in space and time. It is impractical to specify the precise boundary conditions and solve the field equations for the detailed velocity and pressure distributions. However, the equations for the mean motion, in which turbulent fluctuations have been averaged out in some sense, are more tractable.

It is assumed that the dependent variables may be represented by the Reynolds decompositions

$$\begin{aligned} u &= \bar{u} + u', & v &= \bar{v} + v', & w &= \bar{w} + w', \\ p &= \bar{p} + p', & \eta &= \bar{\eta} + \eta' & \text{and } X_i &= \bar{X}_i + X_i', \end{aligned} \quad (1)$$

where dashed quantities denote turbulent fluctuations and over-bars denote mean quantities.

For a flow which is statistically stationary the mean quantity is averaged over a time scale T which is sufficiently large to smooth

out turbulent fluctuations, e.g. the time averaged velocity component u may be expressed as $\bar{u} = \frac{1}{T} \int_{t_0}^{t_0+T} u \, dt$. In the case of a time-dependent turbulent flow field an ensemble average (i.e. the mean value from a large number of conceptual experiments) of fluctuating quantities is more appropriate since this type of averaging process will smooth out turbulent fluctuations but will not affect the long term trends of the flow within, for instance, the tidal time scale, (Bradshaw, 1975). The time-averaging of such a non-stationary field, however, produces a succession of discontinuous steady states, the limiting form of which approaches the ensemble average.

The conditions $\bar{\bar{u}} = \bar{u}$ and $\overline{u'} = 0$ apply to both the time-averaging and ensemble averaging procedures. It follows that the mean of a product such as uu_x , where u_x denotes the partial derivative with respect to x , may be written as $\overline{uu_x} = \bar{u} \bar{u_x} + \overline{u'u'_x}$ and by taking the continuity equation (22.1) into account we may write

$$\overline{u'u'_x} + \overline{v'u'_y} + \overline{w'u'_z} = \frac{\partial}{\partial x} (\overline{u'u'}) + \frac{\partial}{\partial y} (\overline{u'v'}) + \frac{\partial}{\partial z} (\overline{u'w'}).$$

Upon substituting the Reynolds decompositions (1) into the Navier-Stokes equation (23.3) and taking the ensemble average, we obtain the Reynolds equation of mean-mean motion which we may express as

$$\rho \frac{D\bar{u}_i}{Dt} = \bar{X}_i + \frac{\partial}{\partial x_j} \bar{\sigma}_{ij} + \frac{\partial}{\partial x_j} \bar{\Delta}_{ij}, \quad (2)$$

where

$$\bar{\sigma}_{ij} = -\bar{p} \delta_{ij} + \bar{\Delta}_{ij}, \quad (3)$$

$$\bar{\Delta}_{ij} = \mu \left(\frac{\partial \bar{u}_i}{\partial x_j} + \frac{\partial \bar{u}_j}{\partial x_i} \right) \quad (4)$$

and

$$\bar{\Delta}_{ij} = -\rho \overline{u'_i u'_j} \quad (5)$$

Terms of the form $\overline{u_i' u_j'}$ are referred to as one point velocity correlations or as Reynolds stresses.

In analogy to the way in which the shearing terms of the rate of strain tensor describe the tangential shear stresses in the Stokes hypothesis, equation (21.4), it is permissible to represent the Reynolds stresses by

$$\overline{u_i' u_j'} = \rho N_{ij} \left(\frac{\partial \bar{u}_i}{\partial x_j} + \frac{\partial \bar{u}_j}{\partial x_i} \right) \quad (6)$$

where the kinematic eddy viscosity coefficient N_{ij} is related to the Reynolds stresses and mean velocity gradients by

$$N_{ij} = -\overline{u_i' u_j'} / \left(\frac{\partial \bar{u}_i}{\partial x_j} + \frac{\partial \bar{u}_j}{\partial x_i} \right) \quad (7)$$

Thus we may write the Reynolds equation as

$$\frac{D\bar{u}_i}{Dt} = \frac{1}{\rho} \bar{X}_i - \frac{1}{\rho} \frac{\partial \bar{p}}{\partial x_i} + \nu \nabla^2 \bar{u}_i + \frac{\partial}{\partial x_j} \left[N_{ij} \left(\frac{\partial \bar{u}_i}{\partial x_j} + \frac{\partial \bar{u}_j}{\partial x_i} \right) \right] \quad (8)$$

where $\nu = \mu/\rho$ denotes the kinematic coefficient of viscosity, (c.f. Schlichting, 1968).

The formal averaging of the equation of continuity (22.1) yields

$$\overline{u_x} + \overline{v_y} + \overline{w_z} = 0 \quad (9)$$

26. The parameterization of turbulence

For simplicity we consider a two dimensional, steady, mean flow in the x-direction such that $\bar{u} = \bar{u}(y)$ and $\bar{v} = 0$, where the turbulent shear stress $\tau_t = -\rho \overline{u'v'}$. J. Boussinesq in 1877 introduced a constant mixing coefficient A_τ to model the Reynolds stress by putting $\tau_t = A_\tau \rho \overline{du/dy}$, (see Schlichting, 1968). This hypothesis assumes that the dynamic eddy viscosity coefficient is a property of

the fluid comparable to the dynamic molecular viscosity coefficient μ of Stokes's hypothesis for laminar flow, $\tau_L = \mu \Delta u / \Delta y$. The eddy kinematic viscosity coefficient $k = \tau_L / \rho$ is analogous to the kinematic viscosity coefficient.

More generally, k is assumed to be a property of the flow and a function of position. Von Karman's similarity hypothesis assumes that turbulent fluctuations are similar at all points in the field of flow, i.e. they differ from point to point only by time and length scale factors. The scales of length l , velocity B and energy per unit mass b are given by

$$l = c_0 \left| \Delta \bar{u} / \Delta y / \Delta^2 \bar{u} / \Delta y^2 \right|, \quad (1)$$

$$B = c_1 l \left| \Delta \bar{u} / \Delta y \right| \quad (2)$$

and

$$b = c_2 l^2 \left| \Delta \bar{u} / \Delta y \right|^2 \quad (3)$$

where c_0, c_1, c_2 are constants. According to the hypothesis, the turbulent shear stress is determined by the temporal average $-\rho \overline{u'v'}$ and is proportional to the energy scale. This may be expressed as $\tau_t = \rho k \Delta \bar{u} / \Delta y$, where $k = l^2 \left| \Delta \bar{u} / \Delta y \right|$ and is of the same form as that given by Prandtl's mixing length theory,

(Schlichting, 1968).

By introducing the parameter $\phi' = \left| \Delta \bar{u} / \Delta y \right|^2$, the constants c and χ and rescaling the mixing length in equations (1-3), we may obtain the relations

$$k = l b^{\frac{1}{2}}, \quad (4)$$

$$l = -\chi (\phi' / \phi'') \quad (5)$$

and

$$k^2 \phi' = c b^2, \quad (6)$$

which are used by Kraav (1969) in his computation of North Sea semi-diurnal tidal and turbulence parameters.

Other modellings include a linear friction law of the type $\Delta \tau_x / \Delta y = K\bar{u}$, where K is a constant, (e.g. Heaps, 1973). A quadratic friction law in which the derivative of the Reynolds stress is proportional to the square of the current speed is used by Proudman and Doodson (1924). Davies and Furnes (1980) use an eddy viscosity of the form $k = K\bar{u}^2 / \sigma$ where K is an empirically determined constant and σ is a typical frequency.

However, all such parameterizations of the Reynolds stress are controversial. They are semi-empirical and are not found to satisfactorily transfer from one flow regime to another, (Leslie, 1973).

27. Averaged boundary conditions

The boundary conditions of § 24 produce the following conditions.

1) The formal averaging of the kinematic surface condition yields

$\bar{w} - \bar{u}\bar{\eta}_x - \bar{v}\bar{\eta}_y - \bar{\eta}_t = \overline{u'\eta'_x} + \overline{v'\eta'_y}$ at $z = \bar{\eta}$. If we postulate a laminar boundary layer of a few millimetres thickness on either side of the air-sea interface then all terms containing turbulent fluctuations may be dropped. For low wind speeds ($< 5 \text{ m s}^{-1}$) such a hypothesis appears reasonable, (Krauss, 1973). Thus we obtain

$$\bar{w} - \bar{u}\bar{\eta}_x - \bar{v}\bar{\eta}_y - \bar{\eta}_t = 0 \text{ at } z = \bar{\eta}. \quad (1)$$

2) The averaged shear stresses at the surface are taken to be zero.

This condition will be referred to as the no wind condition. This may be written as

$$\bar{\sigma}_{xz} + \bar{\Delta'_{xz}} = \bar{\sigma}_{yz} + \bar{\Delta'_{yz}} = 0 \text{ at } z = \bar{\eta}$$

where the first subscript indicates the normal plane and the second the direction. Alternatively, we may write

$$(\nu + N_{xz})(\bar{u}_z + \bar{w}_x) = 0 \text{ at } z = \bar{\eta}$$

and

$$(\nu + N_{yz})(\bar{v}_z + \bar{w}_y) = 0 \text{ at } z = \bar{\eta}.$$

However, the Reynolds stresses $N_{xz}(\bar{u}_z + \bar{w}_x)$ etc. are zero under the assumption of a surface laminar boundary layer. The averaged no wind condition may be expressed as

$$\bar{u}_z + \bar{w}_x = \bar{v}_z + \bar{w}_y = 0 \text{ at } z = \bar{\eta}. \quad (2)$$

We note that Davies and Furnes (1980) consider that the condition of zero stress is an appropriate surface boundary condition for tides.

3) The averaged normal stress at the surface is equated to the atmospheric pressure which may be chosen as zero for convenience. Thus the dynamic surface condition is $\overline{\sigma_{zz}} + \overline{d'_{zz}} = 0$ at $z = \bar{\eta}$ or, equivalently, $\bar{p} = 2\rho(\nu + N_{zz})\bar{w}_z$ at $z = \bar{\eta}$.

4) The averaged no-slip condition is given by $\bar{u} = \bar{v} = \bar{w} = 0$ at rigid immobile boundaries.

The averaged kinematic boundary conditions are that the normal component of the flow velocity is zero, i.e. $\overline{\underline{u} \cdot \underline{n}} = 0$, at solid stationary boundaries.

5) The smoothed sea surface elevation $\bar{\eta}$ and averaged current components \bar{u} , \bar{v} , \bar{w} are specified at open sea boundaries.

CHAPTER 3.

EXISTING HYDRODYNAMIC MODELS

We review various hydrodynamic models of increasing complexity which have been successfully applied to the North Sea or similar marginal seas.

31. Two dimensional, linearised, frictionless systems

The classical modelling of the contemporary North Sea typically adopts linearised and frictionless versions of the Reynolds equation (25.8) or the Navier-Stokes equation (21.5), the equation of continuity (25.9) or (22.1) and the boundary conditions of § 27 or § 24 in which the z-dependence of the velocity components u and v is neglected. The sea is taken to be homogeneous, of constant depth and contained in a rotating, semi-infinite channel of rectangular section. The channel is closed by a transverse barrier at the southern end and open to the North Atlantic at its northern extremity.

Crease (1958) explains the mechanism by which a normally incident harmonic plane wave that corresponds to an eastward travelling M_2 tidal wave in the North Atlantic Ocean is diffracted by a semi-infinite barrier that represents the western coastline of the North Sea. The resulting secondary wave is a travelling edge wave of the Kelvin type (i.e. the amplitude decays exponentially with distance away from the barrier and the associated transverse velocity component is zero) which propagates southwards without attenuation.

Buchwald (1968) shows how the incident Kelvin wave is diffracted at the corner of the transverse barrier. A Kelvin wave, with angular frequency σ greater than the Coriolis parameter f , gives rise to cylindrical Poincaré type waves. These are waves of the form

$$\xi = \text{Re} \left[A f(\phi) \exp (i(kr + \sigma t)) / r^{\frac{1}{2}} \right]$$

where the constants A and k and the function $f(\phi)$ are such that the elevation ξ satisfies the Helmholtz equation $(\nabla^2 + k^2)\xi = 0$, and

r and ϕ are polar coordinates with the origin at the corner.

The cylindrical Poincaré waves radiate from the corner. A reflected Kelvin wave of reduced amplitude, which travels parallel to the closed end, is also generated by the incident Kelvin wave.

The process of diffraction is repeated at the eastern corner of the channel. The interference pattern of the cylindrical Poincaré waves which radiate from the corners of the transverse barrier produces a non-propagating standing edge wave system of the Poincaré type near the barrier. The amplitude of the north travelling outgoing Kelvin wave is restored to that of the incoming wave within a short distance of the closed end, in the case of a sufficiently deep and narrow channel such as the North Sea and for waves of sufficiently long period such as the M_2 period, (Brown, 1973).

311. The flow field for a rotating semi-infinite channel was analysed by Taylor (1921) before the mechanism by which Kelvin wave reflection took place was well understood. A right-handed cartesian coordinate system, in which the x-axis is directed towards the north, is used. It is assumed that the pressure p obeys a hydrostatic pressure law of the form $p = \rho g(z + \zeta)$ and that the elevation ζ and velocity components u , v and w are proportional to a simple harmonic time factor $e^{i\sigma t}$. The linearised and frictionless equations of momentum and depth integrated continuity for tides in a rotating sea of uniform depth h may then be written as

$$i\sigma u - fv = -g\zeta_x, \quad (1)$$

$$i\sigma v + fu = -g\zeta_y \quad (2)$$

and

$$u_x + v_y + \frac{i\sigma}{h}\zeta = 0 \quad (3)$$

where only the real parts have significance and all dependent

variables are functions of x , y and t only.

The reduction of x , y and ζ by a factor $L = B/\pi$, where B is the channel width, and the depth h by a factor L^2 does not alter the form of equations (1-3). However, the variables x, y and ζ become dimensionless and the depth parameter h now has the dimension of inverse length.

It follows from equations (1-3) that the field equations for u , v and ζ may be represented by the Helmholtz equations

$$(\nabla^2 + K^2) u, v, \zeta = 0 \quad (4)$$

where the Helmholtz constant $K^2 = (\sigma^2 - f^2)/c^2$ is dimensionless and the reduced phase velocity $c = (gh)^{1/2}$ has the dimension of inverse time.

The velocity components may be shown to be related to the elevation gradients by

$$u = \frac{1}{hK^2} (i\sigma\zeta_x + f\zeta_y) \quad (5)$$

and

$$v = \frac{1}{hK^2} (-f\zeta_x + i\sigma\zeta_y). \quad (6)$$

The interrelationship between the velocity gradients is given by

$$i\sigma u_y - f u_x = i\sigma v_x + f v_y. \quad (7)$$

The kinematic boundary conditions for a channel of reduced width π which has rigid vertical walls along the sides $y = \pm \frac{1}{2}\pi$ and a closed end at $x = x_1$ are that

$$v = 0 \text{ at } y = \pm \frac{1}{2}\pi \quad (8)$$

and

$$u = 0 \text{ at } x = x_1. \quad (9)$$

Taylor's method of solution is to find two separate solutions to the field equations which satisfy the longitudinal boundary conditions (8) and give the same value of u at $x = x_1$. The difference between the two solutions will satisfy the field equations and the full boundary conditions that the transverse velocity vanishes at the longitudinal walls and the longitudinal current vanishes at the section $x = x_1$. Thus a barrier could be erected at $x = x_1$ without disturbing the wave motion. We look at Taylor's analysis in some detail since use is made of it in chapter 4.

One partial solution to the problem is given by a superposed incident and reflected Kelvin wave train. An incident Kelvin wave that travels in the negative x -direction has an elevation ζ_I and associated velocity components u_I and v_I which may be expressed as

$$\zeta_I = a_0 \exp(\alpha y + ikx + i\sigma t), \quad u_I = -\frac{c}{h} \zeta_I \text{ and } v_I = 0.$$

Here the amplitude factor, a_0 , the parameter $\alpha = f/c$ and the reduced wave number $k = \sigma/c$ are dimensionless constants.

An 'equal and opposite' reflected Kelvin wave has an elevation and velocity given by

$$\zeta_R = a_0 \exp(-\alpha y - ikx + i\sigma t), \quad u_R = \frac{c}{h} \zeta_R \text{ and } v_R = 0.$$

The superposed Kelvin wave solution, denoted by subscript K , is

$$\begin{aligned} \zeta_K &= \zeta_I + \zeta_R \\ &= 2a_0 [\text{ch}(\alpha y) \cos(kx) + i \text{sh}(\alpha y) \sin(kx)] e^{i\sigma t}, \end{aligned} \quad (10)$$

$$\begin{aligned} u_K &= u_I + u_R \\ &= S [\text{ch}(\alpha y) \sin(kx) - i \text{sh}(\alpha y) \cos(kx)] e^{i\sigma t} \end{aligned} \quad (11)$$

and

$$v_K = v_I + v_R = 0 \quad (12)$$

where the factor S has the dimensions of velocity and is related to the amplitude factor a_0 by $S = -2ica_0 / h$.

We note that although there are an infinite number of points in the xy -plane where u vanishes there is no section $x = x_1$ where the longitudinal current is everywhere zero.

The superposition of an infinite number of Poincaré wave modes provides another partial solution to the problem. The Poincaré wave elevation ζ_p and the velocity components u_p and v_p are given by

$$\zeta_p = \sum_{m=1}^{\infty} [P_m \sin(my) + iQ_m \cos(my)] \exp(-s_m x + i\sigma t), \quad (13)$$

$$u_p = \sum_{m=1}^{\infty} [A_m \cos(my) + iB_m \sin(my)] \exp(-s_m x + i\sigma t), \quad (14)$$

and

$$v_p = \sum_{m=1}^{\infty} [D_m \sin(my) + iC_m \cos(my)] \exp(-s_m x + i\sigma t), \quad (15)$$

where the Poincaré wave coefficients A_m , B_m , C_m , and D_m have the dimensions of velocity, P_m and Q_m are dimensionless and the dimensionless parameter $s_m = (m^2 - K^2)^{1/2}$, $m = 1, 2, \dots$.

Negative values of s_m would imply a wave of exponentially increasing amplitude with increasing x . These may be precluded on the grounds of energy conservation. Imaginary values of s_m occur if $m^2 < \frac{(\sigma^2 - \sigma_0^2)}{gD} \cdot \frac{B^2}{\pi^2}$ where the unscaled channel depth $D = hB^2/\pi^2$. However, if the channel is sufficiently deep, i.e. $D > D_{crit}$, where the subscript 'crit' denotes some critical value, sufficiently narrow, $B < B_{crit}$, and the tidal motion has a sufficiently long period, $\tau > \tau_{crit}$, then only real values of s_m occur, (Hendershott and Speranza, 1971).

Taylor (1921) considers the tidal regime in the North Sea to be approximated by "the tidal motion in a channel 250 miles wide and 40 fathoms deep situated in latitude 53° N when a tidal wave of period 12 hr. is reflected at the closed end". These parameter values allow us to establish the estimates $D_{crit} = 9_m$, $B_{crit} = 1100$ km and $\tau_{crit} = 7.2$ h.

Thus the North Sea may be considered sufficiently narrow and deep that we may exclude the existence of propagating Poincaré waves of M_2 period (12.42h) and only consider positive values of s_m for which $m^2 > k^2$. The reader is referred to Brown (1973) for an analysis of the imperfect Kelvin wave reflection which occurs for shorter tidal periods.

A relationship between the coefficients for the longitudinal current, A_m and B_m , and the transverse current C_m and D_m , may be obtained by substituting equations (14) and (15) into equation (7) and comparing the coefficients of terms in $\sin(my)$ and $\cos(my)$ separately.

Introducing $r_m = \omega k / ms_m$, Taylor obtains

$$C_m = \frac{-ms_m}{s_m^2 - \omega^2} (r_m A_m + B_m) \quad (16)$$

and

$$D_m = \frac{ms_m}{s_m^2 - \omega^2} (A_m + r_m B_m). \quad (17)$$

The kinematic boundary condition (8) is satisfied

provided that

$$C_m = 0, \quad m \text{ even}, \quad (18)$$

and

$$D_m = 0, \quad m \text{ odd}. \quad (19)$$

Hence it follows from equations (16-19) that

$$A_m = -B_m / r_m, \quad m \text{ even}, \quad (20)$$

$$A_m = -r_m B_m, \quad m \text{ odd}, \quad (21)$$

$$D_m = \frac{mA_m}{s_m} - \frac{f}{\sigma} B_m, \quad m \text{ even}, \quad (22)$$

and

$$C_m = \frac{f}{\sigma} A_m - \frac{m}{s_m} B_m, \quad m \text{ odd}. \quad (23)$$

The expressions for the Poincaré wave surface elevation coefficients,

$$P_m = \frac{h}{\sigma} (s_m B_m + m C_m) \quad (24)$$

and

$$Q_m = \frac{h}{\sigma} (m D_m - s_m A_m), \quad (25)$$

may be obtained by substituting equations (13) to (15) into the continuity equation (3).

Values for the longitudinal velocity coefficients, A_m and B_m , must now be chosen so that the longitudinal velocities of the Kelvin and Poincaré waves, u_K and u_P , of equations (11) and (14), are equal for all values of y at some value x_1 of x . This may be written as the condition that

$$\begin{aligned} \sum_{m=1}^{\infty} [A_m \cos(my) + i B_m \sin(my)] \exp(-s_m x_1) \\ = S [\operatorname{ch}(\alpha y) \sin(kx_1) - \operatorname{sh}(\alpha y) \cos(kx_1)]. \end{aligned} \quad (26)$$

Taylor solves equation (26) by expanding the hyperbolic functions as trigonometric series which contain the undetermined multipliers β_s and γ_s , where s is a positive integer. The functions $\operatorname{ch}(\alpha y)$, $\operatorname{sh}(\alpha y)$, $\cos(sy)$ and $\sin(sy)$ are expressed as half range Fourier series which are valid for all values of y within the interval $+\frac{1}{2}\pi$. These Fourier representations are

$$\operatorname{ch}(\alpha y) = \frac{4\alpha}{\pi} \operatorname{sh}\left(\frac{\alpha\pi}{2}\right) \left[\frac{1}{2\alpha^2} + \sum_{m \text{ odd}} (-1)^{\frac{1}{2}m} \frac{\cos(my)}{\alpha^2 + m^2} \right], \quad (27a)$$

$$\operatorname{sh}(\alpha y) = \frac{4\alpha}{\pi} \operatorname{ch}\left(\frac{\alpha\pi}{2}\right) \sum_{m \text{ odd}} (-1)^{\frac{1}{2}(m-1)} \frac{\sin(my)}{\alpha^2 + m^2}, \quad (27b)$$

$$\cos(sy) = (-1)^{\frac{1}{2}(s-1)} \frac{4s}{\pi} \left[\frac{1}{2s^2} - \sum_{m \text{ odd}} (-1)^{\frac{1}{2}m} \frac{\cos(my)}{m^2 - s^2} \right], \quad s \text{ odd}, \quad (27c)$$

and

$$\sin(sy) = (-1)^{\frac{1}{2}s} \frac{4s}{\pi} \sum_{m \text{ odd}} (-1)^{\frac{1}{2}(m-1)} \frac{\sin(my)}{m^2 - s^2}, \quad s \text{ even.} \quad (27d)$$

Multiples of the difference between the left and right hand sides of equations (27c) and (27d) may be added to the expansions of $\text{ch}(\alpha y)$ and $\text{sh}(\alpha y)$. This process enables us to write equation (26) as

$$\begin{aligned} & \sum_{m=1} [A_m \cos(my) + i B_m \sin(my)] e^{-s_m x_1} \\ &= u_0 \left(\text{sh}\left(\frac{\alpha \pi}{2}\right) \sin(kx_1) \left[\frac{1}{2\alpha^2} + \sum_{m \text{ even}} (-1)^{\frac{1}{2}m} \frac{\cos(my)}{\alpha^2 + m^2} \right. \right. \\ &+ \left. \sum_{s \text{ odd}} \beta_s \left\{ (-1)^{\frac{1}{2}(s-1)} \frac{\pi \cos(sy)}{4s} - \frac{1}{2s^2} + \sum_{m \text{ even}} (-1)^{\frac{1}{2}m} \frac{\cos(my)}{m^2 - s^2} \right\} \right] \\ &- i \text{ch}\left(\frac{\alpha \pi}{2}\right) \cos(kx_1) \left[\sum_{m \text{ odd}} (-1)^{\frac{1}{2}(m-1)} \frac{\sin(my)}{\alpha^2 + m^2} \right. \\ &+ \left. \sum_{s \text{ even}} \gamma_s \left\{ (-1)^{\frac{1}{2}s} \frac{\pi \sin(sy)}{4s} - \sum_{m \text{ odd}} (-1)^{\frac{1}{2}(m-1)} \frac{\sin(my)}{m^2 - s^2} \right\} \right] \end{aligned} \quad (28)$$

where $u_0 = 4\alpha S/\pi$.

The coefficients of similar terms in equation (28) may now be compared. The requirement that the constant terms sum to zero produces

$$\frac{1}{\alpha^2} - \sum_{s \text{ odd}} \frac{\beta_s}{s^2} = 0. \quad (29)$$

Taking the relations between A_m and B_m , equations (20) and (21), into account, a comparison of the terms in $\cos(my)$ and $\sin(my)$ yields

$$m \text{ odd, } \frac{1}{\alpha^2 + m^2} - \sum_{s \text{ even}} \frac{\gamma_s}{m^2 - s^2} = \frac{\beta_m \pi}{4m\alpha} \text{th}\left(\frac{\alpha \pi}{2}\right) \tan(kx_1) \quad (30)$$

and

$$m \text{ even, } \frac{1}{\alpha^2 + m^2} + \sum_{\substack{s \\ \text{Odd}}} \frac{\beta_s}{m^2 - s^2} = \frac{\gamma_m \pi}{4 m r_m} \coth\left(\frac{\alpha \pi}{2}\right) \cot(kx_1). \quad (31)$$

We introduce the parameters

$$z_1 = \tan(kx_1),$$

$$L_m = \frac{\pi \operatorname{th}\left(\frac{\alpha \pi}{2}\right)}{4 m r_m},$$

$$M_m = \frac{\pi \coth\left(\frac{\alpha \pi}{2}\right)}{4 m r_m}$$

and

$$B_{ms} = \begin{cases} \frac{1}{m^2 + s^2}, & m = 0, s \neq 0; \\ & m \text{ odd, } s \text{ even;} \\ & m \text{ even, } s \text{ odd,} \end{cases}$$

$$= \frac{(-1)^m}{\alpha^2 + m^2}, \quad s = 0,$$

$$= 0, \quad \text{otherwise.}$$

Equations (29-31) may then be expressed as the matrix equation

$$\begin{bmatrix} B_{00} & B_{01} & 0 & B_{02} & 0 & \dots \\ B_{10} & L_1 z_1 & B_{12} & 0 & B_{14} & \dots \\ B_{20} & B_{21} & \frac{-M_2}{z_1} & B_{23} & 0 & \dots \\ B_{30} & 0 & B_{32} & L_3 z_1 & B & \dots \\ B_{40} & B_{41} & 0 & B_{43} & \frac{-M_4}{z_1} & \dots \\ \vdots & \vdots & \vdots & \vdots & \vdots & \vdots \end{bmatrix} \begin{bmatrix} 1 \\ \beta_1 \\ \gamma_2 \\ \beta_3 \\ \gamma_4 \\ \vdots \end{bmatrix} = \begin{bmatrix} 0 \\ 0 \\ 0 \\ 0 \\ 0 \\ \vdots \end{bmatrix}. \quad (32)$$

Non-trivial solutions to equation (32) exist only if the coefficient matrix is singular and the corresponding determinant is zero. By dividing the first, third, fifth etc. columns of this determinant by z_1 , multiplying the second, fourth, sixth etc. rows by z_1 and writing it as a sum of

two determinants, we obtain the determinantal equation

$$z_1 \begin{vmatrix} B_{00} & B_{01} & 0 & B_{02} & \dots \\ 0 & L_1 & B_{10} & 0 & \dots \\ B_{20} & B_{21} & -M_2 & B_{22} & \dots \\ 0 & 0 & B_{31} & L_3 & \dots \\ B_{40} & B_{41} & 0 & B_{42} & \dots \\ \vdots & \vdots & \vdots & \vdots & \vdots \end{vmatrix} = - \begin{vmatrix} 0 & B_{01} & 0 & B_{02} & \dots \\ B_{10} & L_1 & B_{12} & 0 & \dots \\ 0 & B_{21} & -M_2 & B_{23} & \dots \\ B_{30} & 0 & B_{31} & L_3 & \dots \\ 0 & B_{41} & 0 & B_{42} & \dots \\ \vdots & \vdots & \vdots & \vdots & \vdots \end{vmatrix} \quad (33)$$

A reduced order system for equation (33) is solved and z_1 found. We note that Brown (1978) shows that the quotient of the determinants is convergent.

Equations (30) and (31) may be written as

$$\beta_1 = \frac{-1}{L_1 z_1} (B_{10} + B_{12} \gamma_2 + B_{14} \gamma_4 + \dots), \quad (34a)$$

$$\gamma_2 = \frac{z_1}{M_2} (B_{20} + B_{21} \beta_1 + B_{23} \beta_3 + \dots), \quad (34b)$$

$$\beta_3 = \frac{-1}{L_2 z_1} (B_{30} + B_{31} \gamma_2 + B_{34} \gamma_4 + \dots), \quad (34c)$$

etc. Taylor solves this system by the Gauss-Seidel method. The undetermined multipliers on the right hand sides of equations (34) are initialised to zero. A first approximation to β_1 is found from equation (34a). This value of β_1 is substituted into equation (34b) and γ_2 is calculated. The updated values of β_1 and γ_2 are used to calculate β_3 from equation (34c). First order approximations for the first n undetermined multipliers $\beta_1, \gamma_2, \beta_3, \gamma_4, \dots, \beta_n$ are used to calculate second order approximations. The procedure may be repeated and higher order approximations generated.

The longitudinal velocity coefficients A_m , m odd, and B_m , m even,

are found from equation (28). They are given by

$$m \text{ odd, } A_m = \frac{\pi u_0}{4} \operatorname{sh}\left(\frac{\alpha\pi}{2}\right) e^{s_m x_1} \sin(kx_1) (-1)^{\frac{1}{2}(m-1)} \frac{P_m}{m} \quad (35)$$

and

$$m \text{ even, } B_m = \frac{-\pi u_0}{4} \operatorname{sh}\left(\frac{\alpha\pi}{2}\right) e^{s_m x_1} \cos(kx_1) (-1)^{\frac{1}{2}m} \frac{Q_m}{m} \quad (36)$$

The remaining coefficients A_m , m even, B_m , m odd, C_m , D_m , P_m and Q_m may be obtained from equations (18-25).

The complete solution is given by the difference between the Kelvin wave solution of equations (10-12) and the Poincaré wave solution of equations (13-15). Relative to a coordinate system with its origin at the mid-point of the channel end, the elevation is

$$\zeta = 2a_0 [\operatorname{ch}(\alpha y) \cos(k(x + x_1)) + i \operatorname{sh}(\alpha y) \sin(k(x + x_1))] - \sum_{m=1}^{\infty} [P_m \sin(my) + i Q_m \cos(my)] e^{-s_m x + i\sigma t} \quad (37)$$

the longitudinal component of velocity is

$$u = S [\operatorname{ch}(\alpha y) \sin(k(x + x_1)) - i \operatorname{sh}(\alpha y) \cos(k(x + x_1))] - \sum_{m=1}^{\infty} [A_m \cos(my) + i B_m \sin(my)] e^{-s_m x + i\sigma t} \quad (38)$$

and the transverse component of velocity is

$$v = - \sum_{m=1}^{\infty} [D_m \sin(my) + i C_m \cos(my)] e^{-s_m x + i\sigma t} \quad (39)$$

where the coefficients A_m , B_m etc. have been reduced by a factor $\exp(s_m x_1)$.

The parameter values $\alpha = 0.7$ and $K = 0.5$ are chosen by Taylor (1921) as representative of the North Sea. These values produce $k = (\alpha^2 + K^2)^{\frac{1}{2}} = 0.860$, $z = 0.385$ and $x_1 = 0.427$. The factor $u_0 = 4\alpha S/\pi$ is taken as an arbitrary unit of velocity, whence the velocity factor $S = \frac{\pi u_0}{4\alpha} = 1.122 u_0$ is obtained.

The amplitude factor $a_0 = i h k S / 2 \sigma$ is expressed in units of σ/h , i.e. $2 a_0 \sigma / h = 0.965 u_0$.

For a wave of M_2 period, $\tau = 12.42h$, we obtain $\sigma = 2\pi/\tau = 1.4052 \times 10^{-4} s^{-1}$, $c = \frac{\sigma}{k} = 1.634 \times 10^{-4} s^{-1}$, $h = c^2/g = 2.720 \times 10^{-9} m^{-1}$ where $g = 9.81 ms^{-2}$ and $f = \alpha c = 1.144 \times 10^{-4} s^{-1}$.

The length scale L , channel width B and depth D are interrelated by $L = \frac{B}{\pi} = \alpha (gD)^{1/2} / f$. In the case of a channel of depth 74m (approximately 40 fathoms), $L = 1.649 \times 10^5 m$ and $B = 5.179 \times 10^5 m$. The corresponding latitude of such a basin is given by $\theta = \sin^{-1} \left(\frac{f}{2\Omega} \right)$ where $\Omega = 2\pi/1$ sidereal day $= 7.292 \times 10^{-5} s^{-1}$, whence we obtain $\theta = 51.7^\circ$.

Thus the flow field may be specified by such four parameter combinations as α , K , τ and D or B , D , τ and θ .

The spatial variation of ζ may be conveniently displayed by a chart of the co-range lines, i.e. contours of constant displacement. The elevation may be represented by

$$\zeta(x,y,t) = (\zeta_1(x,y) + i\zeta_2(x,y)) e^{i\sigma t}$$

where ζ_1 and ζ_2 are real functions of x and y . The co-range lines are given by

$$\zeta_1^2 + \zeta_2^2 = \text{constant.} \quad (41)$$

The solution set for different constants forms a series of elliptical contours which are concentric about a system of amphidromes, i.e. nodal points where the tidal range vanishes. The amphidromes lie on the mid-channel axis with a separation of $\frac{1}{2} \lambda_K$, where the wavelength of M_2 Kelvin waves is given by $\lambda_K = 2\pi \left(\frac{gD}{\sigma} \right)^{1/2}$. The distance of the first amphidrome from the barrier is $D_A = \frac{1}{2} (\frac{1}{2} \lambda_K - B - 2\Delta)$, where Δ is the phase shift as the Kelvin wave turns a right-angle corner, (Hendershott and Speranza, 1971).

The co-tidal lines, i.e. lines of constant phase which radiate from the amphidromic points, illustrate the temporal variation of ζ . These may be obtained from $\partial \zeta / \partial t = 0$ which implies the condition

$$\frac{\zeta_2}{\zeta_1} = -\tan \sigma t, \quad (42)$$

(Krauss, 1973). Equation (42) may be solved for different times, e.g. successive lunar hours where 1 lunar hour = 24.84/24 h.

The velocity components may be expressed as

$$u(x,y,t) = (u_1(x,y) + i u_2(x,y)) e^{i\sigma t}$$

and

$$v(x,y,t) = (v_1(x,y) + i v_2(x,y)) e^{i\sigma t}$$

where subscripted functions are independent of time and real. The speed q of the current is given by

$$q = [(u_1 \cos \sigma t - u_2 \sin \sigma t)^2 + (v_1 \cos \sigma t - v_2 \sin \sigma t)^2]^{\frac{1}{2}} \quad (43)$$

and the direction ϕ may be expressed as

$$\phi = \tan^{-1} \left(\frac{v_1 \cos \sigma t - v_2 \sin \sigma t}{u_1 \cos \sigma t - u_2 \sin \sigma t} \right) \quad (44)$$

At any particular point the times of maximum and minimum current speed are given by $\partial q / \partial t = 0$. The velocity vectors that correspond to these times form the semi-major and semi-minor axes of a tidal ellipse. Such ellipses can also represent the actual paths of fluid particles during the tidal motion. The co-tidal lines, co-range lines and tidal ellipses for the Taylor model are symmetrically distributed about the mid-channel axis.

312. An alternative method of solution to the Taylor problem was developed by A. Defant in 1925, (see Defant, 1961). This is the method of collocation and is discussed in § 323.

32. Two dimensional dissipative systems

321. Proudman and Doodson (1924) give a qualitative description of the effects of frictional dissipation of wave energy. A wave which travels around the North Sea in the positive sense will have a steadily diminishing amplitude as its energy is dissipated. The tidal ranges at the east coast will be smaller than at the west coast; those at the north-east will be the least. The amphidromic points will be displaced to the east in such a manner that each one falls to the right of its predecessor along the axis of wave propagation.

They take as their equations of motion

$$u_t - fv = -g \zeta_x - \frac{F}{h} \quad (1a)$$

and

$$v_t + fu = -g \zeta_y - \frac{G}{h} \quad (1b)$$

where the frictional terms represented by F/h and G/h are proportional to the square of the current speed. The frictional parameters F and G are appropriate harmonic constituents of $ku(u^2 + v^2)^{\frac{1}{2}}$ and $kv(u^2 + v^2)^{\frac{1}{2}}$ where k is a constant.

We note that equations (1) may be obtained from the Reynolds equation (25.8) by neglecting the advective and viscous terms and assuming that the pressure follows a hydrostatic law and that the derivatives of the Reynolds stresses are governed by a quadratic friction law.

The dynamic equations are not solved. They are used to interpolate between locations where observational data have been obtained. Writing u , v , ζ , F and G as $u = u_1 \cos \sigma t + u_2 \sin \sigma t$ etc., where subscripted variables are functions of space only, the elevation gradients of equations (1) may be expressed as

$$\frac{\partial \zeta_1}{\partial x} = -\frac{f}{g} u_2 + \frac{f}{g} v_1 - \frac{F_1}{gh}$$

etc.

Current data are subjected to harmonic analysis, i.e. they are resolved into such constituents as the principal lunar semi-diurnal M_2 , the principal solar semi-diurnal S_2 , the luni-solar diurnal K_1 and the principal lunar diurnal O_1 tidal components. The elevation gradients are evaluated at the locations of various stations in the North Sea, the frictional parameter k being taken as 0.002.

A graphical interpolation procedure is used to estimate the elevations at locations that are intermediate to stations for which the elevations and gradients are known. The expression

$$d\zeta = \zeta_x dx + \zeta_y dy$$

is used to extrapolate the elevations in the neighbourhoods of stations.

The co-range and co-tidal charts that are obtained from these elevations amply support the qualitative description. They do not appear to have been greatly superseded by those obtained from more recent data, numerical techniques and frictional parameterizations, (c.f. Nihoul and Ronday, 1976; Davies and Furnes, 1980).

322. Hendershott and Speranza (1971) model the intensified but localised dissipation effects that are confined to the relatively high energy shallow water region at the head of a bay by a dissipative boundary condition at the transverse barrier, i.e.

$$u = \gamma_0 \zeta \quad \text{at } x = 0. \quad (1)$$

Equation (1) replaces the kinematic boundary condition (311.9) of the Taylor problem, equations (311.4-9). The parameter γ_0 may be adjusted to account for varying amounts of boundary dissipation. It is estimated by $\gamma_0 = (gD')^{1/2} / D$ where D' is the depth of the shallow water region and D is the depth beyond this region.

The elevation that satisfies the modified Taylor problem is composed of an incoming Kelvin wave of coastal amplitude ζ_I , an outgoing Kelvin

wave of coastal amplitude ζ_R and superposed non-propagating Poincaré modes.

It has the form

$$\begin{aligned} \zeta = & \zeta_I \exp[-i\omega t + i\omega x/(gD)^{1/2} - fy/(gD)^{1/2}] \\ & + \zeta_R \exp[-i\omega t - i\omega x/(gD)^{1/2} + f(y-a)/(gD)^{1/2}] \\ & + \sum_m e^{s_m x} [a_m \cos(\frac{m\pi y}{a}) + b_m \sin(\frac{m\pi y}{a})] e^{-i\omega t} \end{aligned} \quad (2)$$

for a sea which occupies the region $x \leq 0$, $0 \leq y \leq a$, where $s_m = [m^2 \pi^2 / a^2 - (\omega^2 - f^2) / gD]^{1/2}$, $m = 1, 2, \dots$, and ω is the circular frequency. The coefficients a_m , b_m are evaluated by Taylor's procedure.

The effect of such an energy absorbing barrier is to displace all amphidromic points from the long channel axis by constant amounts. This is in contrast to the mainstream viewpoint which predicts increasing displacements in the direction of the outgoing wave. Nevertheless, this modelling explains the dissimilarities between the tidal regimes in the Adriatic Sea and the Gulf of California. Both seas have fairly similar basin geometries and appear to meet the criteria for perfect Kelvin wave reflection. The Adriatic Sea exhibits only a slight displacement of the amphidrome in its northern section and would conform quite well to the Taylor model. The Gulf of California has no amphidrome in the basin. Hendershott and Speranza explain this difference as arising from the enhanced dissipation of tidal energy by non-linear bottom friction in the north end of the Gulf of California. The predicted amphidrome is displaced to such an extent as to become virtual.

323. If a linear friction law for the bottom friction is used to model the dissipative terms of the Reynolds equation (25.8), the linearised momentum and depth integrated continuity equations may be written as

$$u_t - fv = -g \zeta_x - \gamma u, \quad (1)$$

wave of coastal amplitude ζ_R and superposed non-propagating Poincaré modes.

It has the form

$$\begin{aligned} \zeta = & \zeta_I \exp\left[-i\omega t + i\omega x/(gD)^{\frac{1}{2}} - fy/(gD)^{\frac{1}{2}}\right] \\ & + \zeta_R \exp\left[-i\omega t - i\omega x/(gD)^{\frac{1}{2}} + f(y-a)/(gD)^{\frac{1}{2}}\right] \\ & + \sum_m e^{s_m x} \left[a_m \cos\left(\frac{m\pi y}{a}\right) + b_m \sin\left(\frac{m\pi y}{a}\right) \right] e^{-i\omega t} \end{aligned} \quad (2)$$

for a sea which occupies the region $x \leq 0$, $0 \leq y \leq a$, where $s_m = [m^2 \pi^2 / a^2 - (\omega^2 - f^2) / gD]^{\frac{1}{2}}$, $m = 1, 2, \dots$, and ω is the circular frequency. The coefficients a_m , b_m are evaluated by Taylor's procedure.

The effect of such an energy absorbing barrier is to displace all amphidromic points from the long channel axis by constant amounts. This is in contrast to the mainstream viewpoint which predicts increasing displacements in the direction of the outgoing wave. Nevertheless, this modelling explains the dissimilarities between the tidal regimes in the Adriatic Sea and the Gulf of California. Both seas have fairly similar basin geometries and appear to meet the criteria for perfect Kelvin wave reflection. The Adriatic Sea exhibits only a slight displacement of the amphidrome in its northern section and would conform quite well to the Taylor model. The Gulf of California has no amphidrome in the basin. Hendershott and Speranza explain this difference as arising from the enhanced dissipation of tidal energy by non-linear bottom friction in the north end of the Gulf of California. The predicted amphidrome is displaced to such an extent as to become virtual.

323. If a linear friction law for the bottom friction is used to model the dissipative terms of the Reynolds equation (25.8), the linearised momentum and depth integrated continuity equations may be written as

$$u_t - fv = -g\zeta_x - \gamma u, \quad (1)$$

$$v_t + fu = -g\zeta_y - \tau v \quad (2)$$

and

$$u_x + v_y + \frac{1}{h} \zeta_t = 0 \quad (3)$$

where h denotes the depth and the frictional parameter τ has the dimension of inverse time.

Expressing the velocity components and surface elevation above the mean sea level as

$$u(x,y,t) = \text{Re} \{ U(x,y) e^{-i\omega t} \},$$

$$v(x,y,t) = \text{Re} \{ V(x,y) e^{-i\omega t} \}$$

and

$$\zeta(x,y,t) = \text{Re} \{ Z(x,y) e^{-i\omega t} \},$$

equations (1-3) yield the Helmholtz equation

$$(\nabla^2 + \kappa^2) Z = 0, \quad (4)$$

where

$$\kappa^2 = i\omega(r^2 + \beta^2)/\rho gh \quad \text{and} \quad \beta = \tau - i\omega,$$

and the relations between the time independent parts of the velocity components and the elevation gradients

$$U = \frac{-g}{r^2 + \beta^2} [\beta Z_x + r Z_y] \quad (5)$$

and

$$V = \frac{-g}{r^2 + \beta^2} [-r Z_x + \beta Z_y] . \quad (6)$$

Reinecker and Teubner (1980) assume that the response of the water in a rectangular, semi-infinite channel, that occupies the region $x \geq 0$, $0 \geq y \geq b$, to an inward travelling wave of frequency ω is governed by equations (4-6). These equations are solved subject to the conditions that

$$V = 0 \text{ at } y = 0, b, \quad (7)$$

$$U = 0 \text{ at } x = 0 \quad (8)$$

and the radiation condition that no other inward travelling waves are excited by the input wave. They use both Galerkin and collocation methods to obtain solutions.

The solution to the Helmholtz equation (4) which satisfies the kinematic longitudinal boundary condition (7) and the radiation condition consists of an incident Kelvin wave of unit coastal amplitude, a reflected Kelvin wave of complex coastal amplitude G_0 and superposed, exponentially decaying Poincaré modes. When the effects of bottom friction are included, i.e. $\gamma \neq 0$, all Poincaré modes propagate up-channel. The time independent factor of the elevation may be expressed as

$$Z(x,y) = \exp[-iK_0 x + \alpha_0 y] + G_0 \exp[iK_0 x - \alpha_0 y] + \sum_{n=1}^{\infty} \frac{G_n e^{iK_n x}}{\rho \alpha_n - i f K_n} \left\{ \rho \alpha_n \cos\left(\frac{n\pi y}{b}\right) - f K_n \sin\left(\frac{n\pi y}{b}\right) \right\} \quad (9)$$

where $K_0 = (1\omega\rho/gh)^{1/2}$, $\alpha_0 = -ifK_0/\rho$, $\alpha_n = in\pi/b$ and $K_n = (\alpha_n^2 + k_n^2)^{1/2}$. The constraints $\text{Re}(K_n) \geq 0$ and $\text{Im}(K_n) > 0$, $n = 1, 2, \dots$, are imposed. These ensure that all propagating Poincaré modes travel in the positive x-direction and are exponentially decaying. However, Kelvin waves of exponentially increasing amplitude are not precluded.

The kinematic boundary condition (8) is used to determine the complex coefficients G_n , $n = 0, 1, \dots$. The longitudinal velocity component is approximated by the truncated series

$$U_T(x,y) = \frac{g\alpha_0}{f} [-\exp(-iK_0 x + \alpha_0 y) + G_0 \exp(iK_0 x - \alpha_0 y)] - ig \sum_{n=1}^N \left\{ G_n \frac{K_n \alpha_n e^{iK_n x}}{\rho \alpha_n - i f K_n} x \left[\cos\left(\frac{n\pi y}{b}\right) - \phi_n \sin\left(\frac{n\pi y}{b}\right) \right] \right\} \quad (10)$$

where $\phi_n = if\omega/(gh\alpha_n K_n)$. The system of integral equations

$$\int_0^b U_T(0,y) w_m(y) dy = 0, \quad m = 0, 1, \dots, N, \quad (11)$$

where $w_m(y)$ are appropriate weighting functions, are solved in order to determine the $N + 1$ coefficients of equation (10). If the weighting functions form a complete set then the approximate solution will converge to the exact solution.

By choosing the weighting functions $w_m(y) = \delta(y - y_m)$, where $\delta(y)$ is the Dirac delta function and y_m are specified points along the boundary $x = 0$, equations (10) and (11) produce the system of equations

$$\sum_{n=0}^N A_{mn} G_n = C_m, \quad m = 0, 1, \dots, N, \quad (12)$$

where

$$A_{m0} = \alpha_0 e^{-\alpha_0 y_m} / f,$$

$$A_{mn} = \frac{-iG_n K_n \alpha_n}{f\alpha_n - ifK_n} [\cos(n\pi y_m/b) - \phi_n \sin(n\pi y_m/b)],$$

$$n = 1, 2, \dots, N,$$

and

$$C_m = \alpha_0 e^{-\alpha_0 y_m} / f.$$

This is equivalent to the method of collocation in accordance with which values of the approximate series representation of a function must coincide with the exact values at prescribed points. Reinecker and Teubner (1980) obtain solutions to equation (12) for two sets of collocation points, namely, $y_m = mb/N$ and $y_m = (m + \frac{1}{2})b / (N + 1)$.

The principle of the Galerkin technique is that if $U(x,y)$ is represented by $\sum_{\alpha=1}^{\infty} U_{\alpha}(x) w_{\alpha}(y)$ and the approximation $U_T(x,y)$ is given by $\sum_{\alpha=1}^N U_{\alpha}(x) w_{\alpha}(y)$ then the residual $R = U - U_T$ is minimised by imposing the condition that

$$\int_0^b R w_p dy = 0, \quad p = 1, 2, \dots, N.$$

The choice of $w_p(y)$ is arbitrary, (c.f. Owen, 1980).

Reinecker and Teubner choose the weighting functions from the y -dependent part of the series in equation (10), namely,

$$w_0(y) = e^{-\alpha_0 y} \quad (13a)$$

and

$$w_m(y) = \cos\left(\frac{m\pi y}{b}\right) - \phi_m \sin\left(\frac{m\pi y}{b}\right), \quad m = 1, 2, \dots, N. \quad (13b)$$

For the Galerkin weighting functions of equations (13), the system of equations (11) may be expressed as

$$\sum_{n=0}^N A'_{mn} G_n = C'_m, \quad m = 0, 1, \dots, N. \quad (14)$$

The coefficients of the G_n , $n = 0, 1, \dots, N$ and constants are given by

$$A'_{00} = (1 - e^{-2\alpha_0 b}) / 2r,$$

$$A'_{0n} = \frac{-1 G_n K_n \alpha_n}{p \alpha_n - i f K_n} \cdot \frac{\alpha_0 \frac{n\pi}{b} \phi_n}{\alpha_0^2 - \alpha_n^2} [1 - (-1)^n e^{-\alpha_0 b}], \quad n \neq 0,$$

$$C'_0 = \alpha_0 b / r,$$

$$A'_{m0} = \frac{\alpha_0}{r} \cdot \frac{\alpha_0 - \frac{m\pi}{b} \phi_m}{\alpha_0^2 - \alpha_m^2} [1 - (-1)^m e^{-\alpha_0 b}], \quad m \neq 0,$$

$$A'_{mm} = \frac{-i \alpha_m K_m b}{2(p \alpha_m - i f K_m)} (1 + \phi_m^2), \quad m \neq 0,$$

$$A'_{mn} = \frac{-1 \alpha_n K_n}{p \alpha_n - i f K_n} \cdot \frac{\frac{n\pi}{b} \phi_n - \frac{m\pi}{b} \phi_m}{\alpha_n^2 - \alpha_m^2} [1 - (-1)^{n+m}],$$

$$m \neq n; n \neq 0,$$

and

$$C'_m = \frac{-\alpha_0}{r} \cdot \frac{\alpha_0 + \frac{m\pi}{b} \phi_m}{\alpha_0^2 - \alpha_m^2} [1 - (-1)^m e^{-\alpha_0 b}], \quad m \neq 0.$$

The systems of linear equations (12) and (14) are solved numerically for the case $\tau = 12.4$ h and $\nu = 0.0$. Reinecker and Teubner find that convergence as N increases is satisfactory for both methods but that the Galerkin technique gives better overall results than the collocation method.

The Galerkin method is used to obtain solutions for $\tau = 12.4$, 9.0 and 8.3h and $\nu = 0.0, 10^{-5}, 5 \times 10^{-5}, 10^{-4} \text{ s}^{-1}$. Using the parameter values $b = 500.5$ km, $h = 74$ m and $f = 1.19 \times 10^{-4} \text{ s}^{-1}$ at latitude 54.46°N , they produce co-range and co-tidal line plots for the different periods and values of the friction parameter. In the case of $\tau = 12.4$ h and $\nu = 0.0$, the results are similar to those of Taylor (1921). For the cases $\tau = 9.0, 8.3$ h and $\nu = 0.0$, the results agree with the findings of Brown (1973).

As the friction parameter ν is increased the long-channel spacing of amphidromic points remains virtually unchanged but the amphidromes are displaced from the mid-channel axis in the manner suggested by Proudman and Doodson (1924) until they eventually become virtual. The modulus of decay, i.e. the distance in which a wave decays to e^{-1} of its amplitude, becomes smaller for both Kelvin and propagating Poincaré waves. The interference pattern becomes independent of the wave period. Finally, the input wave dies out before reaching the head of the channel.

33 Three dimensional, advectionless, dissipative systems.

A two dimensional model of the flow may provide a satisfactory description of depth mean currents or of the tidal regime above the region of bottom frictional influence. However, there are many features of the vertical current structure that require a three dimensional analysis. These features include the no-slip condition at the bed, the logarithmic velocity profile of the mainstream current, the Ekman current

spiral and Ekman pumping effects, (Schlichting, 1968 ; Durance and Johnson, 1970; Krauss, 1973; Pond and Pickard, 1978).

331. Kraav (1969) introduces a more realistic z dependence by using a boundary layer model which is solved numerically. The governing equations, in which the advective contributions to the inertial terms have been neglected, within a boundary layer of thickness H are taken to be

$$\frac{\partial u_1}{\partial t} - fv_1 = -g \frac{\partial \xi}{\partial x} + k \frac{\partial^2 u_1}{\partial z^2}, \quad (1)$$

$$\frac{\partial v_1}{\partial t} + fu_1 = -g \frac{\partial \xi}{\partial y} + k \frac{\partial^2 v_1}{\partial z^2}, \quad (2)$$

$$\frac{\partial u_1}{\partial x} + \frac{\partial v_1}{\partial y} + \frac{\partial w_1}{\partial z} = 0, \quad (3)$$

$$k^2 \Phi' - cb^2 H = 0, \quad (4)$$

$$k = L b^{\frac{1}{2}} \quad (5)$$

and

$$L = -\tau \Phi' / \Phi'' \quad (6)$$

where $z = 0$ is the plane of the bottom, k is the vertical eddy coefficient, b and L are energy and length scales of turbulence averaged over the vertical and with respect to the tidal period τ , and τ and c are constants. The subscript '1' refers to the boundary layer, the prime denotes differentiation with respect to z and

$$\Phi' = \frac{1}{\tau} \int_0^H \int_0^\tau \left[\left(\frac{\partial u_1}{\partial z} \right)^2 + \left(\frac{\partial v_1}{\partial z} \right)^2 \right] dt dz.$$

The equations governing the motion above the boundary layer are similar to the field equations used by Taylor (1921), namely

$$\frac{\partial u}{\partial t} - fv = -g \frac{\partial \xi}{\partial x}, \quad (7)$$

$$\frac{\partial v}{\partial t} + fu = -g \frac{\partial \xi}{\partial y} \quad (8)$$

and

$$\frac{\partial u}{\partial x} + \frac{\partial v}{\partial y} + \frac{\partial w}{\partial z} = 0. \quad (9)$$

The boundary conditions which apply to the system of equations (1-9) are that there is no motion at the bed, i.e.

$$u_1 = v_1 = w_1 = 0 \quad \text{when } z = 0, \quad (10)$$

a condition of continuity of velocity at the upper limit of the boundary layer, i.e.

$$u_1 = u, \quad v_1 = v, \quad w_1 = w \quad \text{when } z = H, \quad (11)$$

a kinetic relationship at the sea surface $z = D$, i.e.

$$w = \partial \zeta / \partial t \quad \text{when } z = D, \quad (12)$$

and that the sea level fluctuations at the boundary, denoted by the contour Γ , are known, i.e.

$$\zeta(P) = \phi(P) \quad \text{if } P \in \Gamma. \quad (13)$$

The boundary layer thickness, $H = \pi \left(\frac{2k}{\sigma + f} \right)^{\frac{1}{2}}$, is a modification of the Ekman depth, $D_E = \pi \left(\frac{2k}{f} \right)^{\frac{1}{2}}$.

Using an asymptotic matching method, Kraav obtains the following equations for the elevations ζ' and ζ'' at two instants of time separated by a quarter of a tidal period. In the case of a deep sea, i.e. $H < D$, these equations are

$$\nabla^2 \zeta' + \frac{\sigma^2 - f^2}{gD} \frac{(1-M)\zeta' - M\zeta''}{(1-M)^2 + M^2} = 0, \quad (14)$$

$$\nabla^2 \zeta'' + \frac{\sigma^2 - f^2}{gD} \frac{(1-M)\zeta'' + M\zeta'}{(1-M)^2 + M^2} = 0, \quad (15)$$

where

$$M = \frac{1}{4\sigma D} \left[\frac{\sigma + f}{\alpha} + \frac{\sigma - f}{\beta} \right],$$

$$\alpha = \left(\frac{\sigma - f}{2k} \right)^{\frac{1}{2}}$$

and

$$\beta = \left(\frac{\sigma + f}{2k} \right)^{\frac{1}{2}}.$$

The expression for the eddy viscosity is given by

$$k = \frac{\gamma}{\sigma + f} \cdot \frac{[M_1 + M_2 (\sigma - f)^{\frac{1}{2}} / (\sigma + f)^{\frac{1}{2}}]^5}{[M_1 + M_2 (\sigma - f) / (\sigma + f)]^4} \quad (16)$$

where

$$\gamma = \frac{\lambda^2}{16 \pi}$$

$$M_1 = \left(\frac{B}{\sigma + f}\right)^2 \left[\left(\frac{\partial \xi'}{\partial x} + \frac{\partial \xi''}{\partial y}\right)^2 + \left(\frac{\partial \xi''}{\partial x} - \frac{\partial \xi'}{\partial y}\right)^2 \right]$$

and

$$M_2 = \left(\frac{B}{\sigma + f}\right)^2 \left[\left(\frac{\partial \xi'}{\partial x} - \frac{\partial \xi''}{\partial y}\right)^2 + \left(\frac{\partial \xi''}{\partial x} + \frac{\partial \xi'}{\partial y}\right)^2 \right].$$

Equations for the eddy viscosity and surface elevations of a shallow sea, i.e. $H > D$, are also obtained.

The derivatives in the equations for a deep sea and a shallow sea are replaced by central finite differences. The depths at internal points are obtained by averaging the surrounding depths. The elevations and eddy coefficients are found by a method of successive approximations, i.e. trial values of the elevations are used to determine approximations to the eddy viscosity and the boundary layer thickness.

The patterns of isolines for the boundary layer thickness, eddy viscosity and the maximum tidal current velocities are shown by Kraav to be very similar. The largest eddy coefficients are $900 \text{ cm}^2 \text{ s}^{-1}$ and occur near the English coast and in the southern North Sea. The velocities of the tidal currents, 70 to 90 cm s^{-1} , are also greatest in these regions. The smallest eddy coefficients are found in the Skaggerak region and are less than $1 \text{ cm}^2 \text{ s}^{-1}$. These values rapidly increase in the south of this region, e.g. the coefficients reach values of 40 to $60 \text{ cm}^2 \text{ s}^{-1}$ near the Danish coast and in the Heligoland Bight. Turbulence affects the entire depth of the sea near the English coast and in the southern North Sea, whereas in the Heligoland Bight the thickness of the boundary layer is from 15 to 35 m .

332. Davies and Furnes (1980) compute the M_2 tidal currents in the North Sea by using a three dimensional numerical model in which the hydrodynamic equations are transformed by a weighted depth averaging procedure into a two dimensional system. An inverse transformation of the solutions restores the z dependency, (c.f. Heaps, 1973).

Neglecting advective terms, the equations of continuity and momentum are expressed in a left handed spherical coordinate system as

$$\frac{\partial \xi}{\partial t} + \frac{1}{R \cos \phi} \left(\frac{\partial}{\partial \lambda} \int_0^h u dz + \frac{\partial}{\partial \phi} \int_0^h v \cos \phi dz \right) = 0, \quad (1)$$

$$\frac{\partial u}{\partial t} - \tau v = \frac{-g}{R \cos \phi} \frac{\partial \xi}{\partial \lambda} + \frac{\partial}{\partial z} \left(N \frac{\partial u}{\partial z} \right) \quad (2)$$

and

$$\frac{\partial v}{\partial t} + \tau u = \frac{-g}{R} \frac{\partial \xi}{\partial \phi} + \frac{\partial}{\partial z} \left(N \frac{\partial v}{\partial z} \right). \quad (3)$$

Here λ and ϕ are the east longitude and north latitude, respectively, ξ is the elevation of the sea surface above the undisturbed level $z = 0$, the bed is at $z = h$, R is the radius of the earth, the Coriolis parameter $\tau = 2\omega \sin \phi$, ω is the angular speed of the earth, u and v are the east and north-going components of current and N is the coefficient of vertical eddy viscosity.

The boundary conditions are that at the sea surface there is zero stress, i.e.

$$- \rho \left(N \frac{\partial u}{\partial z} \right)_0 = - \rho \left(N \frac{\partial v}{\partial z} \right)_0 = 0 \quad (4)$$

where the subscript 0 indicates evaluation at $z = 0$. At the sea bed it is assumed that there is a slip condition and a quadratic law of bottom friction holds. This is expressed as

$$- \left(N \frac{\partial u}{\partial z} \right)_h = k u_h (u_h^2 + v_h^2)^{\frac{1}{2}} \quad (5)$$

and

$$- \left(N \frac{\partial v}{\partial z} \right)_h = k v_h (u_h^2 + v_h^2)^{\frac{1}{2}} \quad (6)$$

where k is a constant coefficient of bottom friction and the script h denotes evaluation of $z = h$. An M_2 tidal input is specified along open sea boundaries. A radiation condition allows interior disturbances to propagate outwards.

The velocity components u and v are represented by the m term expansions

$$u(\gamma, \phi, z, t) = \sum_{r=1}^m A_r(\gamma, \phi, t) f_r(z) \quad (7)$$

and

$$v(\gamma, \phi, z, t) = \sum_{r=1}^m B_r(\gamma, \phi, t) f_r(z) \quad (8)$$

where the coefficients A_r and B_r are independent of z and the depth dependent basis functions f_r are differentiable.

Davies and Furnes note that the basis set of functions may be the eigenfunctions of a differential operator or, in the Galerkin method, arbitrarily chosen functions such as B-splines, Chebyshev or Legendre polynomials. They use a set of ten cosine functions,

$$f_r = \cos(\alpha_r z/h), \quad r = 1, 2, \dots, 10, \quad (9)$$

where $\alpha_r = (r-1)\pi$.

An appropriate parameterization of the eddy viscosity is considered to be a depth independent formulation in which the eddy coefficient is proportional to the square of depth mean current, i.e.,

$$N(\gamma, \phi, t) = K(\bar{u}^2 + \bar{v}^2) / \sigma, \quad (10)$$

where the overbar denotes a depth mean velocity, i.e. $\bar{u} = \frac{1}{h} \int_0^h u dz$, K is a dimensionless constant and σ is a typical frequency. The values $\sigma = 10^{-4} \text{ s}^{-1}$ and $K = 2 \times 10^{-5}$ are used.

The expansions for u and v , equations (7-8), are substituted into the equations of continuity and momentum, equations (1-3).

The use of the Galerkin method in the vertical space domain entails that the momentum equations are multiplied by each of the basis functions f_k , $k = 1, 2, \dots, m$, and integrated with respect to z over the interval 0 to h . The $(2m + 1)$ equations which result contain only the depth independent unknowns ξ , A_k and B_k , $k = 1, 2, \dots, m$. These equations are

$$\sum_{r=1}^m \frac{\partial A_r}{\partial t} \int_0^h f_r f_k dz = -\nu \sum_{r=1}^m B_r \int_0^h f_r f_k dz - \frac{g}{R \cos \phi} \frac{\partial \xi}{\partial x} \int_0^h f_k dz - f_k(h) k u_h (u_h^2 + v_h^2)^{\frac{1}{2}} - \lambda_k \sum_{r=1}^m A_r \int_0^h f_r f_k dz, \quad k = 1, 2, \dots, m, \quad (11)$$

$$\sum_{r=1}^m \frac{\partial B_r}{\partial t} \int_0^h f_r f_k dz = -\nu \sum_{r=1}^m A_r \int_0^h f_r f_k dz - \frac{g}{k} \frac{\partial \xi}{\partial \phi} \int_0^h f_k dz - f_k(h) k v_h (u_h^2 + v_h^2)^{\frac{1}{2}} - \lambda_k \sum_{r=1}^m B_r \int_0^h f_r f_k dz, \quad k = 1, 2, \dots, m, \quad (12)$$

and

$$\frac{\partial \xi}{\partial t} + \frac{1}{R \cos \phi} \left(\frac{\partial}{\partial x} \sum_{r=1}^m A_r \int_0^h f_r dz + \frac{\partial}{\partial \phi} \sum_{r=1}^m B_r \cos \phi \int_0^h f_r dz \right) = 0. \quad (13)$$

Here $\lambda_k(\chi, \phi, t) = N(\chi, \phi, t) \alpha_r^2 / h^2$, $k = 1, 2, \dots, m$, are the eigenvalues of the equation

$$\frac{d}{dz} [N(\lambda, \phi, t) r'_k(z)] = -\lambda_k(\lambda, \phi, t) r_k(z)$$

which is subject to the implied boundary conditions of equation (9).

Equations (11 - 13) are discretised in the horizontal by using a staggered finite difference grid in which ξ , u and v are evaluated at different grid points, and discretised with time by using a forward time-stepping method.

The initial state is one of zero displacement and motion, i.e.

$$\xi, A_r, B_r = 0 \quad \text{at } t = 0, r = 1, 2, \dots, m. \quad (14)$$

The normal component of velocity at a closed boundary is zero, thus

$$A_r \cos \psi + B_r \sin \psi = 0, \quad r = 1, 2, \dots, m, \quad (15)$$

where ψ denotes the inclination of the normal.

Along open sea boundaries the M_2 tidal input is specified and a radiation condition is used in which a relation between the total normal component of the depth mean current q and the total elevation ξ is prescribed. This relation is expressed as

$$q = q_T + \frac{c}{h} (\xi - \xi_T) \quad (16)$$

where

$$c = (gh)^{\frac{1}{2}},$$

$$\xi_T = H(\lambda, \phi) \cos[\sigma t - G(\lambda, \phi)],$$

$$q_T = Q(\lambda, \phi) \cos[\sigma t - \gamma(\lambda, \phi)].$$

σ , H and G denote the frequency, amplitude and phase of the M_2 tidal elevation, Q and γ denote the amplitude and phase of the normal component of the depth mean M_2 tidal current, respectively.

The M_2 tidal input at open boundaries and the tidal terms H , G , Q and γ are obtained from a two dimensional model of Flather (1976). It is assumed that the vertical distribution of current has as its expansion coefficients

$$A_1 = q_u / a_1, \quad B_1 = q_v / a_1 \quad (17a)$$

and

$$A_r = B_r = 0, \quad r = 2, 3, \dots, m, \quad (17b)$$

where q_u and q_v are the u and v components of the depth mean current q of equation (16) and $a_1 = \frac{1}{h} \int_0^h f_1 dz$.

Observational data from the Joint North Sea Data Acquisition Program (JONSDAP 76) are found to be in good agreement with the theoretical predictions when the bottom friction parameter $k = 5 \times 10^{-3}$, despite the crudeness of the formulation of the eddy viscosity and the lack of detailed information about the current structure at the open sea boundaries in the model.

Davies and Furnes find that the bottom current, measured at some reference height above the bed, and the depth mean current have a phase difference which is typically of the order of $+10^\circ$. The sense of rotation of the tidal ellipse in the Southern Bight is generally positive (the rotation is in the opposite direction in the northern section of the North Sea). The major axis of the ellipse is oriented in an east-west direction in regions away from coastal influence. The currents in this area are of the order of 25 cm s^{-1} . The orientation of the ellipse becomes nearly parallel to the shoreline, i.e. in a north-south direction, and current magnitudes increase to around 80 cm s^{-1} in regions that are further south. There is also an increase in current magnitude in the east to west direction.

The decrease in current magnitude with depth is accurately modelled, errors in phase and velocity being generally less than 7° and 3 cm s^{-1} , respectively. Co-phase lines for the u and v components of current at the sea surface and bed are obtained. The nodal points, where either the u or v component of velocity is zero, at the sea bed are not identical

to those at the surface. The phase change through depth of the u or v velocity component may be of the order of 100° near a nodal point of u or v .

34 Three dimensional, non-linear, dissipative systems.

The advective terms of the Navier-Stokes equation (23.3), e.g. $u \frac{\partial u}{\partial x} + v \frac{\partial u}{\partial y} + w \frac{\partial u}{\partial z}$, supply the mechanism by which the process of energy transfer between waves of different wave lengths and frequencies can occur, (Krauss, 1973). The irregular small scale motions of a turbulent flow regime which lead to the frictional dissipation of energy as heat are taken into account by the Reynolds stress terms of the Reynolds equation (25.8), (Pond and Pickard, 1978). However, non-linear wave interactions may also result in the localised production of steady currents or tidal constituents of higher frequencies than M_2 in shallow coastal waters. The pronounced quarter-diurnal tide at Southampton is an example of this, (Muir Wood, 1969). Such effects may be more explicitly modelled by the inclusion of the advective terms in the Reynolds equation than by a non-linear parameterization of the Reynolds stresses.

341. Owen (1980) solves the three dimensional, non-linear equations of motion numerically. He uses a finite difference grid in the horizontal and the Galerkin method in the vertical.

The system of hydrodynamic equations, referred to a cartesian coordinate system, are the continuity and momentum equations

$$\frac{\partial u}{\partial x} + \frac{\partial v}{\partial y} + \frac{\partial w}{\partial z} = 0, \quad (1)$$

$$\frac{\partial u}{\partial t} + u \frac{\partial u}{\partial x} + v \frac{\partial u}{\partial y} + w \frac{\partial u}{\partial z} = fv - \frac{1}{\rho} \frac{\partial p}{\partial x} + \frac{\partial}{\partial z} (N \frac{\partial u}{\partial z}), \quad (2)$$

$$\frac{\partial v}{\partial t} + u \frac{\partial v}{\partial x} + v \frac{\partial v}{\partial y} + w \frac{\partial v}{\partial z} = -fu - \frac{1}{\rho} \frac{\partial p}{\partial y} + \frac{\partial}{\partial z} (N \frac{\partial v}{\partial z}), \quad (3)$$

the salinity diffusion equation for the partial mass of dissolved salts

$$\frac{\partial s}{\partial t} + u \frac{\partial s}{\partial x} + v \frac{\partial s}{\partial y} + w \frac{\partial s}{\partial z} = \frac{\partial}{\partial z} \left(K \frac{\partial s}{\partial z} \right), \quad (4)$$

the equation of state

$$\rho_1 = \rho_0 (1 + \alpha s) \quad (5)$$

and the hydrostatic approximation

$$\frac{\partial p}{\partial z} = -\rho g. \quad (6)$$

Here ρ , ρ_1 and ρ_0 are the depth mean, depth dependent and fresh water densities, respectively, s is the salinity, α is a constant. K and N are the eddy coefficients of vertical diffusivity and viscosity, respectively, and f is the Coriolis parameter.

The following boundary conditions apply. The normal component of current is zero at land boundaries, i.e.

$$\underline{u} \cdot \underline{n} = 0 \quad (7)$$

where \underline{n} is the outward directed normal. The sea surface elevation ζ and the salinity are specified through time at open sea boundaries.

At the sea surface $z = \zeta$ the applied stress is zero, there is no flux of salt through the surface and the kinematic surface condition is satisfied, i.e. $\rho_1 N \nabla \underline{u} \cdot \underline{n} = K \nabla s \cdot \underline{n}$, $\frac{\partial}{\partial t} (z - \zeta) = 0$. (8-10)
 at the sea bed we have

$$N \nabla \underline{u} \cdot \underline{n} = k \underline{u}_b (u_b^2 + v_b^2)^{\frac{1}{2}} \quad \text{at } z = -h \quad (11)$$

where the suffix b denotes evaluation at the sea bed and k is the coefficient of bottom friction. There is no flux of salt through the sea bed. i.e.

$$K \nabla s \cdot \underline{n} = 0 \quad \text{at } z = -h. \quad (12)$$

The kinematic bed condition that no water passes through the sea bed is satisfied. i.e.

$$\frac{D}{Dt} (z + h) = 0 \quad \text{at } z = -h \quad (13)$$

where h is the mean depth.

The water column interval $[-h, \zeta]$ is mapped onto $[-1, 1]$ by the coordinate transformation

$$\sigma = 1 - 2 \left(\frac{\zeta - z}{h + \zeta} \right) . \quad (14)$$

The dependent variables u , v and s are represented by the expansions

$$u = U_{\alpha} (x, y, t) P_{\alpha} (\sigma) , \quad (15)$$

$$v = V_{\alpha} (x, y, t) P_{\alpha} (\sigma) \quad (16)$$

and

$$s = S_{\alpha} (x, y, t) P_{\alpha} (\sigma) \quad (17)$$

where a repeated subscript indicates summation and the components of P are any set of basis functions. Owen uses Legendre Polynomials as basis functions.

The Galerkin method is applied by substituting the M term truncated forms of expressions (15) to (17) into the transformed equations (2) to (4), taking the product with P_{β} , $\beta = 1, 2, \dots, M$ and integrating over $[-1, 1]$ with respect to σ .

The eddy viscosity and diffusivity coefficients are represented by prescribed functions of the form

$$N (x, y, \sigma, t) = N_0 (x, y, t) n(\sigma) \quad (18)$$

and

$$K (x, y, \sigma, t) = K_0 (x, y, t) n(\sigma) . \quad (19)$$

Owen defines N_0 and K_0 by using the empirical expressions

$$N_0 = k (h + \zeta) (u^2 + v^2 + v_0^2)^{\frac{1}{2}} (1 + 7Ri)^{-\frac{1}{4}} \quad (20)$$

and

$$K_0 = k (h + \zeta) (u^2 + v^2 + v_0^2)^{\frac{1}{2}} (1 + Ri)^{-7/4} \quad (21)$$

where the reference velocity v_0 prevents the system from becoming frictionless, and the depth mean Richardson number Ri indicates the relative importance of buoyancy and mechanical effects in the generation

of turbulence. The Richardson number is given by

$$Ri = \frac{g (h + \frac{1}{2}) \Delta s}{(v^2 + u^2 + v_0^2)^{\frac{1}{2}}} \quad (22)$$

where Δs is the salinity gradient.

In the case of a homogeneous sea, Owen uses the formulation of Davies and Furnes (1980), i.e.

$$N_0 = c (u^2 + v^2) / \omega \quad (23)$$

where ω is a typical frequency and c is a dimensionless constant.

The vertical variation of the eddy coefficients of viscosity and diffusivity is taken to be parabolic with a maximum at mid-depth of ten times the values at the surface and bed, i.e.

$$n(\sigma) = (1 - 0.9 \sigma^2) \quad (24)$$

An advective splitting technique is used to reduce the computational overhead. The solution is split so that the advective terms are only computed every m steps. The one dimensional scheme illustrates the procedure. The momentum equation

$$\frac{\partial u}{\partial t} + u \frac{\partial u}{\partial x} + g \frac{\partial \xi}{\partial x} + ku = 0$$

is split into gravity wave and advective components, denoted by the subscripts g and a , respectively. This yields

$$\frac{\partial u_g}{\partial t} + g \frac{\partial \xi}{\partial x} + ku = 0$$

and

$$\frac{\partial u_a}{\partial t} + u \frac{\partial u}{\partial x} = 0$$

where

$$\frac{\partial u}{\partial t} = \frac{\partial u_g}{\partial t} + \frac{\partial u_a}{\partial t}.$$

After m time steps Δt the computed value of u_g is used to determine u_a from the advective equation.

A staggered finite difference grid is used in which the surface elevation ζ and the salinity s are evaluated at the cell centre and the U and V components of velocity are evaluated at the sides of each cell. The depth dependent solution is obtained from expansions (15) to (17).

The model is applied by Owen to the Bristol Channel for which homogeneous conditions are assumed. The M_2 surface elevation at the open sea boundary is prescribed by

$$\zeta = H \cos(\sigma_0 t - g_0)$$

where H and g_0 are the amplitude and phase relative to lunar transit at Greenwich and σ_0 is the M_2 frequency.

The five Legendre polynomials $P_1(\sigma)$, ..., $P_5(\sigma)$ are used as the set of basic functions in the expansions (15) to (17). The parameter values $k = 0.005$, $c = 10^{-5}$ and $\omega = 10^{-4} \text{ s}^{-1}$ for the coefficient of bottom friction in equation (11) and the terms in equation (23) are found to give the best results in general.

The observed M_2 surface elevation is reproduced by the model to within 13 cm of amplitude and 4° of phase except at the head of the channel.

A comparison of current observations with the model values is found to be less satisfactory, with the errors in amplitude and phase being generally greater than 10% and 10° , respectively. However, the data are mainly for near-bottom currents and would tend to be dominated by local topographic features which are either outside the resolution capabilities of the model or, in the case of bathymetric effects, not represented by the model.

The reproduction of quarter-diurnal M_4 elevations is found to be generally poor for the parameterization of turbulence as given by

equations (20) or (23) and the bottom stress condition (11).

The amplitude is overestimated by approximately 100% in upstream regions where M_{ij} constituents are locally generated.

CHAPTER 4

AN ANALYTIC THREE DIMENSIONAL MODEL

CHAPTER 4

AN ANALYTIC THREE DIMENSIONAL MODEL

We consider the mean turbulent motion of a shallow sea within a semi-infinite rectangular channel of depth D and breadth $L\pi$ which rotates with an angular velocity $\frac{1}{2}f$. A right handed cartesian coordinate system is adopted. Rigid vertical walls are at $\bar{x} = 0$, $\bar{y} = 0$ and $\bar{y} = L\pi$, the sea bed is at $\bar{z} = -D$ and the undisturbed sea surface is at $\bar{z} = 0$, where tilded quantities are dimensional. The sea surface elevation $\bar{\zeta}$ and velocity components \bar{u} , \bar{v} and \bar{w} are prescribed at the open sea boundary. The pressure \bar{p} is specified at the sea surface $\bar{z} = \bar{\zeta}$. A no-slip condition applies at the bed. The enhanced dissipation that arises from shoaling effects is simulated by a controlled eddy viscosity \bar{N} which is some decreasing function of the longitudinal variable. Non-linear effects are taken into account by retaining a contribution from the advective terms of the momentum equations.

41. System parameters

The parameters L , D , A_0 , U_0 , W_0 , σ and N_0 are chosen as the characteristic scales of horizontal length, vertical length, amplitude, horizontal velocity, vertical velocity, circular frequency and vertical turbulent momentum exchange, respectively. They are functions of the historical time in years before present, $T \in [0, 8300]$, but not the local time \bar{t} .

The dimensionless characteristic coefficients R_0 , E_K , F_r , ϵ_1 , δ and α are introduced. They denote, in turn, the Rossby number, i.e. the ratio of the non-linear inertial forces to the Coriolis forces,

$$R_0 = \frac{U_0}{fL}, \quad (1)$$

the vertical Ekman number, i.e. the ratio between the vertical frictional forces and the Coriolis forces,

$$E_k = \frac{N_0}{f D^2}, \quad (2)$$

the Froude number, i.e. the ratio of the current and phase velocity
 $c = (gD)^{\frac{1}{2}}$,

$$F_r = \frac{U_0}{c}, \quad (3)$$

the aspect ratio

$$\epsilon_1 = \frac{D}{L}, \quad (4)$$

the frequency ratio

$$\delta = \frac{\sigma}{f} \quad (5)$$

and the ratio of the Froude and Rossby numbers,

$$\alpha = \frac{fL}{c}, \quad (6)$$

which is similar to the Kelvin number, i.e. the ratio between the period of the basic transverse oscillation of the basin and the inertial period $\frac{2\pi}{f}$, (Krauss, 1973).

The horizontal scales of length and velocity may be expressed as

$$L = \frac{\alpha c}{f} \quad (7)$$

and

$$U_0 = \alpha R_0 c. \quad (8)$$

We note that L is essentially the same as the Rossby radius of deformation, $(gD)^{\frac{1}{2}}/f$, (c.f. Gill, 1976) and of a form consistent with that used by Taylor (1921), provided that α is constant.

The relations

$$W_0 = \epsilon_1 U_0 \quad (9)$$

and

$$A_0 = \alpha R_0 D \quad (10)$$

may be obtained by a comparison of the orders of magnitude of the terms of the continuity equation (25.9) and its depth integrated form.

We assume that throughout the historic time period of interest the following conditions apply:

- 1) The Coriolis parameter is constant, $f = 1.144 \times 10^{-4}$, and the frequency ratio for the M_2 tidal frequency is $\zeta = 1.229$.
- 2) The Froude-Rossby number ratio α is constant. Such an assumption is consistent with the supposition that the Rossby radius of deformation is a measure of the horizontal length scale at all historical times of interest. Taylor (1921) uses $\alpha = 0.7$ and Moore (1970) uses $\alpha = 1$. We adopt the value $\alpha = 0.7$.
- 3) The relationship between the characteristic depth, amplitude and velocity is taken to be

$$cA_0 = U_0 D = \text{constant} . \quad (11)$$

A first order consideration of the characteristic amplitude of the transmitted wave in a canal where there is an abrupt change of cross-section to one that is geometrically similar yields such a relation, (c.f. Lamb, 1932). Alternatively, a constant volume flux model of a canal of constant breadth where there is a depth discontinuity may be used to obtain equation (11), (c.f. Hendershott and Speranza, 1971). We assume that the flow in a basin where the dimensions are varying with historical time approximately corresponds to one of these models.

- 4) The characteristic eddy viscosity and velocity are related by a quadratic law, i.e.

$$N_0 = C_0 U_0^2 / f \quad (12)$$

where C_0 is a constant, (c.f. Davies and Furnes, 1980).

Under these assumptions, we may specify appropriate values of the system parameters for the Southern Bight at any historical time of interest.

For example, at 0 BP:

$$\begin{aligned} D &= 5 \times 10^1 \text{m}, & U_0 &= 1 \text{ms}^{-1}, & c &= 2.22 \times 10^1 \text{ms}^{-1}, \\ L &= 1.36 \times 10^5 \text{m}, & A_0 &= 2.25 \text{m}, & N_0 &= 4 \times 10^{-2} \text{m}^2 \text{s}^{-1}, \\ R_0 &= 6.45 \times 10^{-2}, & E_k &= 1.40 \times 10^{-1}, & \epsilon_1 &= 3.70 \times 10^{-4} \end{aligned}$$

and at 8300 BP:

$$\begin{aligned} D &= 3 \times 10^1 \text{m}, & U_0 &= 1.67 \text{ms}^{-1}, & c &= 1.72 \times 10^1 \text{ms}^{-1}, \\ L &= 1.05 \times 10^5 \text{m}, & A_0 &= 2.91 \text{m}, & N_0 &= 1.11 \times 10^1 \text{m}^{-1} \text{s}, \\ R_0 &= 1.39 \times 10^{-1}, & E_k &= 1.08, & \epsilon_1 &= 2.86 \times 10^{-4}, \end{aligned}$$

where the characteristic depth, velocity and eddy viscosity at 0 BP are as given or implied by Nihoul and Ronday (1976) and Kraav (1969), and the characteristic depth at 8300 BP is obtained from Nio (1976).

We note that the values of the characteristic eddy viscosity and hence the Ekman number carry a wide margin of error. However, the values of E_k are similar to those used by Janowitz (1972) for lake coastal flows, namely $E_k = 0.1, 0.5$ and 1.0 .

From these data it is clear that ϵ_1 is $O(f)$ and that the ordering

$$\delta \gg E_k \gg R_0 \gg \epsilon_1 \quad (13)$$

is applicable.

In order that shallow water approximations may be made, the horizontal and vertical variables are scaled differently, (Stoker, 1957). A set of dimensionless variables $x, y, z, t, \eta, u, v, w, N_{ij}$ and p are defined by

$$\begin{aligned}
(\bar{x}, \bar{y}) &= L(x, y), & \bar{z} &= Dz, & \bar{t} &= \frac{1}{\sigma} t, \\
\bar{\eta} &= \alpha R_0 D \eta, & (\bar{u}, \bar{v}) &= U_0(u, v), & \bar{w} &= \epsilon_1 U_0 w, & (14) \\
\bar{N}_{ij} &= N_0 N_{ij} & \text{and } \bar{p} &= \rho(U_0 L p - g D z),
\end{aligned}$$

where N_{ij} denotes the components of the dimensionless eddy viscosity.

42. Equations of motion

Upon substituting equations (41.14) into the Reynolds equation (25.8) and taking the relations (41.1-10) into account, we obtain the dimensionless momentum equations

$$\begin{aligned}
\delta u_t + R_0 (u u_x + v u_y + w u_z) - v + p_x \\
= \epsilon_1^2 E_k \left\{ 2 \frac{\partial}{\partial x} [N_{xx} u_x] \right. \\
\left. + \frac{\partial}{\partial y} [N_{xy} (u_y + v_x)] + \frac{\partial}{\partial z} [N_{xz} (u_z / \epsilon_1^2 + w_z)] \right\}, & (1)
\end{aligned}$$

$$\begin{aligned}
\delta v_t + R_0 (u v_x + v v_y + w v_z) + u + p_y \\
= \epsilon_1^2 E_k \left\{ \frac{\partial}{\partial x} [N_{xy} (u_y + v_x)] \right. \\
\left. + 2 \frac{\partial}{\partial y} [N_{yy} v_y] + \frac{\partial}{\partial z} [N_{yz} (v_z / \epsilon_1^2 + w_y)] \right\} & (2)
\end{aligned}$$

and

$$\begin{aligned}
\delta w_t + R_0 (u w_x + v w_y + w w_z) + p_z / \epsilon_1^2 \\
= \epsilon_1^2 E_k \left\{ \frac{\partial}{\partial x} [N_{xz} (w_x + u_z / \epsilon_1^2)] \right. \\
\left. + \frac{\partial}{\partial y} [N_{yz} (w_y + v_z / \epsilon_1^2)] + 2 \frac{\partial}{\partial z} [N_{zz} w_z / \epsilon_1^2] \right\}. & (3)
\end{aligned}$$

Here viscous terms have been neglected in relation to the turbulent frictional terms, the f-plane approximation has been made and effects of astronomical tide producing forces have been neglected in comparison with those of the driving force at the open sea boundary.

If we compare terms of $O(\epsilon_1^{-2})$ in equation (3) then we obtain the hydrostatic pressure condition that the reduced pressure gradient vanishes, i.e.

$$p_z = 0, \quad (4)$$

which is correct to $O(\epsilon_1^2)$. Assuming that fluctuations in the atmospheric pressure are negligible and taking the atmospheric pressure at the sea surface as zero for convenience, the integration of equation (4) yields the expression

$$p = \frac{1}{\alpha} \rho \quad (5)$$

for the reduced pressure.

If the vertical eddy coefficients are replaced by a longitudinally varying eddy viscosity $N(x)$, i.e.

$$N_{xz} = N_{yz} = N(x), \quad (6)$$

(c.f. Shih-Zao, 1977), terms of order $O(\epsilon_1^2 N_{ij})$ are neglected and equation (5) is taken into account, then the momentum equations (1) and (2) may be reduced to the forms

$$\delta u_t + R_0 (uu_x + vy_y + wu_z) = v - \frac{1}{\alpha} \rho_x + E_k N(x) u_{zz} \quad (7)$$

and

$$\delta v_t + R_0 (uv_x + vv_y + wv_z) = -u - \frac{1}{\alpha} \rho_y + E_k N(x) v_{zz}. \quad (8)$$

We note that the error incurred by neglecting the Coriolis parameter f' and the effect of the orientation of the basin is $O(\epsilon_1)$, (c.f. Johns, 1965; §23). The horizontal eddy viscosity coefficients N_{xx} , N_{xy} , N_{yy} are estimated by Pond and Pickard (1978) to be greater than the vertical eddy coefficients by a factor of 10^6 . Thus the errors $O(\epsilon_1^2 N_{xx})$ etc. may be taken as approximately $O(R_0^2) > O(\epsilon_1)$ and equations (7) and (8) are

correct only to $O(R_0^2)$.

The continuity equation (25.9) may be expressed in terms of non-dimensional variables as

$$u_x + v_y + w_z = 0. \quad (9)$$

43. Boundary conditions.

We look for solutions to the field equations (42.7-9) subject to the boundary conditions of § 27.

The kinematic surface condition (27.1) may be written in the non-dimensional form

$$w - k_0 \eta_t = \alpha R_0 (u \eta_x + v \eta_y) \quad \text{at } z = \alpha R_0 \eta, \quad (1)$$

where $k_0 = \alpha \delta$ is a dimensionless wave number.

A Taylor expansion of the terms in equation (1) enables us to express the kinematic surface condition as the transferred condition

$$w - k_0 \eta_t = \alpha R_0 (u \eta_x + v \eta_y - \eta w_z) \quad \text{at } z = 0 \quad (2)$$

which is correct to $O(R_0^2)$.

The no wind condition (27.2) may be expressed as

$$u_z + \alpha R_0 \eta u_{zz} = v_z + \alpha R_0 \eta v_{zz} = 0 \quad \text{at } z = 0 \quad (3)$$

where terms of $O(R_0^2)$ have been neglected.

The no-slip condition (27.4) at the sea bed gives

$$u = v = w = 0 \quad \text{at } z = -1. \quad (4)$$

Kinematic boundary conditions are assumed to apply at the vertical walls of the channel, where equation (27.5) yields

$$u = 0 \quad \text{at } x = 0 \quad (5)$$

and

$$v = 0 \quad \text{at } y = 0, \pi. \quad (6)$$

The dependent variables η , u , v and w are suitably defined at the open sea boundary.

44. Method of solution.

It is assumed that the flow velocity \underline{u} can be represented by a uniformly valid perturbation expansion of the Latta type, (Nayfeh, 1973). A composite solution is formed from the sum of the functions \underline{F} and \underline{G} , i.e.

$$\underline{u}(x,y,z,t) = \underline{F}(x,y,z,t; \epsilon, \epsilon_0) + \underline{G}(x,y,z,Z,t; \epsilon, \epsilon_0),$$

where x , y and z may be referred to as outer coordinates, the boundary layer or inner variable Z is a magnified vertical coordinate, ϵ and ϵ_0 are small parameters of the system. The functions \underline{F} and \underline{G} are expressed as asymptotic expansions. The form of the special function \underline{G} may be obtained from a matched asymptotic expansions analysis, (c.f. appendix 1).

A suitable Latta expansion is found to be of a form which develops in powers of $\epsilon = \epsilon(R_0)$ and which represents \underline{G} by two special functions of the outer coordinates x , y and z , the boundary layer coordinate Z and time t . This expansion is

$$\begin{aligned} u_j = & \sum_{n=0}^{\infty} \epsilon^n f_j^{(n)}(x,y,z,t) \\ & + \text{Re} \left\{ \exp(-\omega_1(x)Z) \sum_{n=0}^{\infty} \epsilon^n g_j^{(n)}(x,y,z,t) \right. \\ & \left. + \exp(-\omega_2(x)Z) \sum_{n=0}^{\infty} \epsilon^n h_j^{(n)}(x,y,z,t) \right\}, \\ & j = 1, 2, 3, \quad (1) \end{aligned}$$

where $u_1 = u$, $u_2 = v$, $u_3 = w$, $Z = \frac{1+z}{\epsilon_0}$ and $\epsilon_0 = \epsilon_0(E_k)$.

The outer variables $f_j^{(n)}(x,y,z,t)$ are real functions. The 'inner'

variables $g_j^{(n)}$, $h_j^{(n)}$ and boundary layer functions $\omega_1(x)$ and $\omega_2(x)$ are complex functions. These functions are determined in the course of the analysis.

The boundary layer functions $\omega_1(x)$ and $\omega_2(x)$ are analogous to the parameters α and β used by Kraav (1969) and the circularly polarised to the left and circularly polarised to the right inertial wave vector components mentioned by Bergstrom and Cogley (1976). The effect of their introduction is to produce two overlapping boundary layer regions.

The derivatives of the velocity components with respect to x are

$$u_{j,x} = \sum_{n=0}^{\infty} \epsilon^n r_{j,x}^{(n)} + \text{Re} \left\{ e^{-\omega_1 z} \sum_{n=0}^{\infty} \epsilon^n \left(g_{j,x}^{(n)} - \frac{1+z}{\epsilon_0} \omega_1' g_j^{(n)} \right) + e^{-\omega_2 z} \sum_{n=0}^{\infty} \epsilon^n \left(h_{j,x}^{(n)} - \frac{1+z}{\epsilon_0} \omega_2' h_j^{(n)} \right) \right\}, \quad j = 1, 2, 3, \quad (2)$$

where the prime suffix denotes differentiation.

The first and second derivatives with respect to z are

$$u_{j,z} = \sum_{n=0}^{\infty} \epsilon^n r_{j,z}^{(n)} + \text{Re} \left\{ e^{-\omega_1 z} \sum_{n=0}^{\infty} \epsilon^n \left(g_{j,z}^{(n)} - \frac{\omega_1}{\epsilon_0} g_j^{(n)} \right) + e^{-\omega_2 z} \sum_{n=0}^{\infty} \epsilon^n \left(h_{j,z}^{(n)} - \frac{\omega_2}{\epsilon_0} h_j^{(n)} \right) \right\}, \quad j = 1, 2, 3, \quad (3)$$

and

$$u_{j,zz} = \sum_{n=0}^{\infty} \epsilon^n r_{j,zz}^{(n)} + \text{Re} \left\{ e^{-\omega_1 z} \sum_{n=0}^{\infty} \epsilon^n \left(g_{j,zz}^{(n)} - \frac{2\omega_1}{\epsilon_0} g_{j,z}^{(n)} + \frac{\omega_1^2}{\epsilon_0^2} g_j^{(n)} \right) + e^{-\omega_2 z} \sum_{n=0}^{\infty} \epsilon^n \left(h_{j,zz}^{(n)} - \frac{2\omega_2}{\epsilon_0} h_{j,z}^{(n)} + \frac{\omega_2^2}{\epsilon_0^2} h_j^{(n)} \right) \right\}, \quad j = 1, 2, 3. \quad (4)$$

The surface elevation $\eta(x,y,t)$ is represented by a perturbation expansion about the zero order state,

$$\eta = \sum_{n=0}^{\infty} \epsilon^n \eta^{(n)} \quad (5)$$

where $\eta^{(n)}$ are real functions of x , y and t .

The difficulties that are inherent in the solving of a two-parameter problem are circumvented by prescribing a relation between E_k and R_0 , (Bergstrom and Cogley, 1976). The functional forms of ϵ and ϵ_0 are chosen so that both are of the same order of magnitude as the n -th root of the coefficient of the highest n -th order derivative in the governing equations, (c.f. Durance and Johnson, 1970).

We consider three cases in which the balance between the frictional and non-linear effects, as measured by the Ekman and Rossby numbers, is such that:

$$1) \quad E_k = O(R_0), \quad \epsilon = \epsilon_0 = R_0^{\frac{1}{2}},$$

$$2) \quad E_k = O(R_0^{\frac{1}{2}}), \quad \epsilon = \epsilon_0 = R_0^{\frac{1}{4}}$$

and

$$3) \quad E_k = \Phi(T) + O(R_0) \text{ where } \Phi \text{ maps the historical time into some subinterval of } [0,1].$$

In each case the perturbation expansions (1 - 5) are substituted into the field equations (42.7-9) and the boundary conditions (43.2-6). Terms of $O(\epsilon^n)$, $O(\epsilon^n e^{-\alpha_1 z})$ and $O(\epsilon^n e^{-\alpha_2 z})$, $n = -1, 0, 1, \dots$, are separately equated. This process generates a set of linearised systems for which analytic solutions are obtained.

45. $E_k = O(R_0)$.

We consider the formulation of case 1, §44, in which the Ekman and Rossby numbers are of the same order of magnitude. We assume that $\epsilon^2 = R_0 = E_k$ and $Z = \frac{1+z}{|\epsilon|}$. The full equations yield the following systems of equations where only the real parts of expressions have significance.

451. The $O(\epsilon^{-1} e^{-\omega_1 Z})$ terms of the expanded continuity equation (42.9) give the relation

$$g_3^{(0)} = - (1+z) \frac{\omega_1'}{\omega_1} g_1^{(0)}. \quad (1)$$

452. The $O(\epsilon^{-1} e^{-\omega_2 Z})$ system is

$$h_3^{(0)} = - (1+z) \frac{\omega_2'}{\omega_2} h_1^{(0)}. \quad (1)$$

453. The $O(\epsilon^0)$ terms of the expanded momentum and continuity equations (42.7-9) yield

$$\delta f_{1,t}^{(0)} = f_2^{(0)} - \frac{1}{\alpha} \eta_x^{(0)}, \quad (1)$$

$$\delta f_{2,t}^{(0)} = -f_1^{(0)} - \frac{1}{\alpha} \eta_y^{(0)} \quad (2)$$

and

$$f_{1,x}^{(0)} + f_{2,y}^{(0)} + f_{3,z}^{(0)} = 0. \quad (3)$$

The $O(\epsilon^0)$ terms of the expanded boundary conditions (43.2-6)

produce the relations

$$f_j^{(0)} + g_j^{(0)} + h_j^{(0)} = 0 \quad \text{at } z = -1, \quad j = 1, 2, 3, \quad (4)$$

$$f_{1,z}^{(0)} = f_{2,z}^{(0)} \quad \text{at } z = 0, \quad (5)$$

$$f_3^{(0)} = k_0 \eta_t^{(0)} \quad \text{at } z = 0, \quad (6)$$

$$f_2^{(0)} = 0 \quad \text{at } y = 0, \quad \pi \quad \text{from equations (14)} \quad (7)$$

and

$$f_1^{(0)} = 0 \quad \text{at } x = 0. \quad (8)$$

We shall refer to equations (1 - 8) as the zeroth order outer system. We note that the zeroth order outer system bed condition (4) relates the zeroth order inner and outer velocity components.

Assuming that all zeroth order dependent variables exhibit a harmonic time dependence of the form e^{it} , we may write

$$\eta^{(0)} = \text{Re} \{ A^{(0)}(x,y) e^{it} \}, \quad (9)$$

$$f_j^{(0)} = \text{Re} \{ F_j^{(0)}(x,y,z) e^{it} \}, \quad (10)$$

$$g_j^{(0)} = G_j^{(0)}(x,y,z) e^{it}, \quad j = 1, 2, 3, \quad (11)$$

and

$$h_j^{(0)} = H_j^{(0)}(x,y,z) e^{it}, \quad j = 1, 2, 3. \quad (12)$$

If we take equations (451.1) and (452.1) into account, we may express equations (1 - 8) as

$$(\nabla^2 + K^2) A^{(0)} = 0, \quad (13)$$

$$F_1^{(0)} = \frac{\alpha}{K^2} (i \delta A_x^{(0)} + A_y^{(0)}), \quad (14)$$

$$F_2^{(0)} = \frac{\alpha}{K^2} (-A_x^{(0)} + i A_y^{(0)}), \quad (15)$$

$$F_3^{(0)} = i k_0 (1+z) A^{(0)}, \quad (16)$$

$$F_2^{(0)} = 0 \quad \text{at } y = 0, \pi, \quad (17)$$

$$F_1^{(0)} = 0 \quad \text{at } x = 0 \quad (18)$$

and

$$F_j^{(0)} + G_j^{(0)} + H_j^{(0)} = 0 \quad \text{at } z = -1, j = 1, 2, 3, \quad (19)$$

where $K^2 = \alpha^2 (\delta^2 - 1)$. It follows from equations (14) and

(15) that $F_1^{(0)}$ and $F_2^{(0)}$ are independent of z and thus the vanishing surface shear stress condition (5) is met.

The system of equations (13 - 19) constitutes a rescaling of the Taylor problem, (Taylor, 1921; § 311). It has the solution

$$A^{(0)} = \frac{i\pi}{4\alpha} [\text{ch}(\alpha \bar{y}) \cos(k_0 \bar{x}) + i \text{sh}(\alpha \bar{y}) \sin(k_0 \bar{x})] - \sum_{m=1}^{\infty} [P_m \sin(m\bar{y}) + i Q_m \cos(m\bar{y})] e^{-s_m x}, \quad (20)$$

$$F_1^{(0)} = \frac{\pi}{4\alpha} [\text{ch}(\alpha \bar{y}) \sin(k_0 \bar{x}) - i \text{sh}(\alpha \bar{y}) \cos(k_0 \bar{x})] - \sum_{m=1}^{\infty} [A_m \cos(m\bar{y}) + i B_m \sin(m\bar{y})] e^{-s_m x} \quad (21)$$

and

$$F_2^{(0)} = - \sum_{m=1}^{\infty} [D_m \sin(m\bar{y}) + i C_m \cos(m\bar{y})] e^{-s_m x} \quad (22)$$

where $\bar{y} = y - \frac{\pi}{2}$, $\bar{x} = x + x_1$, $s_m = (m^2 - K^2)^{\frac{1}{2}}$ and subscripted variables are real and dimensionless.

The coefficients P_m and Q_m are related to A_m , B_m , C_m and D_m by

$$P_m = \frac{1}{k_0} (s_m B_m + m C_m) \quad (23)$$

and

$$Q_m = \frac{1}{k_0} (m D_m - s_m A_m). \quad (24)$$

The parameter values $\alpha = 0.7$ and $\delta = 1.229$ imply that $K = 0.500$ and $k_0 = 0.8602$. These are the same parameter values as used by Taylor (1921), whence we obtain $x_1 = 0.427$.

The dimensionless variables A_m , B_m , C_m and D_m , $m = 1, 2, \dots, 10$, are of the same magnitude as the corresponding dimensional variables

calculated by Taylor. They have the values:

m	A _m	B _m	C _m	D _m
1	0.7560	-1.1000	1.8920	0.0000
2	-0.4270	0.0660	0.0000	0.4950
3	-0.0090	0.1320	-0.1380	0.0000
4	0.1000	-0.0040	0.0000	0.1030
5	0.0012	-0.0500	0.5100	0.0000
6	-0.0425	0.0010	0.0000	-0.0430
7	-0.0003	0.0170	-0.0270	0.0000
8	0.0245	-0.0002	0.0000	0.0240
9	0.0001	-0.0170	0.0170	0.0000
10	-0.0147	0.0001	0.0000	-0.0150

454. The $O(e^{-\omega_1 z})$ momentum equations are

$$\delta g_{1,t}^{(0)} = g_2^{(0)} + N\omega_1^2 g_1^{(0)} \quad (1)$$

and

$$\delta g_{2,t}^{(0)} = -g_1^{(0)} + N\omega_1^2 g_2^{(0)}. \quad (2)$$

The continuity equation for this order of approximation is

$$\omega_1 g_3^{(1)} + (1+z)\omega_1 g_1^{(1)} = g_{1,x}^{(0)} + g_{2,y}^{(0)} + g_{3,z}^{(0)}. \quad (3)$$

The momentum equations (1) and (2) may be expressed as the matrix equation

$$\begin{bmatrix} \delta & -N\omega_1^2 & -1 \\ 1 & \delta & -N\omega_1^2 \end{bmatrix} \begin{bmatrix} g_1^{(0)} \\ g_2^{(0)} \end{bmatrix} = \begin{bmatrix} 0 \\ 0 \end{bmatrix}. \quad (4)$$

Non-trivial solutions exist only if the coefficient matrix is singular. Taking the negative root of the characteristic equation, we obtain an expression for the boundary layer function,

$$\omega_1 = (1 + i) \left(\frac{\delta + 1}{2N} \right)^{\frac{1}{2}}, \quad (5)$$

and the relation

$$G_2^{(0)} = -i G_1^{(0)}. \quad (6)$$

455. The $O(\epsilon^0 e^{-\omega_2 Z})$ system is of a similar structure to the previous system. The positive root of the characteristic equation yields

$$\omega_2 = (1 + i) \left(\frac{\delta - 1}{2N} \right)^{\frac{1}{2}} \quad (1)$$

whence we obtain

$$H_2^{(0)} = i H_1^{(0)}. \quad (2)$$

The continuity equation for this system is

$$\omega_2 h_3^{(1)} + (1+z) \omega_2' h_1^{(1)} = h_{1,x}^{(0)} + h_{2,y}^{(0)} + h_{3,z}^{(0)}. \quad (3)$$

The $O(\epsilon^0 e^{-\omega_1 Z})$ and $O(\epsilon^0 e^{-\omega_2 Z})$ systems will be referred to as the zeroth order inner system of equations. We note that the zeroth order inner system continuity equations (454.3) and (455.3) yield relations between the zeroth and first order inner variables.

456. The $O(\epsilon e^{-\omega_2 Z})$ momentum equations of the first order inner system yield additional information about the functional forms of the zeroth and first order inner variables $g_j^{(0)}$ and $g_j^{(1)}$. These equations may be written as

$$\delta g_{1,t}^{(1)} - \omega_1^2 N g_1^{(1)} - g_2^{(1)} = \omega_1 g_1^{(0)} - 2 \omega_1 N g_{1,z}^{(0)} \quad (1)$$

and

$$\delta g_{2,t}^{(1)} - \omega_1^2 N g_2^{(1)} + g_1^{(1)} = \omega_1 f g_2^{(0)} - 2 \omega_1 N g_{2,z}^{(0)} \quad (2)$$

where $f = (1+z) \frac{\omega_1'}{\omega_1} r_1^{(0)} + r_3^{(0)}$.

The function f is a real function of x, y, z and t since $r_1^{(0)}$ and $r_3^{(0)}$ are real functions and it follows from equation (454.5) that $\frac{\omega_1'}{\omega_1} = -\frac{1}{2} \frac{N'}{N}$ is also real.

By writing

$$f = F e^{it} + \bar{F} e^{-it}, \quad (3)$$

where the overbar denotes the complex conjugate and F is independent of time, the non-linear terms of equations (1) and (2) may be expressed as

$$\omega_1 f g_j^{(0)} = \omega_1 F G_j^{(0)} e^{2it} + \omega_1 \bar{F} G_j^{(0)}, \quad (4)$$

$j = 1, 2,$

where

$$F = \frac{1}{4}(1+z) (2i k_0 A^{(0)} - \frac{N'}{N} F_1^{(0)}). \quad (5)$$

The particular integral terms of equations (1) and (2) are either proportional to e^{2it} or e^{it} or they are independent of time. This suggests that the first order inner flow variables may be represented by the harmonic expansion

$$g_j^{(1)} = \sum_{n=0}^{\infty} G_{j,n}^{(1)} e^{int}, \quad j = 1, 2, 3, \quad (6)$$

where $G_{j,n}^{(1)}$, $n = 0, 1, 2, \dots$, are independent of time.

Expansion (6) is substituted into equations (1) and (2) and terms that are proportional to the same time factor are compared.

For the terms which are independent of time we obtain

$$\begin{bmatrix} -\omega_1^2 N & -1 \\ 1 & -\omega_1^2 N \end{bmatrix} \begin{bmatrix} G_{1,0}^{(1)} \\ G_{2,0}^{(0)} \end{bmatrix} = \omega_1 F G_1^{(0)} \begin{bmatrix} 1 \\ -1 \end{bmatrix}. \quad (7)$$

Thus the first order, steady, inner flow components are

$$G_{1,0}^{(1)} = \frac{1\omega_1}{\delta} F G_1^{(0)} \quad (8)$$

and

$$G_{2,0}^{(1)} = \frac{\omega_1}{\delta} F G_1^{(0)}. \quad (9)$$

The terms that are proportional to e^{it} produce the relation

$$\begin{bmatrix} 1\delta - \omega_1^2 N & -1 \\ 1 & 1\delta - \omega_1^2 N \end{bmatrix} \begin{bmatrix} G_{1,1}^{(1)} \\ G_{2,1}^{(1)} \end{bmatrix} = -2\omega_1 N G_{1,z}^{(0)} \begin{bmatrix} 1 \\ -1 \end{bmatrix}. \quad (10)$$

The coefficient matrix of this system is singular and we obtain

$$G_{1,z}^{(0)} = 0 \quad (11)$$

and

$$G_{2,1}^{(1)} = -1 G_{1,1}^{(1)}. \quad (12)$$

Comparing terms that are proportional to e^{2it} , we get the relation

$$\begin{bmatrix} 21\delta - \omega_1^2 N & -1 \\ 1 & 21\delta - \omega_1^2 N \end{bmatrix} \begin{bmatrix} G_{1,2}^{(1)} \\ G_{2,2}^{(1)} \end{bmatrix} = \omega_1 F G_1^{(0)} \begin{bmatrix} 1 \\ -1 \end{bmatrix} \quad (13)$$

which has the solutions

$$G_{1,2}^{(1)} = \frac{-1 \omega_1}{\delta} F G_1^{(0)} \quad (14)$$

and

$$G_{2,2}^{(1)} = \frac{-\omega_1}{\delta} F G_1^{(0)}. \quad (15)$$

The matrix systems for terms with e^{int} , $n > 2$, time dependencies are of the form

$$\begin{bmatrix} in\delta - \omega_1^2 N & -1 \\ 1 & in\delta - \omega_1^2 N \end{bmatrix} \begin{bmatrix} G_{1,n}^{(1)} \\ G_{2,n}^{(1)} \end{bmatrix} = \begin{bmatrix} 0 \\ 0 \end{bmatrix}, \quad n=3, 4, \dots \quad (16)$$

The coefficient matrix of equation (16) is, in general, non-singular. Thus only the trivial solution pertains to the harmonic constituents of those first order inner flow variables that have time dependencies at frequencies higher than quarter-diurnal, i.e.

$$G_{j,n}^{(0)} = 0; \quad j = 1, 2; \quad n = 3, 4, \dots \quad (17)$$

457. The $O(\epsilon e^{-\omega_2 z})$ momentum equations are

$$\delta h_{1,t}^{(1)} - \omega_2^2 N h_1^{(1)} - h_2^{(1)} = \omega_2^f h_1^{(0)} - 2\omega_2 N h_{1,z}^{(0)} \quad (1)$$

and

$$\delta h_{2,t}^{(1)} - \omega_2^2 N h_2^{(1)} + h_1^{(1)} = \omega_2^f h_2^{(0)} - 2\omega_2 N h_{2,z}^{(0)} \quad (2)$$

where we have used equation (455.1) to obtain the relation

$$\omega_2^f / \omega_2 = -\frac{1}{2} N' / N.$$

$$\text{Writing } h_j^{(1)} = \sum_{n=0}^{\infty} H_{j,n}^{(1)} e^{int}, \quad j = 1, 2, 3, \dots,$$

where the terms $H_{j,n}^{(1)}$ are independent of time, the following

relations may be obtained by the same methods used in § 456:

$$H_{1,0}^{(1)} = \frac{1 \omega_2}{\delta} F H_1^{(0)}, \quad (3)$$

$$H_{2,0}^{(1)} = \frac{-\omega_2}{\delta} F H_1^{(0)}, \quad (4)$$

$$H_{2,1}^{(1)} = 1 H_{1,1}^{(1)}, \quad (5)$$

$$H_{1,2}^{(1)} = -\frac{1}{\delta} \omega_2 F H_1^{(0)}, \quad (6)$$

$$H_{2,2}^{(1)} = \frac{\omega_2}{\delta} F H_1^{(0)}, \quad (7)$$

$$H_{j,n}^{(1)} = 0; \quad j = 1,2; \quad n = 3,4,\dots \quad (8)$$

and

$$H_{1,z}^{(0)} = 0. \quad (9)$$

458. The solutions for the zeroth order inner variables may now be expressed in terms of the zeroth order outer variables. The first order inner system equations (456.11) and (457.9) in conjunction with the zeroth order inner system equations (454.6) and (455.2.) imply that $G_1^{(0)}$, $G_2^{(0)}$, $H_1^{(0)}$ and $H_2^{(0)}$ are independent of z . The zeroth order outer system condition (453.19) may be used to establish that

$$G_1^{(0)} = -\frac{1}{2} (F_1^{(0)} + 1 F_2^{(0)}), \quad (1)$$

$$G_2^{(0)} = \frac{1}{2} (1 F_1^{(0)} - F_2^{(0)}), \quad (2)$$

$$G_3^{(0)} = -\frac{1}{4} (1+z) \frac{N'}{N} (F_1^{(0)} + 1 F_2^{(0)}), \quad (3)$$

$$H_1^{(0)} = -\frac{1}{2} (F_1^{(0)} - 1 F_2^{(0)}), \quad (4)$$

$$H_2^{(0)} = -\frac{1}{2} (1 F_1^{(0)} + F_2^{(0)}) \quad (5)$$

and

$$H_3^{(0)} = -\frac{1}{4} (1+z) \frac{N'}{N} (F_1^{(0)} - 1 F_2^{(0)}) \quad (6)$$

where we have taken the $O(\epsilon^{-1} e^{-\omega_1 z})$ and $O(\epsilon^{-1} e^{-\omega_2 z})$ equations (451.1) and (452.1) into account.

The functional forms of the zeroth order outer variables $F_1^{(0)}$ and $F_2^{(0)}$ are given by equations (453.21-22). Thus we may now construct a zeroth order composite solution from the truncated Latta expansion (44.1) that is uniformly valid from the bed to the surface.

459. We next look at the first order outer system of equations of motion and boundary conditions for information about the first order outer and inner flow variables. If we assume that the first order perturbation of the surface elevation has a time dependency which is similar to that of the basic state, i.e.

$$\eta^{(1)} = \text{Re} \left\{ A^{(1)} e^{it} \right\}, \quad (1)$$

then the first order outer flow variables may be expressed as

$$r_j^{(1)} = \text{Re} \left\{ F_j^{(1)} e^{it} \right\}, \quad j = 1, 2, 3, \quad (2)$$

where $A^{(1)}$ and $F_j^{(1)}$ are independent of time.

The $O(\epsilon)$ momentum equations are given by

$$i \delta F_1^{(1)} - F_2^{(1)} = -\frac{1}{\alpha} A_x^{(1)} \quad (3)$$

and

$$i \delta F_2^{(1)} + F_1^{(1)} = -\frac{1}{\alpha} A_y^{(1)}. \quad (4)$$

Clearly $F_1^{(1)}$ and $F_2^{(1)}$ are independent of z .

By taking the $O(\epsilon)$ surface and bed conditions, (c.f. §453), together with the $O(\epsilon^0 e^{-\omega_1 z})$ etc. continuity equations (454.3) and (455.3.) into account, the continuity equation for this system may be expressed in the form

$$F_{1,x}^{(1)} + F_{2,y}^{(1)} + i k_0 A^{(1)} = -\hat{E} A^{(0)}. \quad (5)$$

Here the linear dissipation operator \hat{E} is given by

$$\hat{E} = k^2 \nu_1 - \nu_1' \frac{\partial}{\partial x} - i \nu_2' \frac{\partial}{\partial y}, \quad (6)$$

γ_1 and γ_2 are functions of x which are defined by

$$\gamma_1 = \frac{1\alpha}{2K^2} \left(\frac{\delta-1}{\omega_1} + \frac{\delta+1}{\omega_2} \right) \quad (7)$$

and

$$\gamma_2 = \frac{1\alpha}{2K^2} \left(\frac{\delta-1}{\omega_1} - \frac{\delta+1}{\omega_2} \right) \quad (8)$$

and the derivatives γ_1' and γ_2' are such that

$$\gamma_1' = \gamma_1 N' / 2N \quad (9)$$

and

$$\gamma_2' = \gamma_2 N' / 2N. \quad (10)$$

The kinematic boundary conditions may be written as

$$\frac{\partial^n F_2^{(1)}}{\partial x^n} = 0, \quad n = 0, 1, \dots, \text{ at } y = 0, \pi \quad (11)$$

and

$$\frac{\partial^n F_1^{(1)}}{\partial y^n} = 0, \quad n = 0, 1, \dots, \text{ at } x = 0. \quad (12)$$

After some manipulation equations (3 - 5) yield

$$\hat{H} A^{(1)} = \frac{1K^2}{K_0} \hat{E} A^{(0)}, \quad (13)$$

$$F_1^{(1)} = \frac{\alpha}{K^2} (1 \delta A_x^{(1)} + A_y^{(1)}) \quad (14)$$

and

$$F_2^{(1)} = \frac{\alpha}{K^2} (1 \delta A_y^{(1)} - A_x^{(1)}) \quad (15)$$

where \hat{H} denotes the Helmholtz operator ($\nabla^2 + K^2$). It follows

that $F_2^{(1)}$ satisfies the inhomogeneous Helmholtz equation

$$\hat{H} F_2^{(1)} = p(x,y) \quad (16)$$

where the function $p(x,y)$ is given by

$$p(x,y) = \frac{1}{\delta} (1 \delta \frac{\partial}{\partial y} - \frac{\partial}{\partial x}) \hat{E} A^{(0)}. \quad (17)$$

The kinematic boundary condition for the first order outer longitudinal component of velocity, equation (12), may be expressed as a mixed derivative condition for the transverse component. This form of expression is

$$F_{2,xy}^{(1)} + 1 \ll k_0 F_2^{(1)} = q(y) \quad \text{at } x = 0 \quad (18)$$

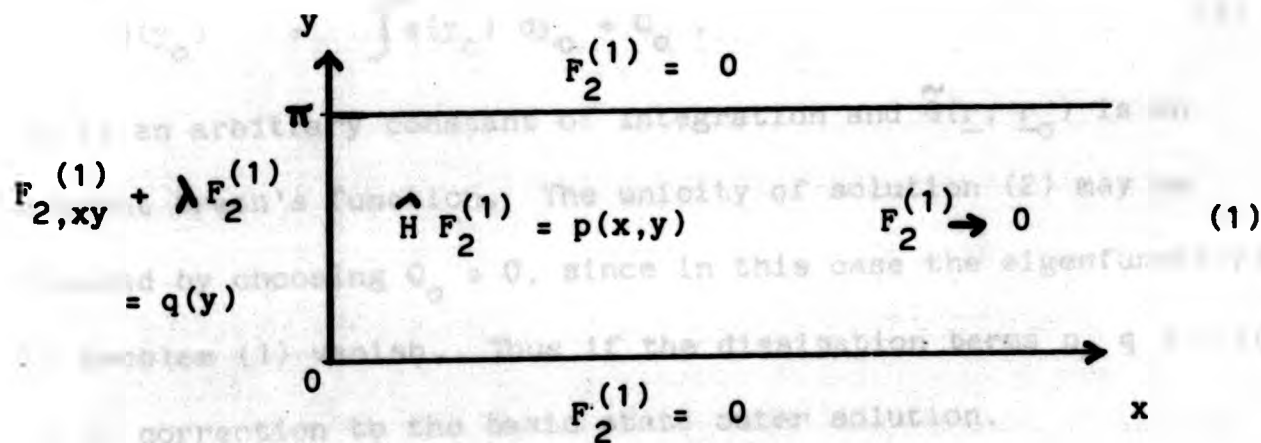
where

$$q(y) = \frac{-1}{\xi} \frac{\partial}{\partial y} [\hat{E} A^{(0)}]_{x=0} \quad (19)$$

Following Brown (1978), we shall assume that frictional effects at the mouth of the channel are negligible in comparison with those at the head, i.e. $\lim_{x \rightarrow \infty} N(x) = 0$. The inhomogeneous term $p(x,y)$ of equation (16) will become vanishingly small and the first order outer solution will tend to the same form as the zeroth order outer solution at far upchannel regions. Thus we obtain the condition

$$\lim_{x \rightarrow \infty} F_2^{(1)}(x,y) = 0 \quad (20)$$

4510. The $O(\epsilon)$ equations (459.11, 16, 18 and 20) pose a boundary value problem for the first order outer transverse current that may be diagrammatically represented as:



where we have introduced $\lambda = 1 \ll k_0$.

We note that the field equation of problem (1) is an elliptic

equation and the mixed derivative condition on $x = 0$ is of a non-Dirichlet, non-Neumann and non-Robin type, i.e. neither the dependent variable, nor the normal derivative, nor a linear combination of these are specified at the transverse barrier. Such a problem is, in general, ill-posed and no unique solution exists, (Williams, 1980; Morse and Feshbach, 1953). However, in this particular case we are able to show that a unique solution does exist, (c.f. Brown, 1978).

The solution to the inhomogeneous problem (1) for the first order outer transverse velocity component is obtained by an adaptation of the method of Green's functions, (see appendix 2). It may be written as

$$F_2^{(1)}(\underline{r}) = \int_{y_0=0}^{\pi} \int_{x_0=0}^{\infty} p(\underline{r}_0) \tilde{G}(\underline{r}; \underline{r}_0) d\underline{r}_0 + \int_{y_0=0}^{\pi} Q(y_0) \tilde{G}(\underline{r}; \underline{r}_0) \Big|_{x_0=0} dy_0 \quad (2)$$

where $\underline{r} = (x, y)$ and $\underline{r}_0 = (x_0, y_0)$ represent field and source variables, respectively, $Q(y_0)$ is the indefinite integral

$$Q(y_0) = \int q(y_0) dy_0 + Q_0, \quad (3)$$

Q_0 is an arbitrary constant of integration and $\tilde{G}(\underline{r}; \underline{r}_0)$ is an adjoint Green's function. The unicity of solution (2) may be ensured by choosing $Q_0 = 0$, since in this case the eigenfunctions of problem (1) vanish. Thus if the dissipation terms $p, q = 0$ there is no correction to the basic state outer solution.

The expression for the adjoint Green's function is given by

$$\begin{aligned} \tilde{G}(\underline{r}; \underline{r}_0) = & \sum_{r=1}^{\infty} \left\{ \frac{\epsilon_r}{s_r} \sin(ry) \sin(ry_0) [\exp(-s_r |x-x_0|) \right. \\ & - \exp(-s_r (x+x_0))] \\ & \left. + a_r(x,y) \exp(-s_r x_0) \sin(ry_0) \right\}. \end{aligned} \quad (4)$$

The adjoint Green's function coefficients $a_r(x,y)$ are generated by the recurrence relations

$$\lambda \sum_{n=1}^{\infty} \alpha_{rn} a_n - s_r a_r = -2\epsilon_r \sin(ry) \exp(-s_r x), \quad r = 1, 2, \dots, \quad (5)$$

where the coefficients α_{rn} are given by

$$\alpha_{rn} = \begin{cases} 0, & r+n \text{ even}, \\ 4r/(\pi n(r^2 - n^2)), & r+n \text{ odd} \end{cases} \quad (6)$$

for integer values of r and n , ϵ_r is a constant and

$$s_r = (r^2 - k^2)^{1/2}, \quad r=1, 2, \dots \quad (7)$$

The y -derivative of the transverse current is given by

$$\begin{aligned} F_{2,y}^{(1)}(\underline{r}) = & \int_{y_0=0}^{\pi} \int_{x_0=0}^{\infty} p(\underline{r}_0) \tilde{G}_y(\underline{r}; \underline{r}_0) dr_0 \\ & + \int_{y_0=0}^{\pi} Q(y_0) \tilde{G}_y(\underline{r}; \underline{r}_0) \Big|_{x_0=0} dy_0 \end{aligned} \quad (8)$$

where the y -derivative of the adjoint Green's function has the form

$$\begin{aligned} \tilde{G}_y(\underline{r}; \underline{r}_0) = & \sum_{r=1}^{\infty} \left\{ \frac{r\epsilon_r}{s_r} \cos(ry) \sin(ry_0) [\exp(-s_r |x-x_0|) \right. \\ & - \exp(-s_r (x+x_0))] \\ & \left. + \partial a_r(x,y)/\partial y \sin(ry_0) \exp(-s_r x_0) \right\} \end{aligned} \quad (9)$$

and the recurrence relations for the coefficients $\partial a_r/\partial y$ are

$$\lambda \sum_{n=1}^{\infty} \alpha_{rn} \partial a_n/\partial y - s_r \partial a_r/\partial y = -2r\epsilon_r \cos(ry) \exp(-s_r x), \quad r = 1, 2, \dots \quad (10)$$

The x-derivative of the transverse current is

$$F_{2,x}^{(1)}(\underline{r}) = \int_{y_0=0}^{\pi} \int_{x_0=0}^{\infty} p(\underline{r}_0) \tilde{G}_x(\underline{r}; \underline{r}_0) d\underline{r}_0 + \int_{y_0=0}^{\pi} q(y_0) \tilde{G}_x(\underline{r}; \underline{r}_0) \Big|_{x_0=0} dy_0 \quad (11)$$

where the x-derivative of the adjoint Green's function is given by the expression

$$\tilde{G}_x(\underline{r}; \underline{r}_0) = \sum_{r=1}^{\infty} \left\{ d_0 \epsilon_r \sin(ry) \sin(ry_0) \times [\exp(d_0 s_r (x-x_0)) + d_0 \exp(-s_r (x+x_0))] + \partial a_r(x,y) / \partial x \sin(ry_0) \exp(-s_r x_0) \right\}, \quad (12)$$

in which $d_0 = \text{sgn}(x_0 - x)$ and the recurrence relations for the coefficients $\partial a_r / \partial x$ are

$$\lambda \sum_{n=1}^{\infty} \alpha_{rn} \partial a_n / \partial x - s_r \partial a_r / \partial x = 2 \epsilon_r s_r \sin(ry) \exp(-s_r x), \quad r = 1, 2, \dots \quad (13)$$

4511. The $O(\epsilon)$ surface elevation $A^{(1)}$ is found from the second order equation

$$A_{xx}^{(1)} + k_0^2 A^{(1)} = \mathcal{E}(x,y) \quad (1)$$

where

$$\mathcal{E}(x,y) = i k_0 \left(\frac{-1}{8} F_{2,x}^{(1)} + F_{2,y}^{(1)} + \hat{E} A^{(0)} \right). \quad (2)$$

Equation (1) may be obtained by differentiating equation (459.3) with respect to x and eliminating $F_{1,x}^{(1)}$ from equation (459.5).

The method of variation of parameters may be used to solve equation (1). The solution may be written as

$$A^{(1)}(x,y) = \mathcal{E}_1(x,y) e^{ik_0 x} + \mathcal{E}_2(x,y) e^{-ik_0 x} \quad (3)$$

where

$$\mathcal{L}_1(x,y) = \frac{1}{2k_0} \int_x^\infty \mathcal{L} e^{-ik_0 x} dx + \mathcal{L}_1(\infty, y) \quad (4)$$

and

$$\mathcal{L}_2(x,y) = \frac{-1}{2k_0} \int_x^\infty \mathcal{L} e^{ik_0 x} dx + \mathcal{L}_2(\infty, y). \quad (5)$$

The derivative with respect to x is given by

$$A_x^{(1)}(x,y) = ik_0 (\mathcal{L}_1 e^{ik_0 x} - \mathcal{L}_2 e^{-ik_0 x}). \quad (6)$$

The relation

$$F_1^{(1)} = \frac{1}{k_0} (A_x^{(1)} - F_2^{(1)}) \quad (7)$$

follows from equation (459.4). It may be used to obtain the first order outer longitudinal current.

The functions $\mathcal{L}_1(\infty, y)$ and $\mathcal{L}_2(\infty, y)$ are specified by a radiation condition. A convenient form of radiation condition involves the assumption that the first order amplitude tends to a Kelvin wave solution at infinity, i.e.

$$\lim_{x \rightarrow \infty} A^{(1)} = \beta_1 \exp(ik_0 x + \alpha y) + \beta_2 \exp(-ik_0 x - \alpha y) \quad (8)$$

where β_1 and β_2 are complex constants. The kinematic boundary condition at the transverse barrier, i.e. $F_1^{(1)} = 0$ at $x = 0$, is used to determine β_1 and β_2 .^(*)

4512. The second order inner system produces information about the z dependency of the first order inner variables. The terms that are proportional to e^{it} of the $O(\epsilon^2 e^{-\omega_1 z})$ momentum equations yield the matrix relation

$$\begin{bmatrix} -1 & -1 \\ 1 & -1 \end{bmatrix} \begin{bmatrix} G_{1,1}^{(2)} \\ G_{2,1}^{(2)} \end{bmatrix} = \omega_1 (G_{1,0}^{(1)} F + G_{1,2}^{(1)} \bar{F} - 2N \frac{\partial}{\partial z} G_{1,1}^{(1)}) \begin{bmatrix} 1 \\ -1 \end{bmatrix} \quad (1)$$

(*) The usual radiation condition demands that β_1 is prescribed, (Stoker, 1957). Here β_1 is implicitly determined by the Green's function solution for $F_2^{(1)}$, equation (4510.2).

where $G_{1,1}^{(2)}$ and $G_{2,1}^{(2)}$ are the time independent parts of the M_2 constituents of the second order inner velocity

$$g_j^{(2)} = \sum_{n=0}^{\infty} G_{j,n}^{(2)}(x,y,z) e^{int}, \quad j = 1, 2, 3.$$

The existence of solutions to equation (1) implies that the particular integral terms vanish, whence we obtain

$$\frac{\partial}{\partial z} (G_{1,1}^{(1)}) = \frac{1}{2N} (G_{1,0}^{(1)} F + G_{1,2}^{(1)} \bar{F}). \quad (2)$$

It then follows from equations (456.8, 12 and 14) that

$$\frac{\partial}{\partial z} (G_{j,1}^{(1)}) = 0, \quad j = 1, 2, \quad (3)$$

i.e. the first order inner variables $G_{1,1}^{(1)}$ and $G_{2,1}^{(1)}$ are independent of z .

A similar analysis of the $O(\epsilon^2 e^{-\omega_1 z})$ system shows that the first order inner variables $H_{1,1}^{(1)}$ and $H_{2,1}^{(1)}$ are also independent of z , i.e.

$$\frac{\partial}{\partial z} (H_{j,1}^{(1)}) = 0, \quad j = 1, 2. \quad (4)$$

Thus the $O(\epsilon)$ bed condition applies throughout the water column in the case of the first order horizontal components of velocity, i.e.

$$F_j^{(1)} + G_{j,1}^{(1)} + H_{j,1}^{(1)} = 0, \quad j = 1, 2. \quad (5)$$

We may now recall equations (456.12), (457.5) and the $O(\epsilon^0 e^{-\omega_1 z})$ etc. continuity equations (454.3) and (455.3) and write expressions for $G_{j,1}^{(1)}$ and $H_{j,1}^{(1)}$, $j = 1, 2, 3$, in terms of the first order outer variables and zero order inner and outer variables. For clarity we list the expressions for all the $G_{j,n}^{(1)}$ and $H_{j,n}^{(1)}$, $j = 1, 2, 3$. These expressions are:

$$G_{1,0}^{(1)} = \frac{1 \omega_1}{6} F G_1^{(0)}, \quad (6)$$

$$G_{2,0}^{(1)} = \frac{\omega_1}{6} F G_1^{(0)}, \quad (7)$$

$$G_{3,0}^{(1)} = \frac{1 \omega_1}{2 \delta} (1+z) \frac{N'}{N} F G_1^{(0)}, \quad (8)$$

$$G_{1,1}^{(1)} = -\frac{1}{2} (F_1^{(1)} + 1 F_2^{(1)}), \quad (9)$$

$$G_{2,1}^{(1)} = \frac{1}{2} (1 F_1^{(1)} - F_2^{(1)}), \quad (10)$$

$$G_{3,1}^{(1)} = \frac{1}{\omega_1} (G_{1,x}^{(0)} + G_{2,y}^{(0)} + G_{3,z}^{(0)}) \\ - \frac{1}{4} (1+z) \frac{N'}{N} (F_1^{(1)} + 1 F_2^{(1)}), \quad (11)$$

$$G_{1,2}^{(1)} = \frac{-1 \omega_1}{6} F G_1^{(0)}, \quad (12)$$

$$G_{2,2}^{(1)} = \frac{-\omega_1}{6} F G_1^{(0)}, \quad (13)$$

$$G_{3,2}^{(1)} = \frac{-1 \omega_1}{2 \delta} (1+z) \frac{N'}{N} F G_1^{(0)}, \quad (14)$$

$$H_{1,0}^{(1)} = \frac{1 \omega_2}{6} F H_1^{(0)}, \quad (15)$$

$$H_{2,0}^{(1)} = \frac{-\omega_2}{6} F H_1^{(0)}, \quad (16)$$

$$H_{3,0}^{(1)} = \frac{1 \omega_2}{2 \delta} (1+z) \frac{N'}{N} F H_1^{(0)}, \quad (17)$$

$$H_{1,1}^{(1)} = -\frac{1}{2} (F_1^{(1)} - 1 F_2^{(1)}), \quad (18)$$

$$H_{2,1}^{(1)} = -\frac{1}{2} (1 F_1^{(1)} + F_2^{(1)}), \quad (19)$$

$$H_{3,1}^{(1)} = \frac{1}{\omega_2} (H_{1,x}^{(0)} + H_{2,y}^{(0)} + H_{3,z}^{(0)}) \\ - \frac{1}{4} (1+z) \frac{N'}{N} (F_1^{(1)} - 1 F_2^{(1)}), \quad (20)$$

$$H_{1,2}^{(1)} = \frac{-1 \omega_2}{6} F H_1^{(0)}, \quad (21)$$

$$H_{2,2}^{(1)} = \frac{\omega_2}{\xi} F H_1^{(0)} \quad (22)$$

and

$$H_{3,2}^{(1)} = \frac{-i\omega_2}{2\xi} (1+z) \frac{N}{N'} F H_1^{(0)} \quad (23)$$

4513. The perturbation expansions which are correct to first order for the amplitude and the current components, equations (44.5 and 1), are given by the real parts of

$$\eta = (A^{(0)} + \epsilon A^{(1)}) e^{it} \quad (1)$$

and

$$\begin{aligned} u_j = & (F_j^{(0)} + e^{-\omega_1 Z} G_j^{(0)} + e^{-\omega_2 Z} H_j^{(0)}) e^{it} \\ & + \epsilon \left\{ e^{-\omega_1 Z} G_{j,0}^{(1)} + e^{-\omega_2 Z} H_{j,0}^{(1)} \right. \\ & + (F_j^{(1)} + e^{-\omega_1 Z} G_{j,1}^{(1)} + e^{-\omega_2 Z} H_{j,1}^{(1)}) e^{it} \\ & \left. + (e^{-\omega_1 Z} G_{j,2}^{(1)} + e^{-\omega_2 Z} H_{j,2}^{(1)}) e^{2it} \right\}, \\ & j = 1, 2, 3. \quad (2) \end{aligned}$$

The results of §§ 453, 458, 4510, 4511 and 4512 provide analytic expressions for each of the terms in equations (1) and (2). The characteristic depth may be estimated at any historical time of interest from the data of Nio (1976). The remaining system parameters are obtained from the relations of § 41. Thus the flow regime is specified in three dimensions x , y and z , at any local time t and for any historical time T .

$$46. \quad \underline{E_k} = O(R_0^{\frac{1}{2}}).$$

We now consider the case (2) formulation of § 44 for a flow regime in which dissipational effects are an order of magnitude greater than non-linear effects. The relations

$\epsilon^4 = R_0 = E_k^2$ and $Z = \frac{1+z}{|\epsilon|}$ are assumed to apply.

The expanded field equations (42.7-9) and boundary conditions (43.2-6) generate systems of equations and relations that are analogous to those of § 45 where $E_k = O(R_0)$. No contribution from the non-linear terms of the momentum equations (42.7-8) occurs until the third order inner system is considered. Thus zeroth and first order inner and outer variables contain no steady or quarter-diurnal components. The constituent of the $E_k = O(R_0)$ system that is governed by the harmonic time factor e^{it} is identical to that of the $E_k = O(R_0^{\frac{1}{2}})$ system up to the first order.

The solution, which is correct to first order, is given by the real parts of

$$\eta = (A^{(0)} + \epsilon A^{(1)}) e^{it} \quad (1)$$

and

$$u_j = \left(F_j^{(0)} + e^{-\omega_1 Z} G_j^{(0)} + e^{-\omega_2 Z} H_j^{(0)} + \epsilon (F_j^{(1)} + e^{-\omega_1 Z} G_{j,1}^{(1)} + e^{-\omega_2 Z} H_{j,1}^{(1)}) \right) e^{it} \quad (2)$$

where the functional forms of the zeroth and first order inner and outer variables and boundary layer functions are the same as in § 45.

$$47. \quad \underline{E_k} = \underline{\Phi}(T) + O(R_0).$$

In the formulation of case (3), § 44, the order of magnitude of the frictional terms in the momentum equations (42.7-8) is permitted to vary from $O(R_0)$ at 0 BP to $O(1)$ at 8300 BP by a suitable choice of the historical time dependent function $\underline{\Phi}(T)$. The relationship between the eddy viscosity, Ekman and Rossby

numbers is taken to be such that

$$E_k N(x) u_{j,zz} = -\delta \sigma_0(T) u_j + \epsilon^2 N(x) u_{j,zz} ,$$

$$j = 1, 2, \quad (1)$$

where $\epsilon = R_0^{\frac{1}{2}}$ and $\sigma_0(T)$ is a dimensionless frictional parameter.

This parameterization enables us to express the momentum equations (42.7-8) in the form

$$\delta \left(\frac{\partial}{\partial t} + \sigma_0 \right) u + \epsilon^2 (uu_x + vu_y + wu_z)$$

$$= v - \frac{1}{\alpha} \eta_x + \epsilon^2 N u_{zz} \quad (2)$$

and

$$\delta \left(\frac{\partial}{\partial t} + \sigma_0 \right) v + \epsilon^2 (uv_x + vv_y + wv_z)$$

$$= -u - \frac{1}{\alpha} \eta_y + \epsilon^2 N v_{zz} . \quad (3)$$

The perturbation expansions (44.1-5) are substituted into the momentum equations (1) and (2), the continuity equation (42.9) and the boundary conditions (43.2-6). The $O(\epsilon^n)$, $O(\epsilon^n e^{-\omega_1 Z})$ and $O(\epsilon^n e^{-\omega_2 Z})$, $n = -1, 0, 1, \dots$, systems are separated out. The time dependence is similar to that of § 45, namely, for $j = 1, 2, 3$,

$$f_j^{(0)} = \text{Re} \left\{ F_j^{(0)} e^{it} \right\} ,$$

$$\eta^{(0)} = \text{Re} \left\{ A^{(0)} e^{it} \right\} ,$$

$$g_j^{(0)} = G_j^{(0)} e^{it} ,$$

$$h_j^{(0)} = H_j^{(0)} e^{it} ,$$

$$f_j^{(1)} = \text{Re} \left\{ F_j^{(1)} e^{it} \right\} ,$$

$$g_j^{(1)} = \sum_{n=0}^{\infty} G_{j,n}^{(1)} e^{it}$$

and

$$h_j^{(1)} = \sum_{n=0}^{\infty} H_{j,n}^{(1)} e^{it}.$$

471. The zeroth order outer system field equations may be written as

$$(\nabla^2 + k^2) A^{(0)} = 0, \quad (1)$$

$$F_1^{(0)} = \frac{1}{k^2 \beta_0} k_0 [\beta_0 A_x^{(0)} + A_y^{(0)}] \quad (2)$$

and

$$F_2^{(0)} = \frac{1}{k^2 \beta_0} k_0 [-A_x^{(0)} + \beta_0 A_y^{(0)}] \quad (3)$$

where we have introduced the dimensionless parameters

$$\beta_0 = \delta (\gamma_0 + 1) \quad (4)$$

and

$$k^2 = \frac{-i \alpha k_0}{\beta_0} (1 + \beta_0^2). \quad (5)$$

The kinematic boundary conditions are that

$$F_1^{(0)} = 0 \quad \text{at } x = 0 \quad (6)$$

and

$$F_2^{(0)} = 0 \quad \text{at } y = 0, \pi. \quad (7)$$

Following Reinecker and Teubner (1980), the solution to equation (1) that is subject to the boundary conditions (6 - 7) is given by

$$A^{(0)} = \exp(-i K_0 x + \alpha_0 y) + G_0 \exp(i K_0 x - \alpha_0 y) + \sum_{n=1}^{\infty} G_n \frac{e^{i K_n x}}{\beta_0 \alpha_n - i K_n} [\beta_0 \alpha_n \cos(ny) - K_n \sin(ny)] \quad (8)$$

where

$$K_0 = (-i \alpha k_0 \beta_0)^{\frac{1}{2}}, \quad (9)$$

$$\alpha_0 = -i K_0 / \beta_0, \quad (10)$$

$$\alpha_n = i n, \quad (11)$$

$$K_n = (\alpha_n^2 + k^2)^{\frac{1}{2}}, \quad (12)$$

$$\operatorname{Re}(K_n) \leq 0 \quad (13)$$

and

$$\operatorname{Im}(K_n) > 0. \quad (14)$$

The coefficients G_n , $n = 0, 1, \dots, N$, may be determined by using the method of collocation. The first $(N+1)$ coefficients are the solutions of the set of $(N+1)$ simultaneous linear equations

$$\begin{aligned} \alpha_0 G_0 e^{-\alpha_0 y_m} - \sum_{n=1}^N G_n \frac{i K_n \alpha_n}{\beta_0 \alpha_n - i K_n} [\cos(ny_m) - \phi_n \sin(ny_m)] \\ = \alpha_0 e^{\alpha_0 y_m}, \quad m = 0, 1, \dots, N \end{aligned} \quad (15)$$

where

$$\phi_n = \frac{-i \alpha_0 k_0}{\alpha_n K_n} \quad (16)$$

and

$$y_m = \frac{m\pi}{N}, \quad m = 0, 1, \dots, N. \quad (17)$$

The $O(\epsilon)$ components of velocity may be expressed as

$$\begin{aligned} F_1^{(0)} &= \frac{i K_0}{\alpha_0 \beta_0} [\exp(-i K_0 x + \alpha_0 y) - G_0 \exp(i K_0 x - \alpha_0 y)] \\ &+ \frac{1}{\alpha_0} \sum_{n=1}^N G_n \frac{e^{i K_n x}}{\beta_0 \alpha_n - i K_n} [\alpha_0 k_0 \sin(ny) + n K_n \cos(ny)], \end{aligned} \quad (18)$$

$$F_2^{(0)} = \frac{-1}{\alpha_0 \beta_0} \sum_{n=1}^N G_n \frac{i \beta_0 \alpha_n^2 + \alpha_0 k_0}{\beta_0 \alpha_n - i K_n} e^{i K_n x} \sin(ny) \quad (19)$$

and

$$F_3^{(0)} = i k_0 (1+z) A^{(0)}. \quad (20)$$

472. The zeroth order inner system momentum equations yield expressions for the boundary layer functions ω_1 and ω_2 . These expressions are

$$\omega_1 = \left(\frac{P_0 + 1}{N}\right)^{\frac{1}{2}} \quad (1)$$

and

$$\omega_2 = \left(\frac{P_0 - 1}{N}\right)^{\frac{1}{2}}. \quad (2)$$

We note that ω_1 and ω_2 satisfy the relation

$$\frac{\omega_1'}{\omega_1} = \frac{\omega_2'}{\omega_2} = \frac{-N'}{2N}. \quad (3)$$

473. The first order outer system of equations reduces to

$$(\nabla^2 + k^2) A^{(1)} = \frac{1}{k_0} \hat{E} A^{(0)}, \quad (1)$$

$$F_1^{(1)} = \frac{1}{P_0 k^2} (P_0 A_x^{(1)} + A_y^{(1)}), \quad (2)$$

$$F_2^{(1)} = \frac{1}{P_0 k^2} (P_0 A_y^{(1)} - A_x^{(1)}), \quad (3)$$

$$F_1^{(1)} = 0 \quad \text{at } x = 0, \quad (4)$$

and

$$F_2^{(1)} = 0 \quad \text{at } y = 0, \pi, \quad (5)$$

where the dissipative term $E A^{(0)}$ has the form

$$\hat{E} A^{(0)} = \left(\gamma_1 k^2 - \gamma_1' \frac{\partial}{\partial x} - \gamma_2' \frac{\partial}{\partial y}\right) A^{(0)} \quad (6)$$

and the x dependent parameters γ_1 , γ_2 and the derivatives are related to the boundary layer functions ω_1 , ω_2 and the eddy viscosity N by the expressions

$$\gamma_1 = \frac{k_0}{2k^2 P_0} \left(\frac{1}{\omega_1} \frac{\partial \omega_1}{\partial x} + \frac{1}{\omega_2} \frac{\partial \omega_2}{\partial x}\right), \quad (7)$$

$$\gamma_2 = \frac{k_0}{2k^2 P_0} \left(\frac{1}{\omega_1} \frac{\partial \omega_1}{\partial y} - \frac{1}{\omega_2} \frac{\partial \omega_2}{\partial y}\right), \quad (8)$$

$$\gamma'_1 = N' \gamma_1 / 2N \quad (9)$$

and

$$\gamma'_2 = N' \gamma_2 / 2N. \quad (10)$$

The boundary value problem for $F_2^{(1)}$ is of a similar shape to that of § 459, namely,

$$(\nabla^2 + k^2) F_2^{(1)} = p(x,y), \quad (11)$$

$$F_{2,xy}^{(1)} + \lambda F_2^{(1)} = q(y) \quad \text{at } x = 0, \quad (12)$$

$$F_2^{(1)} = 0 \quad \text{at } y = 0, \pi \quad (13)$$

and

$$\lim_{x \rightarrow \infty} F_2^{(1)} = 0, \quad (14)$$

where

$$p(x,y) = \frac{-1}{\beta_0} \left(\beta_0 \frac{\partial}{\partial y} - \frac{\partial}{\partial x} \right) \widehat{E} A^{(0)}, \quad (15)$$

$$q(y) = \frac{1}{\beta_0} \frac{\partial}{\partial y} (\widehat{E} A^{(0)})_{x=0} \quad (16)$$

and

$$\lambda = i \alpha k_0. \quad (17)$$

The solution is given by the integral expression

$$F_2^{(1)}(\underline{r}) = \int_{y_0=0}^{\pi} \int_{x_0=0}^{\infty} p(\underline{r}_0) \widetilde{G}(\underline{r}; \underline{r}_0) d \underline{r}_0 + \int_{y_0=0}^{\pi} Q(y_0) \widetilde{G}(\underline{r}; \underline{r}_0) \Big|_{x_0=0} d y_0 \quad (18)$$

where

$$Q(y_0) = \int q(y_0) d y_0 \quad (19)$$

and the adjoint Green's function \widetilde{G} is similar to that given in

§ 4510, K being replaced by k .

The first order amplitude is found from the governing equation

$$(\partial_{xx}^2 + k_1^2) A^{(1)} = e(x,y) \quad (20)$$

where

$$k_1 = (-i \alpha k_0 \beta_0)^{\frac{1}{2}} \quad (21)$$

and

$$\mathcal{L}(x,y) = \alpha \beta_0 \left[-\frac{1}{\beta_0} F_{2,x}^{(1)} + F_{2,y}^{(1)} + \hat{E} A^{(0)} \right]. \quad (22)$$

We obtain the solution

$$A^{(1)} = \mathcal{L}_1(x,y) e^{i k_1 x} + \mathcal{L}_2(x,y) e^{-i k_1 x} \quad (23)$$

in which

$$\mathcal{L}_1(x,y) = \frac{1}{2k_1} \int_x^\infty \mathcal{L} e^{-i k_1 x} dx + \mathcal{L}_1(\infty, y) \quad (24)$$

and

$$\mathcal{L}_2(x,y) = \frac{-1}{2k_1} \int_x^\infty \mathcal{L} e^{i k_1 x} dx + \mathcal{L}_2(\infty, y). \quad (25)$$

The x-derivative of the first order amplitude is given by the expression

$$A_x^{(1)}(x,y) = i k_1 (\mathcal{L}_1 e^{i k_1 x} - \mathcal{L}_2 e^{-i k_1 x}). \quad (26)$$

The first order outer velocity is found from the $O(\epsilon)$ momentum equations. It may be written as

$$F_1^{(1)} = \frac{-1}{\alpha \beta_0} (A_x^{(1)} - \alpha F_2^{(1)}). \quad (27)$$

474. The zeroth and first order inner variables are related to the outer variables by expressions which are identical to those for the $E_k = O(R_0)$ system, i.e. equations (458.1-6) and (4512.6-23) where F is given by equation (456.5).

Thus the solution to first order is of the same form as that given by equations (4513.1-2). We may note that in the special case when $\tau_0 = 0$ (whence $\beta_0 = 1$, $k = K$ and $k_1 = k_0$) the solution is the same as that of § 45.

CHAPTER 5

ANALYSIS OF RESULTS

Velocity profiles and co-range line diagrams which are typical of a flow for which the basic state outer solution is similar to that of Taylor (1921) are obtained from the expressions of § 45. A functional form for the eddy viscosity $N(x)$ is prescribed.

51. Vertical current structure.

The z dependent basic state horizontal velocity components are given by the leading term of equation (4513.2) They may be written as

$$u(x,y,z,t) = \text{Re} \left\{ (F_1^{(0)} + \exp(-\omega_1 Z) G_1^{(0)} + \exp(-\omega_2 Z) H_1^{(0)}) e^{it} \right\} \quad (1)$$

and

$$v(x,y,z,t) = \text{Re} \left\{ (F_2^{(0)} + \exp(-\omega_1 Z) G_2^{(0)} + \exp(-\omega_2 Z) H_2^{(0)}) e^{it} \right\} \quad (2)$$

where we recall that the zeroth order outer and inner velocity components $F_j^{(0)}$, $G_j^{(0)}$ and $H_j^{(0)}$, $j = 1, 2$, are functions of x and y , the magnified boundary layer vertical coordinate $Z = (1+z)/|\epsilon|$ and the boundary layer functions ω_1 and ω_2 are functions of x .

In the case when the zeroth order outer solution is that of Taylor (1921), the functional forms of $F_j^{(0)}$, $G_j^{(0)}$ and $H_j^{(0)}$, $j = 1, 2$, are given by equations (453.21-22) and (458.1, 2, 4 and 5). The boundary layer functions $\omega_1(x)$ and $\omega_2(x)$ are given by equations (454.5) and (455.1).

We introduce an exponentially decaying function to represent the eddy viscosity $N(x)$, i.e.

$$N(x) = b_0 \exp(-2 c_0 x) \quad (3)$$

where b_0 and c_0 are real constants. Brown (1978) shows that such a formulation overestimates the frictional effects near the head of

the channel whilst underestimating them further upchannel. However, this modelling crudely produces the required effects at finite distances from the transverse barrier and it has the advantage of relative simplicity.

The parameter values $b_0 = -1$ and $c_0 = 1$ are chosen and the functions u and v are plotted against Z at successive quarter tidal periods in the region of the first amphidromic point in figure 5.1, (see appendix 3, program 1). The velocity profiles for the u and v components exhibit boundary layer thicknesses which rapidly decrease away from the channel head. The magnified boundary layer coordinate Z lies within the intervals $[0.0, 3.9]$ at 0 BP and $[0.0, 2.7]$ at 8300 BP, under the assumptions of § 41. The mid-channel boundary layer thickness, expressed as a fraction of the total depth, is estimated at various distances from the channel head and at different historical times in the following table:

Distance from head of channel	0.10	1.67	5.00
Boundary layer thickness at 0 BP	0.51	0.08	0.01
Boundary layer thickness at 8300 BP	0.74	0.11	0.02

We note that the use of a negative eddy viscosity generally presupposes a physical mechanism such that there is a transfer of momentum between fluid parcels in the direction of low to high velocity regions and an accentuation of the current differences. This has been found to give an improved account of the effects of meso-scale eddies, i.e. transient motions with relatively large velocities, such as occur in the Gulf Stream flow, (Krauss, 1978).

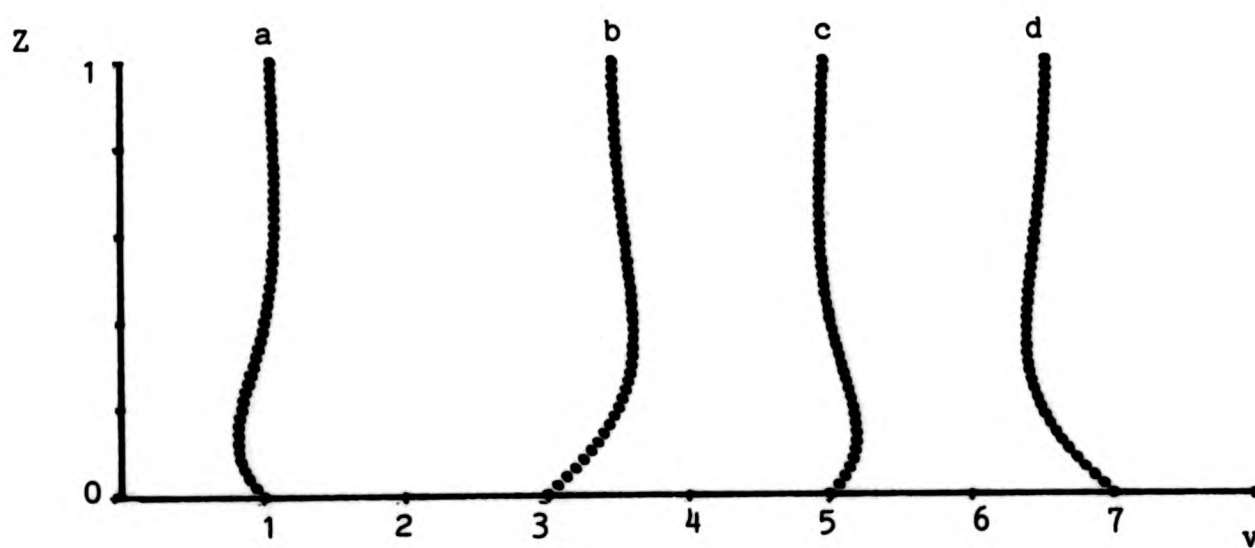
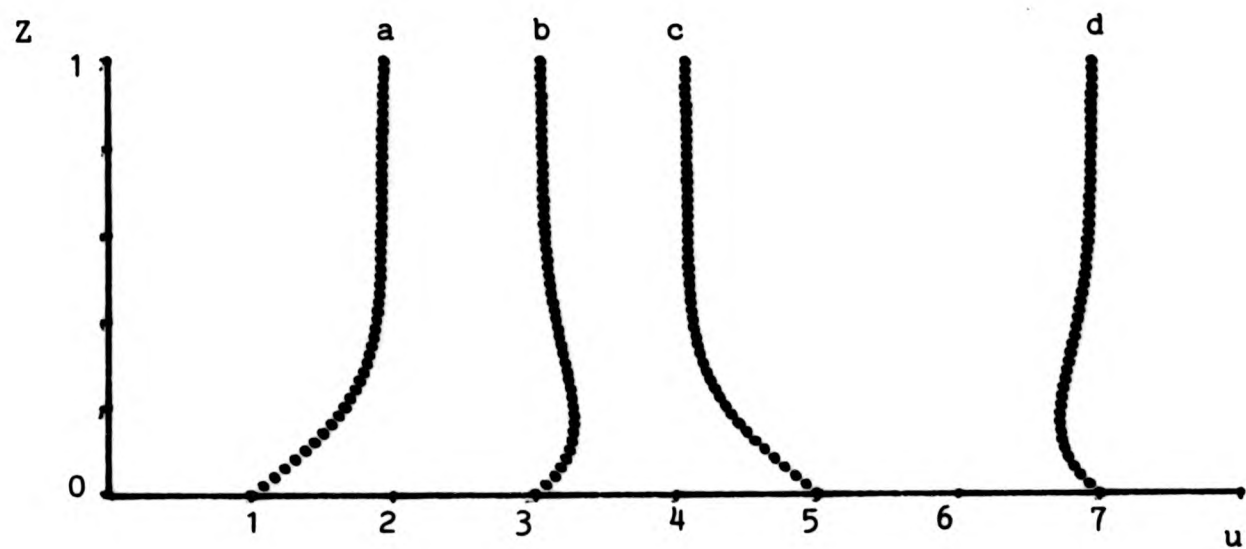


Figure 5.1

Relative velocity profiles for u and v at $x = 1.67$,
 $y = 1.57$, $Z \in [0,1]$ and (a) $t = 0$, (b) $t = 1.57$,
(c) $t = 3.14$, (d) $t = 4.71$.

However, within our modelling we consider complex functions of N for which the real parts are positive and the effect of $b_0 = -1$ when compared with $b_0 = 1$ only shows itself as a difference in the phase relation between the u and v velocity components.

The boundary layer thickness, as measured by the displacement thickness, varies as $|N|^{1/2}$. Thus the boundary layer may be extended throughout the depth by increasing the magnitude of the parameter b_0 . The rate at which the boundary layer thickness decreases with distance from the channel head may be diminished by decreasing the magnitude of the parameter c_0 .

52. First order outer corrections.

Approximations to the real and imaginary parts of the first order outer transverse velocity $F_2^{(1)}$ and its derivatives $F_{2,y}^{(1)}$ and $F_{2,x}^{(1)}$ are found by quadrature of equations (4510.2, 8 and 11). The following procedure may be adopted.

The first N Green's function coefficients and derivatives, a_n , $\partial a_n / \partial y$ and $\partial a_n / \partial x$, $n = 1, 2, \dots, N$, are obtained from the reduced forms of the matrix equations (4510.5, 10 and 13) which are separated into real and imaginary systems and are solved at a representative sample of field points, (see appendix 3, program 2). The field points of interest are taken at the intersections of a regular grid of $(N_x + 1)$ by $(N_y + 1)$ grid lines which covers the region $0 \leq x \leq 2\pi$, $0 \leq y \leq \pi$. The NAG library routines F01AAF and F04AAF may be used to perform the matrix inversions that are required and solve the systems of simultaneous linear equations that are generated.

The complex dissipation terms $p(r_0)$ and $Q(y_0)$, expressions for

which are obtained from equations (459.17 and 19), are evaluated at representative source points, (see appendix 3, program 3). It is convenient to allow the source and field points to coincide. The Taylor solution of § 453 is assumed to apply and the eddy viscosity is given by equation (51.3).

The integrands $p(\underline{r}_0) \tilde{G}(\underline{r}; \underline{r}_0)$ and $Q(y_0) \tilde{G}(\underline{r}; \underline{r}_0) \Big|_{x_0=0}$ are specified at the source points of interest. Space integration is performed by the repeated application of Simpson's rule. The real and imaginary parts of $F_2^{(1)}$ etc. are then evaluated at field points of interest, (see appendix 3, program 4).

The real and imaginary parts of the first order amplitude $A^{(1)}$ are found from equation (4511.3), (see appendix 3, program 5).

A surface fitting method is used to evaluate $F_{2,x}^{(1)}$, $F_{2,y}^{(1)}$ and $\hat{E} A^{(0)}$ at field points in between those specified. A suitable scheme is that of linear interpolation in which $f(x,y)$ is found by averaging the four neighbouring values at grid points (i,j) , $(i+1, j)$, $(i, j+1)$ and $(i+1, j+1)$, i.e.

$$f(x,y) = x_2 y_2 f(i,j) + x_1 y_1 f(i+1, j+1) \\ + x_1 y_2 f(i+1, j) + x_2 y_1 f(i, j+1),$$

where i and j are the rounded down integer values of $xN_x/2\pi$ and yN_y/π , respectively,

$$x_1 = xN_x/2\pi - i, \quad x_2 = 1 - x_1, \\ y_1 = yN_y/\pi - j \quad \text{and} \quad y_2 = 1 - y_1.$$

The function $\mathcal{L}(x,y)$ of equation (4511.2) is expressed in terms of these interpolated values. The functions $\mathcal{L}_1(x,y)$ and $\mathcal{L}_2(x,y)$ are determined by numerical quadrature of equations

(4511.4 and 5) and by choosing $\mathcal{L}_1(\infty, y)$ and $\mathcal{L}_2(\infty, y)$ so as to give the best fit with the form implied by the radiation condition, equation (4511.8).

The corrected amplitude $A = A^{(0)} + \epsilon A^{(1)}$ is determined and the co-range lines are produced by solving $|A| = \text{constant}$ for the values 0.2, 0.4, ..., 1.2. A sign change search procedure is used, (see appendix 3, program 6).

The magnitude of the parameter $\epsilon = \pm R_0^{\frac{1}{2}}$ varies between 0.25 at 0 BP and 0.37 at 8300 BP under the assumptions of § 41. Thus ϵ may be viewed as a measure of historical time.

We see from the co-range lines of figure 5.2 that the lateral displacement of the amphidromic points from the mid-channel axis follows the expected pattern as $|\epsilon|$ increases to 0.4, and the magnitude of the outgoing wave becomes increasingly less than that of the incoming wave. The parameter values for the eddy viscosity are taken as $b_0 = -0.0625$ and $c_0 = 1.0$ and the range of Rossby numbers are such that $\epsilon = 0.00, -0.20$ and -0.40 in figure 5.2. Since the magnitude of the first order elevation $A^{(1)}$ is proportional to $|N|^{\frac{1}{2}}$, an identical set of co-range lines may be obtained for different values of b_0 and ϵ which maintain the invariance of $b_0 \epsilon^2$, e.g. $b_0 = -1.0, \epsilon = 0.00, -0.05$ and -0.10 .

The similar lateral displacements of the first and second amphidromic points in figure 5.2 occurs because of the low level of frictional dissipation away from the head of the channel. The decreasing effects of friction may be reduced by decreasing the frictional parameter c_0 . In figures 5.3 and 5.4 the parameter value $c_0 = 0.1$ is used and the co-range lines show a marked

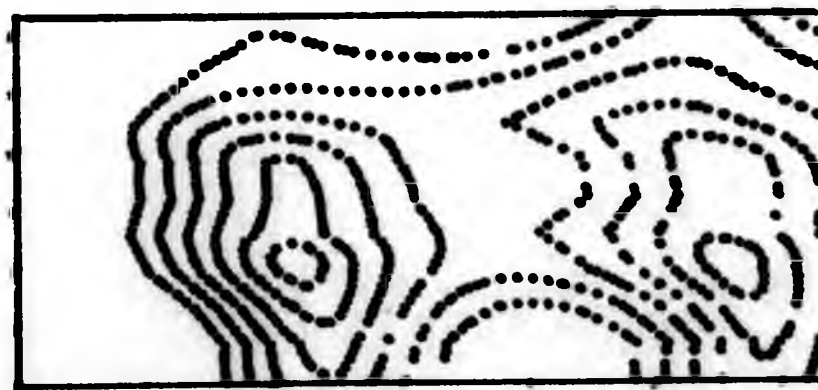
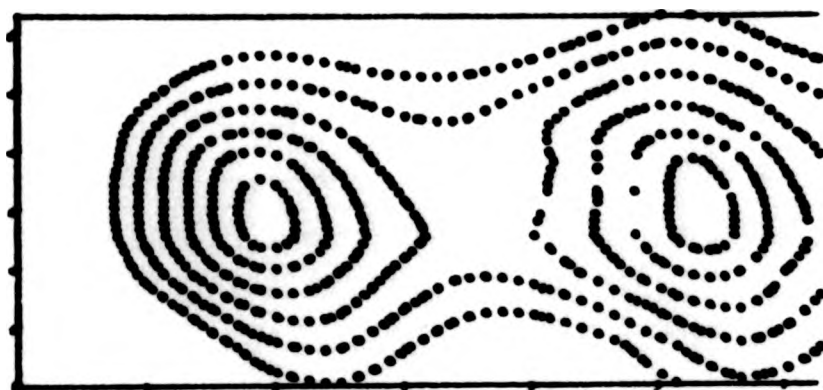
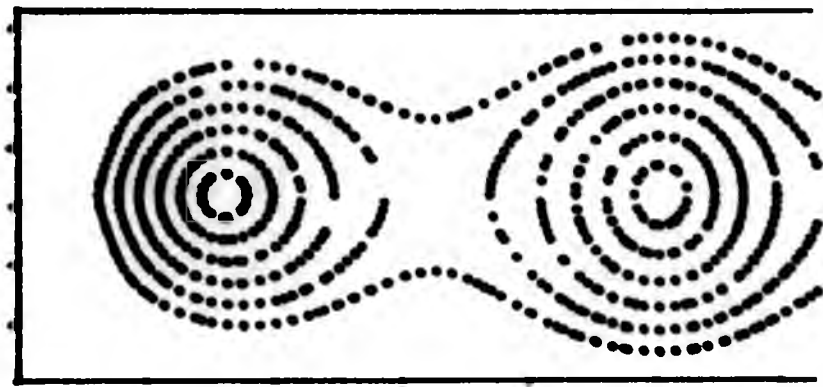


Figure 5.2

Co-range lines for $\nu_0 = -0.0625$, $c_0 = 1.00$,
 $\epsilon = 0.0, -0.2$ and -0.4 .

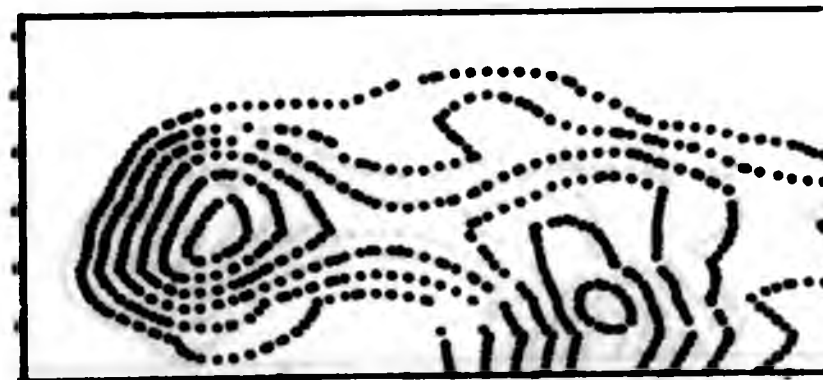
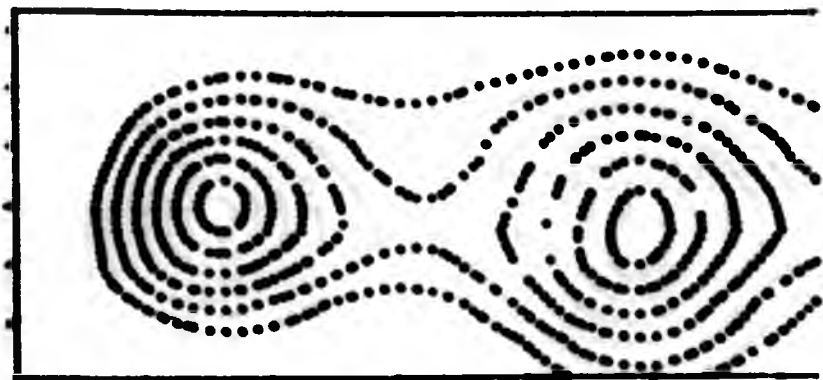


Figure 5.3

Co-range lines for $\nu_0 = -0.11$, $c_0 = 0.1$,
 $\epsilon = -0.15, -0.30$ and -0.45 .

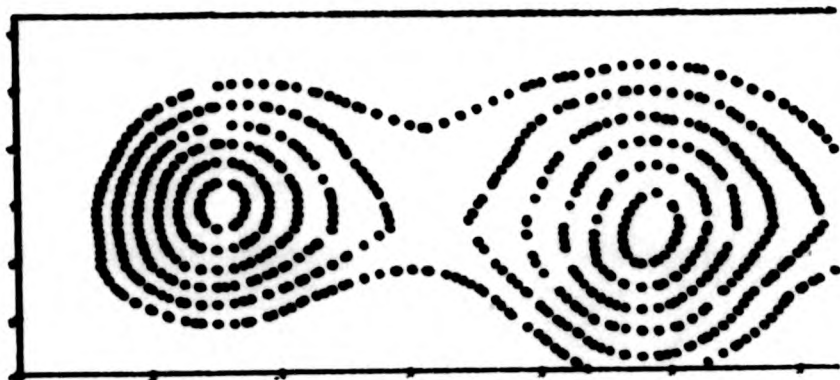


Figure 5.4

Co-range lines for $b_0 = 0.11$, $c_0 = 0.1$,
 $\epsilon = 0.15, 0.30$ and 0.45 .

difference in the lateral displacement of the second amphidromic point.

The co-range contours for large values of $|\epsilon|$ show certain anomalous features such as discontinuity of slope. These, we would suggest, are artefacts that partly arise from the low resolution of the mesh and the crudeness of the algorithms used for the calculation of the first order correction $A^{(1)}$ and the solution set of $|A| = \text{constant}$. However, a more accurate computation, whilst desirable, would have been prohibitively expensive. Furthermore, as $|\epsilon|$ is increased the balance between the zeroth and first order waves becomes such that the incoming part of the corrected wave, $A = A^{(0)} + \epsilon A^{(1)}$, is no longer of greater magnitude than the outgoing constituent. Thus the corrected amplitude, and hence the co-range lines, are nearing the limit at which they become physically meaningless.

53. An alternative method of solution to the Taylor problem.

It is of interest to note that the adapted method of Green's functions (appendix 2) may be used to find the basic state outer solution.

We require that the homogeneous counterpart of the boundary value problem of appendix 2 is a re-statement of the Taylor problem for the v velocity component, (Taylor, 1921). We allow $F_2^{(0)}$ to be piecewise continuous at the boundary and prescribe a relation between $F_2^{(0)}(0,0)$ and $F_2^{(0)}(0,\pi)$ such that the solution to the quasi-homogeneous problem, i.e. p and $q = 0$, $Q_0, F_2^{(0)}(0,0)$ and $F_2^{(0)}(0,\pi) \neq 0$, is identical to that obtained by Taylor's procedure. A unique solution to the quasi-homogeneous problem may be found since the solution to the eigenvalue problem, i.e. $p, q, Q_0, F_2^{(0)}(0,0)$ and

$F_2^{(0)}(0, \pi) = 0$, is trivial. The device of allowing $F_2^{(0)}$ to be discontinuous at the corners of the channel may be regarded as simulating the diffraction effects discussed by Buchwald (1968) and thus is not purely a mathematical artifice.

The Green's function coefficients are generated by the recurrence relations of case 2, appendix 2, i.e.

$$\lambda \sum_{n=1}^{\infty} \alpha_{rn} a_n + s_r a_r = 2 \epsilon_r \sin(ry) e^{-s_r x},$$

$$r = 1, 2, \dots,$$

where

$$\alpha_{rn} = \frac{1}{n} [P_{nr} + P_{or} (1 - (-1)^n \psi) / (\psi - 1)].$$

The parameter $\psi = \int F_2^{(0)}(0, \pi) dy / \int F_2^{(0)}(0, 0) dy$ is taken to be such that it has unit magnitude. This ensures that the magnitudes of the incoming and outgoing wave contribution are similar. The choice of parameter value $\psi = 1$ is found to be satisfactory.

The dissipation terms p and Q_0 are taken as 0 and -0.1131, respectively.

The real and imaginary parts of the basic state outer transverse velocity $F_2^{(0)}$ and the derivatives $F_{2,x}^{(0)}$ and $F_{2,y}^{(0)}$ are evaluated at field points of interest. The details of the procedure are the same as those for the calculation of the first order outer transverse velocity in § 52.

We note that the values obtained for $F_2^{(0)}$ are in very good agreement with those of the Taylor solution in § 453, the two solution sets differing by less than 0.5% at field points not on the transverse barrier. However, at $x = 0$ the discrepancy is around 50%. The values of transverse velocity gradients are generally within 10% of those of the Taylor solution.

The basic state surface elevation $A^{(0)}$ is calculated as in § 52. The amplitudes of the incoming and outgoing waves at $x = 2\pi$ are found to be (0.53, 0.19) and (0.53, -0.20), respectively. These values compare favourably with those of Taylor, namely, (0.52, 0.20) and (0.52, -0.20).

Thus the comparison of the two methods in this special case provides an estimate of the errors incurred and a useful check on the validity of the procedures of § 52.

CHAPTER 6.

CONCLUDING REMARKS.

61. We have shown how the flow regime within a marginal sea of slowly varying topography such as the evolving North Sea may be simply idealised. Feasible relationships between the characteristic lengths, velocities and coefficients and the depth and hence the historical time are indicated in § 41. We then show in §§ 44-47 how a composite expansion of the Latta type may be used to construct a three dimensional solution that is applicable to the problem of a co-oscillating flow within a semi-infinite channel. This composite solution is uniformly valid from the bed to the surface. It is comprised of basic state inner and outer solutions and first order inner and outer corrections which arise from a small perturbation to the system.

The basic state outer solution is essentially two dimensional and may be determined from existing models of flow such as those of Taylor (1921), Hendershott and Speranza (1971), Brown (1978) or Reinecker and Teubner (1980).

The basic state inner solution that applies within the boundary layer region above the bed is shown to be suitably specified by two functions of the outer flow solution and two boundary layer functions of an x dependent vertical eddy viscosity coefficient. Wall effects are assumed to be confined to very thin boundary layers and thus the boundary conditions at the walls are neglected outside of these regions. This assumption is justified in appendix 1. The basic state composite solution is discussed in § 51.

The effects of energy dissipation are accounted for by a perturbation to the system. The first order correction to the

outer flow is an attenuating wave solution. It is found by an adapted Green's function technique (see appendix 2) and is uniquely determined by the basic state outer solution, (see for example §§ 4510, 4511). We show in § 52 how the amphidromic points of the corrected system are laterally displaced from the mid-channel axis as the frictional dissipation effects of the first order outer perturbation increase with historical time. The changes in the amphidromic system conform to the model of Hendershott and Speranza (1971) when the rate of decay of the eddy viscosity with distance from the channel head is sufficiently large and to that of Reinecker and Teubner (1980) when the decay rate is sufficiently small.

The first order inner solution is related to the first order outer and basic state solution in § 4512. It contains a non-linear contribution from the zeroth order solution which provides a mechanism for energy transfer from semi-diurnal constituents of the flow to steady and quarter-diurnal modes. Thus the mass transport velocity, i.e. the mean Lagrangian velocity which is often represented as the sum of the mean Eulerian current and a Stokes drift component, (Longuet-Higgins, 1953), undergoes an inertial enhancement at sub-surface regions. The magnitude of the mean Eulerian current within the boundary layer region is of the order of the product of the characteristic velocity and the Rossby number. It varies with depth approximately as $Z \exp(-\omega_2 Z)$. Thus, under the assumptions of § 41, the magnitude of the steady current at 8300 BP is greater than that of the present day by about a factor of four. It is clear that observational data of steady current velocity profiles in the contemporary

North Sea would provide a means of estimating the magnitude of the eddy viscosity and verifying our assumptions. However, such data as exist tend to have sufficient variability as to obscure any residual contribution from M_2 wave interactions.

We note here that we have neglected the effects of various other interaction effects in our model. Robinson (1981) considers that the non-linear interaction between topographic features and the tidal stream is an important factor in the production of localised residual currents, e.g. a 10% change in depth may induce a residual velocity greater than 2 cms^{-1} . Nihoul and Roday (1976) are of the opinion that the residual circulation pattern is strongly influenced by the effects of a tidal stress that results from the non-linear interactions of tides and storm surges. These effects become more pronounced in shallow areas because of the rapid spatial variation of the velocity.

Furthermore, the implications for the sequence of scouring and deposition of sediments are far from clear. It is suggested by Hunt and Johns (1963) and Noda (1969) that in the case of standing gravity waves sand-bar formation may occur in the vicinity of alternate nodes of the mass transport velocity. On the other hand, Lamoure and Mei (1977) suggest that mass transport near the bed is directed towards a convex corner. Sediment accumulates near such features rather than at stagnation points.

62. The Green's function solution obtained in appendix 2 may be open to question when it is applied to examples of the quasi-homogeneous type. In such cases there are discontinuities at the boundaries and the use of Green's identity (B1.9) in the

construction of the solution may be invalidated. However, the results of applying the Green's function solution to the Taylor problem in § 53 would appear to provide a measure of supportive evidence for the validity of the method of construction or, at worst, usefulness of the method in forming an approximate solution.

A more rigorous approach might result from the use of a Green's function $G^+(\underline{r}; \underline{r}_0)$ which has the same functional form as $G(\underline{r}; \underline{r}_0)$ in equation (B2.1) but for which the boundary condition at the transverse barrier is

$$G_{xy}^+ + \lambda G^+ = 0 \quad \text{at } x = 0 ,$$

(c.f. equation (B1.6)). It follows from Green's identity that G and G^+ satisfy the reciprocity relation

$$\begin{aligned} G^+(\underline{r}_0; \underline{r}) - G(\underline{r}; \underline{r}_0) \\ = \frac{1}{\lambda} [(G_x^+(\underline{r}_1; \underline{r}) G_x(\underline{r}_1; \underline{r}_0))_{x_1=0}]_{y_1=0}^{\pi} . \end{aligned}$$

The solution $\phi(x,y)$ to the boundary value problem of equations (B1.1-4) is then given by an integral expression of the form

$$\begin{aligned} \phi(x,y) = \int_{x_0}^x \int_{y_0}^y p(\underline{r}_0) G^+(\underline{r}; \underline{r}_0) d\underline{r}_0 \\ + \int_{y_0}^y Q(y_0) G^+(\underline{r}; \underline{r}_0) \Big|_{x_0=0} dy_0 , \end{aligned}$$

Clearly such a solution would be more efficient to use than equation (B5.2) since it would only require one set of Green's function coefficients to be computed for the calculation of $\phi(x,y)$ and its derivatives. The difficulty is, of course, to demonstrate that this integral representation is a solution.

63. Additional boundary layer structures would be required to form a composite solution that is uniformly valid near the walls and head of the channel as well as throughout the water column. These, we suggest, might be taken into account by incorporating special functions which contain factors of the type $\exp(-\alpha X)$ and $\exp(-\beta Y)$ into the Latta expansion (44.1). Here X and Y are suitably magnified horizontal coordinates and α, β are functions of the horizontal coefficient of eddy viscosity.

A numerical solution that took account of a more realistic coastal and bed topography might be attempted.

APPENDIX 1

AN INFINITE CHANNEL BOUNDARY LAYER MODEL

A1. We consider the flow regime of a sea within a rotating infinite channel when there is a no-slip condition at the walls and bed. It is assumed that frictional effects are confined to boundary layer regions and that the sea has as its basic state the surface form of a non-attenuating Kelvin wave that travels in the negative x-direction. In all other respects the sea is similar to that described in chapter 4.

Thus the field equations that govern the motion are the momentum and continuity equations (42.1, 2, 3 and 9). The boundary conditions are the surface conditions (43.2-3) and the no-slip condition (43.4) which now applies at $z = -1$ and $y = 0, \pi$. This system of equations will be referred to as the full system.

It will be assumed that the Ekman and Rossby numbers are equal to a small parameter ϵ^2 and that the time dependence is simple harmonic, i.e. we can write

$$(u, v, w, \eta) = \text{Re}(U, V, W, A e^{it}).$$

The method of matched asymptotic expansions (Nayfeh, 1981) is used to express the full system as sets of outer and inner equations that are applicable at interior, bed or wall regions.

A2. The outer equations that govern the core flow are obtained by neglecting the no-slip conditions and finding the limit as $\epsilon \rightarrow 0$ of each term in the full system. These equations are

$$i \epsilon U_0 = V_0 - \frac{1}{\alpha} A_x, \quad (1)$$

$$i \epsilon V_0 = -U_0 - \frac{1}{\alpha} A_y \quad (2)$$

and

$$\frac{\partial U_0}{\partial x} + \frac{\partial V_0}{\partial y} + i k_0 A = 0 \quad (3)$$

where the subscript o denotes an outer variable. Equations

(1-3) admit a Kelvin wave solution

$$A = \exp(i k_o x + \alpha y), \quad (4)$$

$$U_o = -A \quad (5)$$

and

$$V_o = 0. \quad (6)$$

The vertical component of velocity is obtained from the equation of continuity. It is

$$W_o = i k_o (1 + z) A. \quad (7)$$

A3. The inner system of equations that applies in the bed region is obtained by expressing the full system in terms of a magnified boundary layer variable $Z = (1 + z) / \epsilon$ and finding the limiting form as $\epsilon \rightarrow 0$. This process yields

$$i \delta U_1 = V_1 + N \frac{\partial^2 U_1}{\partial Z^2} - \frac{1}{\alpha} A_x \quad (1)$$

and

$$i \delta V_1 = -U_1 + N \frac{\partial^2 V_1}{\partial Z^2} - \frac{1}{\alpha} A_y \quad (2)$$

where the subscript 1 denotes an inner variable.

If we substitute

$$\xi_1(Z) A(x,y) = U_1 + i V_1 \quad (3)$$

and

$$\xi_2(Z) A(x,y) = U_1 - i V_1 \quad (4)$$

into equations (1 - 2) we obtain the second order differential equations

$$\xi_1'' - \omega_1^2 \xi_1 - \omega_1^2 = 0 \quad (5)$$

and

$$\xi_2'' - \omega_2^2 \xi_2 - \omega_2^2 = 0. \quad (6)$$

Here the boundary layer parameters ω_1 and ω_2 are given by

$$\omega_1 = (1 + \epsilon) \left(\frac{\epsilon + 1}{2N} \right)^{\frac{1}{2}} \quad (7)$$

and

$$\omega_2 = (1 + \epsilon) \left(\frac{\epsilon - 1}{2N} \right)^{\frac{1}{2}} \quad (8)$$

The solutions to equations (5 - 6) that satisfy the no-slip condition at the bed and contain no terms that increase exponentially with increasing distance from the bed are

$$f_1 = \exp(-\omega_1 Z) - 1 \quad (9)$$

and

$$f_2 = \exp(-\omega_2 Z) - 1 \quad (10)$$

Thus the bed flow velocity components U_1 and V_1 are given by

$$U_1 = \frac{1}{2} (\exp(-\omega_1 Z) + \exp(-\omega_2 Z) - 2) A \quad (11)$$

and

$$V_1 = \frac{1}{2i} (\exp(-\omega_1 Z) - \exp(-\omega_2 Z)) A \quad (12)$$

A4. If the horizontal and vertical coefficients of momentum exchange are taken to be of the same order then the stretching transformation $Y = (y - \pi) / \epsilon \epsilon_1$ is appropriate within the boundary layer region of the channel wall at $y = \pi$. This will ensure that the ratio of the wall and bed boundary layer thicknesses is of the same order of magnitude as the aspect ratio $\epsilon_1 = D/L$.

The limiting form of the full system that applies above the bed boundary layer yields

$$N \frac{\partial^2 U_w}{\partial Y^2} - i \epsilon U_w - \frac{1}{\alpha} \frac{\partial A_w}{\partial x} = 0 \quad (1)$$

where the subscript w indicates the wall region and

$$A_w = \exp(ikx + \alpha \pi) \quad (2)$$

Thus a solution that satisfies the no-slip condition at the wall and asymptotically matches with the core flow is given by

$$U_w = (\exp(-\omega_3 Y) - 1) A_w \quad (3)$$

and

$$V_w = 0 \quad (4)$$

where

$$\omega_3 = -(1 + i) (\epsilon / 2N)^{1/2} \quad (5)$$

Solutions that are analogous to equations (3 - 5) may be obtained for the flow near the channel wall at $y = 0$.

A5. Composite solutions, denoted by subscript c, that are uniformly valid from the bed to the surface are given by

$$U_c = U_o + U_1 - [U_1]_o \quad (1)$$

and

$$V_c = V_o + V_1 - [V_1]_o \quad (2)$$

Here $[U_1]_o$ and $[V_1]_o$ denote the outer limits of the inner solutions and are equal to U_o and V_o , respectively. Hence equations (1 - 2) reduce to

$$U_c = U_1 \quad (3)$$

and

$$V_c = V_1 \quad (4)$$

We may construct a composite solution that is uniformly valid across the width of the channel and above the bed boundary layer in a similar fashion. However, an additional boundary layer treatment is required to form solutions that obey no-slip conditions at the walls in the region of the bottom boundary layer.

APPENDIX 2

AN ADAPTATION OF THE METHOD OF GREEN'S FUNCTIONS

B1. Consider the relationship between a function of position $\phi(\underline{r})$ and a Green's function $G(\underline{r}; \underline{r}_0)$, where $\underline{r} = (x, y)$ and $\underline{r}_0 = (x_0, y_0)$ constitute field source variables, respectively, when ϕ and G are solutions to the boundary value problems

$$\hat{H} \phi = p(\underline{r}), \quad (1)$$

$$\phi_{xy} + \lambda \phi = q(y) \quad \text{on } x = 0, \quad (2)$$

$$\frac{\partial^n \phi}{\partial x^n} = 0, \quad n = 0, 1, \dots, \quad \text{on } y = 0, \pi, \quad (3)$$

$$\lim_{x \rightarrow \infty} \phi = 0, \quad (4)$$

and

$$\hat{H} G = \delta(\underline{r} - \underline{r}_0), \quad (5)$$

$$G_{xy} - \lambda G = 0 \quad \text{on } x = 0, \quad (6)$$

$$\frac{\partial^n G}{\partial x^n} = 0, \quad n = 0, 1, \dots, \quad \text{on } y = 0, \pi, \quad (7)$$

$$\lim_{x \rightarrow \infty} G = 0. \quad (8)$$

Here the Helmholtz operator $\hat{H} = (\nabla^2 + k^2)$, k is a constant within the interval $(0, 1)$, $\delta(\underline{r} - \underline{r}_0)$ is the Dirac delta function, λ is a complex constant and $p(\underline{r})$ and $q(y)$ are known functions.

The Green's identity

$$\int_D (\phi \nabla^2 G - G \nabla^2 \phi) dS = \int_c (\phi \frac{\partial G}{\partial n} - G \frac{\partial \phi}{\partial n}) ds, \quad (9)$$

where c denotes the contour which bounds the domain

$$D = \{(x, y) : x \geq 0, y \in [0, \pi]\},$$

dS and ds are surface and line elements, respectively, may be used to show that

$$\phi(\underline{r}_0) = \int_D p G dS + \int_0^\pi (G \phi_x - \phi G_x)_{x=0} dy. \quad (10)$$

The integrated forms of the boundary conditions (2) and (6) are

$$\int G dy = \frac{1}{\lambda} (G_x - a_0) \quad \text{on } x = 0 \quad (11)$$

and

$$\int \phi dy = \frac{1}{\lambda} (Q - \phi_x) \quad \text{on } x = 0, \quad (12)$$

where $a_0 = a_0(r_0)$ is an arbitrary function of r_0 , $Q = \int q dy + Q_0$

and Q_0 is an arbitrary constant of integration.

The line integral of equation (10) may be integrated by parts, whence we obtain the expressions

$$\phi(r_0) = \int_0^{\pi} p G dS - \frac{1}{\lambda} \int_0^{\pi} q G_x|_{x=0} dy + \frac{1}{\lambda} \left[(\phi_x G_x)_{x=0} \right]_{y=0}^{\pi} \quad (13)$$

and

$$\phi(r_0) = \int_0^{\pi} p G dS + \int_0^{\pi} Q G|_{x=0} dy + \frac{1}{\lambda} \left[(G_x (\phi_x - Q))_{x=0} \right]_{y=0}^{\pi} \quad (14)$$

Thus $\phi(r_0)$ is the solution to the inhomogeneous Helmholtz equation with inhomogeneous boundary conditions, equations (1 - 4), except, possibly, at the corners $(0,0)$ and $(0,\pi)$ where ϕ , G and the derivatives may be discontinuous. However, we shall assume that the use of the Green's identity, equation (9) is not invalidated.

It will be convenient to choose G so that $\left[(G_x (\phi_x - Q))_{x=0} \right]_{y=0}^{\pi}$ vanishes and equation (14) takes the form

$$\phi(r_0) = \int_0^{\pi} p G dS + \int_0^{\pi} Q G|_{x=0} dy \quad (15)$$

By choosing $Q_0 = 0$ and $G_x = 0$ at the corners we may ensure that the eigenfunctions of the boundary value problem, equations (1 - 4), vanish. Alternatively, if we wish to ensure that the non-trivial and identical solutions may be obtained from equations (13)

and (15) in the case of the quasi-homogeneous problem when $p = q = 0$ and $Q = Q_0 \neq 0$, it is necessary to impose the constraint that $[(\phi_x G_x)_{x=0}]_{y=0}$ is non-zero. We shall refer to those cases for which the eigenfunctions vanish as case 1 examples and to those for which non-trivial solutions exist for the quasi-homogeneous problem as case 2 examples.

B2. A Green's function which satisfies the governing equation (B1.5) and the boundary conditions (B1.7-8) is given by the infinite series representation

$$G(\underline{r}; \underline{r}_0) = \sum_{r=1}^{\infty} \left\{ \frac{\epsilon_r}{s_r} \sin(ry) \sin(ry_0) \right. \\ \left. x [\exp(-s_r |x - x_0|) - \exp(-s_r(x + x_0))] \right. \\ \left. + a_r(x_0, y_0) e^{-s_r x} \sin(ry) \right\}, \quad (1)$$

where $s_r = (r^2 - k^2)^{1/2}$, $\epsilon_r = -1/\pi$ and the Green's functions coefficients a_r , $r = 1, 2, \dots$, are functions of the source variables, (c.f. Morse and Feshbach, 1953).

At the transverse barrier, the Green's function (1), its x derivative and integral take the forms

$$G|_{x=0} = \sum_{r=1}^{\infty} a_r \sin(ry), \quad (2)$$

$$G_x|_{x=0} = \sum_{r=1}^{\infty} \left\{ 2\epsilon_r \sin(ry_0) e^{-s_r x_0} - s_r a_r \right\} \sin(ry) \quad (3)$$

and, to within an arbitrary function of the source variables,

$$\int G|_{x=0} dy = - \sum_{r=1}^{\infty} \frac{a_r}{r} \cos(ry). \quad (4)$$

B3. The Green's function coefficients $a_r(x_0, y_0)$ must now be found so that the remaining boundary condition (B1.6) is satisfied.

The half range Fourier sine series for the odd extension of $\cos(ry)$,

$$\cos(ry) = \sum_{n=1}^{\infty} \beta_{rn} \sin(ny), \quad r = 1, 2, \dots, \quad (1)$$

where

$$\beta_{rn} = \begin{cases} 0, & r + n \text{ even,} \\ 4n / \pi (n^2 - r^2), & r + n \text{ odd,} \end{cases} \quad (2)$$

is substituted into equation (B2.4). The coefficients of similar terms in the expanded transverse boundary condition (B1.11) are compared. This yields the recurrence relations

$$\lambda \sum_{n=1}^{\infty} \beta_{nr} \frac{a_n}{n} - s_r a_r = a_0 \beta_{0r} - 2 \epsilon_r \sin(ry_0) e^{-s_r x_0}, \quad r = 1, 2, \dots \quad (3)$$

The Green's function coefficients a_1, a_2, \dots, a_N may be determined by specifying $a_0(x_0, y_0)$ and solving the N -th order reduced system of simultaneous linear equations.

The existence of a solution set $a_r, r = 1, 2, \dots, N$, and the convergence to a unique limiting form may be shown by establishing that the coefficient matrix obtained from equation (3) is diagonally dominant and the right hand sides are bounded, (Davis, 1936). Thus a sufficient condition for convergence is that

$$\sum_{n=1}^{\infty} |\beta_{nr}/n| < s_r / |\lambda|, \quad r = 1, 2, \dots$$

It is readily shown that

$$\sum_{\substack{n=1 \\ n \neq r}}^{\infty} \left| \frac{1 - (-1)^{r+n}}{n(r^2 - n^2)} \right| < \frac{1}{r^2} \left\{ \sum_{n=1}^{r-1} \left(\frac{2}{n} + \frac{1}{r-n} - \frac{1}{r+n} \right) \right. \\ \left. - \sum_{n=r+1}^{\infty} \left(\frac{2}{n} + \frac{1}{r-n} - \frac{1}{r+n} \right) \right\}, \quad r = 1, 2, \dots, \\ < \frac{4}{r} - \frac{5}{2r^3}, \quad r = 1, 2, \dots$$

Thus, if $|\lambda| < 0.8$ the convergence criterion is satisfied.

If we write $b_r = s_r a_r$ in equation (3) then a solution set $\{b_r\}$ may be shown to exist for all $x_0 \geq 0$, $0 \leq y_0 \leq \pi$. Thus $a_r = 0$ ($1/r$), $r = 1, 2, \dots$, at most.

By taking the recurrence relations (3) into account the expression for the Green's function derivative at the transverse barrier, equation (B2.2), may be written as

$$G_x \Big|_{x=0} = \sum_{r=1}^{\infty} (c_r + d_r) \sin(ry)$$

where

$$c_r = -\lambda \sum_{n=1}^{\infty} \beta_{nr} a_n / n$$

and

$$d_r = a_0 \beta_{or}$$

The uniform convergence of this expression is shown as follows.

We may show that $|c_r| = 0$ ($1/r$) and $|c_r - c_{r+2}| = 0(1/r^2)$. Thus $\sum_r c_r \sin(ry)$ is uniformly convergent in $(0, \pi)$, (see, for example, Copson, 1935). The constants $d_r = 4a_0 / \pi r$, $r = 1, 2, \dots$, are monotonically converging to zero, thus $\sum_r d_r \sin(ry)$ is uniformly convergent in the interval $(0, 2\pi)$. Hence the series representation of $G_x \Big|_{x=0}$ is uniformly convergent for all $y \in (0, \pi)$.

B4. For convenience we shall assume that we may choose $a_0 = 0$ for the case 1 formulation.

A suitable form for $a_0(x_0, y_0)$ that is compatible with case 2 type problems is found by taking the constraints that were inherent in equation (B1.15) into consideration. We recall that these were

$$[\{G_x (\phi_x - Q)\}_{x=0}]_{y=0}^{\pi} = 0 \quad (1)$$

whilst

$$Q_0, [\{\phi_x G_x\}_{x=0}]_{y=0}^{\pi} \neq 0. \quad (2)$$

If we take the integrated boundary conditions (B1.11-12) and the expansion for $\int G|_{x=0} dy$, equation (B2.4), into account, introduce

$$\sigma_1 = \sum_{r=1}^{\infty} (-1)^r \frac{a_r}{r}, \quad (3)$$

$$\sigma_2 = \sum_{r=1}^{\infty} \frac{a_r}{r}, \quad (4)$$

$$\Phi(x, y) = \int \phi dy \quad (5)$$

and assume that for some constant μ

$$\Phi(0, \pi) = \mu \Phi(0, 0), \quad (6)$$

then we may express equation (1) as

$$\lambda \Phi(0, 0) [(1 - \mu) a_0 + \lambda (\mu \sigma_1 - \sigma_2)] = 0. \quad (7)$$

Thus if $\Phi(0, 0)$ is finite and non-zero, it follows from equation (7) that

$$a_0(x_0, y_0) = \frac{\lambda (\mu \sigma_1 - \sigma_2)}{\mu - 1}, \quad \mu \neq 1. \quad (8)$$

B5. The solution to equations (B1.1-4) is given by equations (B1.15), (B2.1), (B3.3) and (B4.8) in which source and field variables have been interchanged. This may be written as

$$\phi(\underline{r}) = \int_{y_0=0}^{\pi} \int_{x_0=0}^{\infty} p(\underline{r}_0) \tilde{G} dx_0 dy_0 + \int_{y_0=0}^{\pi} Q(y_0) \tilde{G}|_{x=0} dy_0 \quad (1)$$

Here the adjoint Green's function $\tilde{G}(\underline{r}; \underline{r}_0) = G(\underline{r}_0; \underline{r})$. It is given by

$$\tilde{G}(\underline{r}; \underline{r}_0) = \sum_{r=1}^{\infty} \left\{ \frac{\epsilon_r}{s_r} \sin(ry) \sin(ry_0) \times [\exp(-s_r |x - x_0|) - \exp(-s_r (x + x_0))] + a_r(x, y) e^{-s_r x_0} \sin(ry_0) \right\} \quad (2)$$

The coefficients a_1, a_2, \dots , are generated by the recurrence relations

$$-\lambda \sum_{n=1}^{\infty} \alpha_{rn} a_n + s_r a_r = 2 \epsilon_r \sin(ry) e^{-s_r x}, \quad r = 1, 2, \dots, \quad (3)$$

where for case 1 examples

$$\alpha_{rn} = \beta_{nr} / n \quad (4)$$

and for case 2 examples

$$\alpha_{rn} = \frac{1}{n} [\beta_{nr} + \beta_{or} (1 - (-1)^n p) / (p - 1)] \quad (5)$$

APPENDIX 3

PROGRAMS

The programs referred to in chapter 5 are listed here. Identifier names follow a notation similar to that of § 45. The language used is VAX-11 PASCAL since it has the advantage of relative clarity for the user whilst allowing an interface with efficient FORTRAN utilities such as NAG or SIMPLEPLOT.

The depth variation of the horizontal components of velocity is calculated in program 1, (see § 51). Programs 2 - 5 are used to compute the amplitude and velocity components for the zeroth and first order outer system, (see §§ 52 and 53). Co-range lines are computed and plotted by means of programs 6 - 7.

PROGRAM 1.

(* THE DEPTH VARIATION OF U AND V
IS DETERMINED FROM THE EXPRESSIONS
OF SECTION 45.

THE EDDY VISCOSITY N(X) IS ASSUMED
TO BE GIVEN BY

$N(X) = -\exp(-2.00 \cdot X)$ *)

VAR X,Y,Z,T,ALPHA,K,DELTA,PI,CO,CNST,
KO,X1,UR,VR:REAL;
A,B,C,D:ARRAY [1..10] OF REAL;
ZERO:ARRAY [0..100] OF REAL;
I,J,COUNT,NZERO:INTEGER;
UVSZ,VVSZ:TEXT;

FUNCTION S(M:INTEGER):REAL;
BEGIN S:=SQRT(M*M-K*K) END;

FUNCTION CH(X:REAL):REAL;
BEGIN
CH:=(EXP(X)+EXP(-X))/2
END;

FUNCTION SH(X:REAL):REAL;
BEGIN
SH:=(EXP(X)-EXP(-X))/2
END;

FUNCTION REF1(X,Y:REAL):REAL;
VAR Z,XBAR,YBAR:REAL;M:INTEGER;
BEGIN
XBAR:=X+X1;YBAR:=Y-PI/2;Z:=0;
FOR M:=1 TO 10 DO
Z:=Z+A[M]*COS(M*YBAR)/EXP(S(M)*X);
REF1:=PI*CH(ALPHA*YBAR)*SIN(KO*XBAR)
/(4*ALPHA) -Z
END;

FUNCTION IMF1(X,Y:REAL):REAL;
VAR Z,XBAR,YBAR:REAL;M:INTEGER;
BEGIN
XBAR:=X+X1;YBAR:=Y-PI/2;Z:=0;
FOR M:=1 TO 10 DO
Z:=Z+B[M]*SIN(M*YBAR)/EXP(S(M)*X);
IMF1:=-PI*SH(ALPHA*YBAR)*COS(KO*XBAR)
/(4*ALPHA) -Z
END;

FUNCTION REF2(X,Y:REAL):REAL;
VAR Z,YBAR:REAL;M:INTEGER;
BEGIN
YBAR:=Y-PI/2;Z:=0;
FOR M:=1 TO 10 DO
Z:=Z+D[M]*SIN(M*YBAR)/EXP(S(M)*X);
REF2:=-Z
END;

FUNCTION IMF2(X,Y:REAL):REAL;
VAR Z,YBAR:REAL;M:INTEGER;

```

BEGIN
  YBAR:=Y-PI/2;Z:=0;
  FOR M:=1 TO 10 DO
    Z:=Z+CCM]*COS(M*YBAR)/EXP(S(M)*X);
  IMF2:=-Z
END;

FUNCTION REG1(X,Y:REAL):REAL;
BEGIN
  REG1:=- (REF1(X,Y)-IMF2(X,Y))/2
END;

FUNCTION IMG1(X,Y:REAL):REAL;
BEGIN
  IMG1:=- (IMF1(X,Y)+REF2(X,Y))/2
END;

FUNCTION REG2(X,Y:REAL):REAL;
BEGIN
  REG2:=- (IMF1(X,Y)+REF2(X,Y))/2
END;

FUNCTION IMG2(X,Y:REAL):REAL;
BEGIN
  IMG2:=(REF1(X,Y)-IMF2(X,Y))/2
END;

FUNCTION REH1(X,Y:REAL):REAL;
BEGIN
  REH1:=- (REF1(X,Y)+IMF2(X,Y))/2
END;

FUNCTION IMH1(X,Y:REAL):REAL;
BEGIN
  IMH1:=- (IMF1(X,Y)-REF2(X,Y))/2
END;

FUNCTION REH2(X,Y:REAL):REAL;
BEGIN
  REH2:=- (-IMF1(X,Y)+REF2(X,Y))/2
END;

FUNCTION IMH2(X,Y:REAL):REAL;
BEGIN
  IMH2:=- (REF1(X,Y)+IMF2(X,Y))/2
END;

FUNCTION T1(X,Z:REAL):REAL;
BEGIN
  T1:=SQRT((DELTA+1)/2)*EXP(CO*X)*Z
END;

FUNCTION T2(X,Z:REAL):REAL;
BEGIN
  T2:=SQRT((DELTA-1)/2)*EXP(CO*X)*Z
END;

FUNCTION C1(X,Z:REAL):REAL;
BEGIN
  IF T1(X,Z)>80 THEN C1:=0

```

```

        ELSE C1:=COS(T1(X,Z))/EXP(T1(X,Z))
END;

FUNCTION C2(X,Z:REAL):REAL;
BEGIN
    IF T2(X,Z)>80 THEN C2:=0
    ELSE C2:=COS(T2(X,Z))/EXP(T2(X,Z))
END;

FUNCTION S1(X,Z:REAL):REAL;
BEGIN
    IF T1(X,Z)>80 THEN S1:=0
    ELSE S1:=+SIN(T1(X,Z))/EXP(T1(X,Z))
END;

FUNCTION S2(X,Z:REAL):REAL;
BEGIN
    IF T2(X,Z)>80 THEN S2:=0
    ELSE S2:=+SIN(T2(X,Z))/EXP(T2(X,Z))
END;

FUNCTION REU(X,Y,Z:REAL):REAL;
BEGIN
    REU:=REF1(X,Y) +C1(X,Z)*REG1(X,Y) +S1(X,Z)*IMG1(X,Y)
        +C2(X,Z)*REH1(X,Y) +S2(X,Z)*IMH1(X,Y)
END;

FUNCTION IMU(X,Y,Z:REAL):REAL;
BEGIN
    IMU:=IMF1(X,Y) +C1(X,Z)*IMG1(X,Y) -S1(X,Z)*REG1(X,Y)
        +C2(X,Z)*IMH1(X,Y) -S2(X,Z)*REH1(X,Y)
END;

FUNCTION REV(X,Y,Z:REAL):REAL;
BEGIN
    REV:=REF2(X,Y) +C1(X,Z)*REG2(X,Y) +S1(X,Z)*IMG2(X,Y)
        +C2(X,Z)*REH2(X,Y) +S2(X,Z)*IMH2(X,Y)
END;

FUNCTION IMV(X,Y,Z:REAL):REAL;
BEGIN
    IMV:=IMF2(X,Y) +C1(X,Z)*IMG2(X,Y) -S1(X,Z)*REG2(X,Y)
        +C2(X,Z)*IMH2(X,Y) -S2(X,Z)*REH2(X,Y)
END;

FUNCTION U(X,Y,Z,T:REAL):REAL;
BEGIN
    U:=REU(X,Y,Z)*COS(T)-IMU(X,Y,Z)*SIN(T)
END;

FUNCTION V(X,Y,Z,T:REAL):REAL;
BEGIN
    V:=REV(X,Y,Z)*COS(T)-IMV(X,Y,Z)*SIN(T)
END;

BEGIN
    ALPHA:=0.7;K:=0.5;K0:=0.8602;C0:=1;
    DELTA:=1.229;PI:=4*ARCTAN(1);X1:=0.427;

    AC1:=0.765;AC2:= -0.427;AC3:= -0.009;

```

```
AC4]:=0.100;AC5]:=0.0012;AC6]:= -0.0425;  
AC7]:= -0.0003;AC8]:=0.0245;AC9]:=0.0001;  
AC10]:= -0.0147;
```

```
BC1]:= -1.100;BC2]:=0.056;BC3]:=0.132;  
BC4]:= -0.004;BC5]:= -0.050;BC6]:=0.001;  
BC7]:=0.027;BC8]:= -0.0002;BC9]:= -0.017;  
BC10]:=0.0001;
```

```
CC1]:=1.892;CC2]:=0.0;CC3]:= -0.138;  
CC4]:=0.0;CC5]:=0.510;CC6]:=0.0;  
CC7]:= -0.027;CC8]:=0.0;CC9]:=0.017;  
CC10]:=0.0;
```

```
DC1]:=0.0;DC2]:= -0.495;DC3]:=0.0;  
DC4]:=0.103;DC5]:=0.0;DC6]:= -0.043;  
DC7]:=0.0;DC8]:=0.024;DC9]:=0.0;  
DC10]:= -0.015;
```

```
X:=0.1;Y:=PI/2;
```

```
REWRITE(UVSZ);WRITELN(UVSZ);  
WRITELN(UVSZ,' 0 8 0 1');  
FOR J:=0 TO 3 DO  
FOR I:=0 TO 50 DO  
BEGIN  
T:=J*PI/2;  
Z:=4*I/50;  
UR:=1 +2*J +U(X,Y,Z,T);  
WRITELN(UVSZ,UR:9:5,Z:9:5)  
END;  
WRITELN(UVSZ,' -9999 ');
```

```
REWRITE(VVSZ);WRITELN(VVSZ);  
WRITELN(VVSZ,' 0 8 0 1');  
FOR J:=0 TO 3 DO  
FOR I:=0 TO 50 DO  
BEGIN  
T:=J*PI/2;  
Z:=4*I/50;  
VR:=1 +2*J +V(X,Y,Z,T);  
WRITELN(VVSZ,VR:9:5,Z:9:5)  
END;  
WRITELN(VVSZ,' -9999 ')  
END.
```

PROGRAM 2.

(* GREEN'S FUNCTION COEFFICIENTS
OF SECTION 4510 *)

TYPE MATRIX=ARRAY [1..20,1..20] OF DOUBLE;
VECTOR=ARRAY [1..20] OF DOUBLE;

VAR X,Y,LAMDA1,LAMDA2,MU1,MU2,PI,KH,EPS:DOUBLE;
I,J,N,IA,IUNIT,IFAIL:INTEGER;
B,C,D,INVB,INVC,INVD,M0,M1,M2:MATRIX;
U,V,R,S,P,Q,V0,V1,V2,V3,V4:VECTOR;
GFC:TEXT;

FUNCTION DELTA(I,J:INTEGER):DOUBLE;
BEGIN
IF I=J THEN DELTA:=1.0
ELSE DELTA:=0.0
END;

FUNCTION EXPNTL(X:DOUBLE):DOUBLE;
BEGIN
IF X<88 THEN EXPNTL:=EXP(X)
ELSE EXPNTL:=1D+36
END;

FUNCTION NU(I:INTEGER):DOUBLE;
BEGIN NU:=SQRT(I*I-KH*KH) END;

FUNCTION BETA(I,J:INTEGER):DOUBLE;
BEGIN
IF I=0 THEN BETA:=0 ELSE
IF (I+J) MOD 2=1 THEN
BETA:=4*J/(PI*(J*J-I*I))
ELSE BETA:=0
END;

FUNCTION REALPHA(I,J:INTEGER):DOUBLE;
BEGIN
REALPHA:=BETA(J,I)/J+BETA(0,I)*((MU1-1)
-COS(J*PI)*(MU1*(MU1-1)+MU2**2))
/(J*((MU1-1)**2+MU2**2))
END;

FUNCTION IMALPHA(I,J:INTEGER):DOUBLE;
BEGIN
IMALPHA:=-BETA(0,I)*MU2*(1-COS(J*PI))
/(J*((MU1-1)**2+MU2**2))
END;

(*ADDS MATRICES A,B ASSIGNS RESULT TO C*)
PROCEDURE MATADD(VAR A,B,C:MATRIX);
VAR I,J:INTEGER;
BEGIN
FOR I:=1 TO 20 DO FOR J:=1 TO 20 DO
C[I,J]:=A[I,J]+B[I,J]
END;

(*MULTIPLIES MATRICES A,B, ASSIGNS RESULT TO C*)
PROCEDURE MATMULT(VAR A,B,C:MATRIX);

```

VAR I,J,K:INTEGER;Z:DOUBLE;
BEGIN
  FOR I:=1 TO 20 DO FOR J:=1 TO 20 DO
    BEGIN
      Z:=0;
      FOR K:=1 TO 20 DO
        Z:=Z+ACI,K]*BCK,J];
      CCI,J]:=Z
    END
  END;

(* C=A.B *)
PROCEDURE VECTMULT(VAR A:MATRIX;VAR B,C:VECTOR);
VAR I,J:INTEGER;Z:DOUBLE;
BEGIN
  FOR I:=1 TO 20 DO
    BEGIN
      Z:=0;
      FOR J:=1 TO 20 DO
        Z:=Z+ACI,J]*B[J];
        CCI]:=Z
      END
    END;

(* C=A+B *)
PROCEDURE VECTADD(VAR A,B,C:VECTOR);
VAR J:INTEGER;
BEGIN
  FOR J:=1 TO 20 DO
    C[J]:=A[J]+B[J]
  END;

(* C=B-A *)
PROCEDURE VECTSUB(VAR A,B,C:VECTOR);
VAR J:INTEGER;
BEGIN
  FOR J:=1 TO 20 DO
    C[J]:=B[J]-A[J]
  END;

(*NAG FORTRAN SUBROUTINE F01AAF,CALCULATES THE
APPROXIMATE INVERSE OF A REAL MATRIX BY CROUT'S METHOD*)
PROCEDURE F01AAF(VAR A:MATRIX; IA,N:INTEGER;VAR UNIT:MATRIX;
  IUNIT:INTEGER;VAR WKSPACE:VECTOR;VAR IFAIL:INTEGER);
EXTERN;

(*NAG FORTRAN SUBROUTINE F04AAF, CALCULATES THE
APPROXIMATE SOLUTION OF A SET OF REAL LINEAR
EQUATIONS BY CROUT'S FACTORISATION METHOD*)

BEGIN

  PI:=4*ARCTAN(1);KH:=0.5;
  LAMDA1:=0;LAMDA2:=0.6021;
  MU1:=0;MU2:=2;EPS:=-1/PI;

  FOR I:=1 TO 20 DO FOR J:=1 TO 20 DO
    BEGIN
      BCI,J]:=LAMDA2*REALPHA(I,J)
      +LAMDA1*IMALPHA(I,J);

```

```

      CCI,JJ:=LAMDA2*IMALPHA(I,J)
      -LAMDA1*REALPHA(I,J)
      +NU(I)*DELTA(I,J)
END:

(* INVERSE OF MATRIX B *)
IA:=20;N:=20;IUNIT:=20;IFAIL:=0;
FOR I:=1 TO 20 DO FOR J:=1 TO 20 DO
MOEI,JJ:=BCI,JJ;
FO1AAF(MO,IA,N,INVB,IUNIT,VO,IFAIL);
IF IFAIL<>0 THEN WRITELN(' FAIL AT 1');

(* INVERSE OF MATRIX C *)
FOR I:=1 TO 20 DO FOR J:=1 TO 20 DO
MOEI,JJ:=CCI,JJ;
FO1AAF(MO,IA,N,INVC,IUNIT,VO,IFAIL);
IF IFAIL<>0 THEN WRITELN(' FAIL AT 2');

(* MATRIX D *)
MATMULT(INVB,C,M1);
MATMULT(INVC,B,M2);
MATADD(M1,M2,D);

(* INVERSE OF MATRIX D *)
FOR I:=1 TO 20 DO FOR J:=1 TO 20 DO
MOEI,JJ:=DCI,JJ;
FO1AAF(MO,IA,N,INVD,IUNIT,VO,IFAIL);

REWRITE(GFC);

(* REAL AND IMAGINARY PARTS OF THE
GREEN'S FUNCTION COEFFICIENTS,
U AND V, ARE FOUND BY SOLVING
D.U=R AND D.V=S AT DIFFERENT
FIELD POINTS (X,Y):X=0,PI/5,---,2.PI
AND Y=0,PI/10,---,PI.
Y AND X DERIVATIVES ARE ALSO OBTAINED *)

FOR J:=1 TO 3 DO
BEGIN X:=0;Y:=0;
REPEAT
BEGIN
REPEAT
FOR I:=1 TO 20 DO
BEGIN
PEIJ:=0;
CASE J OF
1:QCIJ:=2*EPS*SIN(I*Y)
/EXPNTL(NU(I)*X);
2:QCIJ:=2*EPS*I*COS(I*Y)
/EXPNTL(NU(I)*X);
3:QCIJ:=-2*EPS*NU(I)*SIN(I*Y)
/EXPNTL(NU(I)*X)
END
END:

(* VECTOR R *)
VECTMULT(INVC,P,V1);
VECTMULT(INVB,Q,V2);
VECTADD(V1,V2,R);

```

```
(* VECTOR S *)  
VECTMULT(INVC,Q,V3);  
VECTMULT(INVB,P,V4);  
VECTSUB(V4,V3,S);
```

```
(* SOLUTIONS U AND V *)  
VECTMULT(INVD,R,U);  
VECTMULT(INVD,S,V);
```

```
WRITELN(GFC);WRITELN(GFC);  
FOR I:=1 TO 10 DO  
WRITELN(GFC,X:9:6,Y:9:6,UCIJ:10:6,VEIJ:10:6);
```

```
Y:=Y+PI/10
```

```
UNTIL Y>PI  
END:X:=X+PI/5;Y:=0  
UNTIL X>2*PI  
END
```

```
END.
```

PROGRAM 3.

(* DISSIPATION TERMS P AND Q
ARE CALCULATED FROM THE
EXPRESSIONS OF SECTION 459 *)

VAR I,J,K:INTEGER;
X,Y,PI,KH,DELTA,ALPHA,KO,CO:REAL;
A,B,C,D,P,Q:ARRAY [1..10] OF REAL;
ABCD,EA0,PANDQ:TEXT;

FUNCTION SH(X:REAL):REAL;
BEGIN
SH:=(EXP(X)-EXP(-X))/2
END;

FUNCTION CH(X:REAL):REAL;
BEGIN
CH:=(EXP(X)+EXP(-X))/2
END;

FUNCTION S(I:INTEGER):REAL;
BEGIN S:=SQRT(I*I-KH*KH) END;

FUNCTION READ(X,Y:REAL):REAL;
VAR M:INTEGER;XBAR,YBAR,Z:REAL;
BEGIN
XBAR:=X+0.427;YBAR:=Y-PI/2;
Z:=0;FOR M:=1 TO 10 DO
Z:=Z+PCM]*SIN(M*YBAR)/EXP(S(M)*X);
READ:=-PI*SH(ALPHA*YBAR)*SIN(KO*XBAR)
/(4*ALPHA) -Z
END;

FUNCTION IMA0(X,Y:REAL):REAL;
VAR M:INTEGER;XBAR,YBAR,Z:REAL;
BEGIN
XBAR:=X+0.427;YBAR:=Y-PI/2;
Z:=0;FOR M:=1 TO 10 DO
Z:=Z+QCM]*COS(M*YBAR)/EXP(S(M)*X);
IMA0:=PI*CH(ALPHA*YBAR)*COS(KO*XBAR)
/(4*ALPHA) -Z
END;

FUNCTION REF1(X,Y:REAL):REAL;
VAR M:INTEGER;XBAR,YBAR,Z:REAL;
BEGIN
XBAR:=X+0.427;YBAR:=Y-PI/2;
Z:=0;FOR M:=1 TO 10 DO
Z:=Z+AEM]*COS(M*YBAR)/EXP(S(M)*X);
REF1:=PI*CH(ALPHA*YBAR)*SIN(KO*XBAR)/(4*ALPHA) -Z
END;

FUNCTION IMF1(X,Y:REAL):REAL;
VAR M:INTEGER;XBAR,YBAR,Z:REAL;
BEGIN
XBAR:=X+0.427;YBAR:=Y-PI/2;
Z:=0;FOR M:=1 TO 10 DO
Z:=Z+BEH]*SIN(M*YBAR)/EXP(S(M)*X);
IMF1:=-PI*SH(ALPHA*YBAR)*COS(KO*XBAR)/(4*ALPHA) -Z
END;

```

FUNCTION REF2(X,Y:REAL):REAL;
VAR M:INTEGER;YBAR,Z:REAL;
BEGIN
  YBAR:=Y-PI/2;Z:=0;
  FOR M:=1 TO 10 DO
    Z:=Z+DCM]*SIN(M*YBAR)/EXP(S(M)*X);
  REF2:=-Z
END;

```

```

FUNCTION IMF2(X,Y:REAL):REAL;
VAR M:INTEGER;YBAR,Z:REAL;
BEGIN
  YBAR:=Y-PI/2;Z:=0;
  FOR M:=1 TO 10 DO
    Z:=Z+CEM]*COS(M*YBAR)/EXP(S(M)*X);
  IMF2:=-Z
END;

```

```

FUNCTION REF1X(X,Y:REAL):REAL;
VAR M:INTEGER;XBAR,YBAR,Z:REAL;
BEGIN
  XBAR:=X+0.427;YBAR:=Y-PI/2;
  Z:=0;FOR M:=1 TO 10 DO
    Z:=Z+S(M)*ACM]*COS(M*YBAR)/EXP(S(M)*X);
  REF1X:=PI*DELTA*CH(ALPHA*YBAR)*COS(KO*XBAR)/4 +Z
END;

```

```

FUNCTION IMF1X(X,Y:REAL):REAL;
VAR M:INTEGER;XBAR,YBAR,Z:REAL;
BEGIN
  XBAR:=X+0.427;YBAR:=Y-PI/2;
  Z:=0;FOR M:=1 TO 10 DO
    Z:=Z+S(M)*BCM]*SIN(M*YBAR)/EXP(S(M)*X);
  IMF1X:=PI*DELTA*SH(ALPHA*YBAR)*SIN(KO*XBAR)/4 +Z
END;

```

```

FUNCTION REF1Y(X,Y:REAL):REAL;
VAR M:INTEGER;XBAR,YBAR,Z:REAL;
BEGIN
  XBAR:=X+0.427;YBAR:=Y-PI/2;
  Z:=0;FOR M:=1 TO 10 DO
    Z:=Z+M*ACM]*SIN(M*YBAR)/EXP(S(M)*X);
  REF1Y:=PI*SH(ALPHA*YBAR)*SIN(KO*XBAR)/4 +Z
END;

```

```

FUNCTION IMF1Y(X,Y:REAL):REAL;
VAR M:INTEGER;XBAR,YBAR,Z:REAL;
BEGIN
  XBAR:=X+0.427;YBAR:=Y-PI/2;
  Z:=0;FOR M:=1 TO 10 DO
    Z:=Z+M*BCM]*COS(M*YBAR)/EXP(S(M)*X);
  IMF1Y:=-PI*CH(ALPHA*YBAR)*COS(KO*XBAR)/4 -Z
END;

```

```

FUNCTION REF2X(X,Y:REAL):REAL;
VAR M:INTEGER;YBAR,Z:REAL;
BEGIN
  YBAR:=Y-PI/2;
  Z:=0;FOR M:=1 TO 10 DO
    Z:=Z+S(M)*DCM]*SIN(M*YBAR)/EXP(S(M)*X);

```

```

REF2X:=Z
END;

FUNCTION IMF2X(X,Y:REAL):REAL;
VAR M:INTEGER;YBAR,Z:REAL;
BEGIN
  YBAR:=Y-PI/2;
  Z:=0;FOR M:=1 TO 10 DO
  Z:=Z+S(M)*CCM]*COS(M*YBAR)/EXP(S(M)*X);
  IMF2X:=Z
END;

FUNCTION REF2Y(X,Y:REAL):REAL;
VAR M:INTEGER;YBAR,Z:REAL;
BEGIN
  YBAR:=Y-PI/2;
  Z:=0;FOR M:=1 TO 10 DO
  Z:=Z+M*DCM]*COS(M*YBAR)/EXP(S(M)*X);
  REF2Y:=-Z
END;

FUNCTION IMF2Y(X,Y:REAL):REAL;
VAR M:INTEGER;YBAR,Z:REAL;
BEGIN
  YBAR:=Y-PI/2;
  Z:=0;FOR M:=1 TO 10 DO
  Z:=Z+M*CCM]*SIN(M*YBAR)/EXP(S(M)*X);
  IMF2Y:=Z
END;

FUNCTION REAOX(X,Y:REAL):REAL;
BEGIN
  REAOX:=ALPHA*REF2(X,Y)+K0*IMF1(X,Y)
END;

FUNCTION IMAOX(X,Y:REAL):REAL;
BEGIN
  IMAOX:=ALPHA*IMF2(X,Y)-K0*REF1(X,Y)
END;

FUNCTION REAOY(X,Y:REAL):REAL;
BEGIN
  REAOY:=-ALPHA*REF1(X,Y)+K0*IMF2(X,Y)
END;

FUNCTION IMAOY(X,Y:REAL):REAL;
BEGIN
  IMAOY:=-ALPHA*IMF1(X,Y)-K0*REF2(X,Y)
END;

FUNCTION REAOXX(X,Y:REAL):REAL;
BEGIN
  REAOXX:=ALPHA*REF2X(X,Y)+K0*IMF1X(X,Y)
END;

FUNCTION IMAOXX(X,Y:REAL):REAL;
BEGIN
  IMAOXX:=ALPHA*IMF2X(X,Y)-K0*REF1X(X,Y)
END;

FUNCTION REAOYY(X,Y:REAL):REAL;

```

```

3BEGIN
  REAOYY:=-ALPHA*REF1Y(X,Y)+K0*IMF2Y(X,Y)
END:

FUNCTION IMAOYY(X,Y:REAL):REAL;
BEGIN
  IMAOYY:=-ALPHA*IMF1Y(X,Y)-K0*REF2Y(X,Y)
END:

FUNCTION REAOXY(X,Y:REAL):REAL;
BEGIN
  REAOXY:=ALPHA*REF2Y(X,Y)+K0*IMF1Y(X,Y)
END:

FUNCTION IMAOXY(X,Y:REAL):REAL;
BEGIN
  IMAOXY:=ALPHA*IMF2Y(X,Y)-K0*REF1Y(X,Y)
END:

FUNCTION REOMEGA1(X:REAL):REAL;
3BEGIN
  REOMEGA1:=SQRT((DELTA+1)/2)*EXP(C0*X)*3
END:

FUNCTION IMOMEGA1(X:REAL):REAL;
3BEGIN IMOMEGA1:=REOMEGA1(X) END:

FUNCTION REOMEGA2(X:REAL):REAL;
3BEGIN
  REOMEGA2:=SQRT((DELTA-1)/2)*EXP(C0*X)*3
END:

FUNCTION IMOMEGA2(X:REAL):REAL;
3BEGIN IMOMEGA2:=REOMEGA2(X) END:

FUNCTION MODOMEGA1(X:REAL):REAL;
BEGIN
  MODOMEGA1:=SQRT(REOMEGA1(X)**2+IMOMEGA1(X)**2)
END:

FUNCTION MODOMEGA2(X:REAL):REAL;
BEGIN
  MODOMEGA2:=SQRT(REOMEGA2(X)**2+IMOMEGA2(X)**2)
END:

FUNCTION REGAMMA1(X:REAL):REAL;
BEGIN
  REGAMMA1:=ALPHA*((DELTA-1)*IMOMEGA1(X)
    /MODOMEGA1(X)**2 +(DELTA+1)*IMOMEGA2(X)
    /MODOMEGA2(X)**2) /(2*KH*KH)
END:

FUNCTION IMGAMMA1(X:REAL):REAL;
BEGIN
  IMGAMMA1:=ALPHA*((DELTA-1)*REOMEGA1(X)
    /MODOMEGA1(X)**2 +(DELTA+1)*IMOMEGA2(X)
    /MODOMEGA2(X)**2) /(2*KH*KH)
END:

FUNCTION REGAMMA2(X:REAL):REAL;
3BEGIN

```

```

REGAMMA2:=ALPHA*((DELTA-1)*IMOMEGA1(X)
/MODOMEGA1(X)**2 -(DELTA+1)*IMOMEGA2(X)
/MODOMEGA2(X)**2)/(2*KH*KH)
END;

FUNCTION IMGAMMA2(X:REAL):REAL;
BEGIN
IMGAMMA2:=ALPHA*((DELTA-1)*REOMEGA1(X)
/MODOMEGA1(X)**2 -(DELTA+1)*REOMEGA2(X)
/MODOMEGA2(X)**2)/(2*KH*KH)
END;

FUNCTION REEAO(X,Y:REAL):REAL;
BEGIN
REEAO:=KH*KH*REGAMMA1(X)*REAO(X,Y)
-KH*KH*IMGAMMA1(X)*IMAO(X,Y)
+CO*REGAMMA1(X)*REAOX(X,Y)
-CO*IMGAMMA1(X)*IMAOX(X,Y)
-CO*REGAMMA2(X)*REAOY(X,Y)
-CO*IMGAMMA2(X)*IMAOY(X,Y)
END;

FUNCTION IMEAO(X,Y:REAL):REAL;
BEGIN
IMEAO:=KH*KH*REGAMMA1(X)*IMAO(X,Y)
+KH*KH*IMGAMMA1(X)*REAO(X,Y)
+CO*REGAMMA1(X)*IMAOX(X,Y)
+CO*IMGAMMA1(X)*REAOX(X,Y)
+CO*REGAMMA2(X)*REAOY(X,Y)
-CO*IMGAMMA2(X)*IMAOY(X,Y)
END;

FUNCTION REDXEO(X,Y:REAL):REAL;
BEGIN
REDXEO:=-KH*KH*CO*REGAMMA1(X)*REAO(X,Y)
+KH*KH*REGAMMA1(X)*REAOX(X,Y)
+KH*KH*CO*IMGAMMA1(X)*IMAO(X,Y)
-KH*KH*IMGAMMA1(X)*IMAOX(X,Y)
-CO*CO*REGAMMA1(X)*REAOX(X,Y)
+CO*REGAMMA1(X)*REAOXX(X,Y)
+CO*CO*IMGAMMA1(X)*IMAOX(X,Y)
-CO*IMGAMMA1(X)*IMAOXX(X,Y)
+CO*CO*REGAMMA2(X)*IMAOY(X,Y)
-CO*REGAMMA2(X)*IMAOXY(X,Y)
+CO*CO*IMGAMMA2(X)*REAOY(X,Y)
-CO*IMGAMMA2(X)*REAOXY(X,Y)
END;

FUNCTION IMDXEO(X,Y:REAL):REAL;
BEGIN
IMDXEO:=-KH*KH*CO*REGAMMA1(X)*IMAO(X,Y)
+KH*KH*REGAMMA1(X)*IMAOX(X,Y)
-KH*KH*CO*IMGAMMA1(X)*REAO(X,Y)
+KH*KH*IMGAMMA1(X)*REAOX(X,Y)
-CO*CO*REGAMMA1(X)*IMAOX(X,Y)
+CO*REGAMMA1(X)*IMAOXX(X,Y)
-CO*CO*IMGAMMA1(X)*REAOX(X,Y)
+CO*IMGAMMA1(X)*REAOXX(X,Y)
-CO*CO*REGAMMA2(X)*REAOY(X,Y)
+CO*REGAMMA2(X)*REAOXY(X,Y)
+CO*CO*IMGAMMA2(X)*IMAOY(X,Y)

```

```

                                -CO*IMGAMMA2(X)*IMAOXY(X,Y)
END:

FUNCTION REDYEA0(X,Y:REAL):REAL:
BEGIN
  REDYEA0:=KH*KH*REGAMMA1(X)*REAOY(X,Y)
            -KH*KH*IMGAMMA1(X)*IMAOY(X,Y)
            +CO*REGAMMA1(X)*REAOXY(X,Y)
            -CO*IMGAMMA1(X)*IMAOXY(X,Y)
            -CO*REGAMMA2(X)*IMAOYY(X,Y)
            -CO*IMGAMMA2(X)*REAOYY(X,Y)
END:

FUNCTION IMDYEA0(X,Y:REAL):REAL:
BEGIN
  IMDYEA0:=KH*KH*REGAMMA1(X)*IMAOY(X,Y)
            +KH*KH*IMGAMMA1(X)*REAOY(X,Y)
            +CO*REGAMMA1(X)*IMAOXY(X,Y)
            +CO*IMGAMMA1(X)*REAOXY(X,Y)
            +CO*REGAMMA2(X)*REAOYY(X,Y)
            -CO*IMGAMMA2(X)*IMAOYY(X,Y)
END:

FUNCTION REQ(Y:REAL):REAL:
BEGIN
  REQ:=IMEA0(0,Y)/DELTA
END:

FUNCTION IMQ(Y:REAL):REAL:
BEGIN
  IMQ:=-REEA0(0,Y)/DELTA
END:

FUNCTION REP(X,Y:REAL):REAL:
BEGIN
  REP:=-REDYEA0(X,Y)+IMDXEA0(X,Y)/DELTA
END:

FUNCTION IMP(X,Y:REAL):REAL:
BEGIN
  IMP:=-IMDYEA0(X,Y)-REDXEA0(X,Y)/DELTA
END:

BEGIN
  PI:=4*ARCTAN(1);DELTA:=1.229;
  KO:=0.8602;ALPHA:=0.7;KH:=0.5;CO:=0.1;

  RESET(ABCD);
  FOR I:=1 TO 10 DO
  BEGIN
    READ(ABCD,ACIJ);
    READ(ABCD,BCIJ);
    READ(ABCD,CCIJ);
    READ(ABCD,DCIJ);
    PCIJ:=(S(I)*BCIJ+I*CCIJ)/KO;
    QCIJ:=(I*DCIJ-S(I)*ACIJ)/KO
  END:

  (*OUTPUT ON PANDQ.DAT *)
  REWRITE(PANDQ);

```

```

WRITELN(PANDQ);WRITELN(PANDQ);
FOR I:=0 TO 10 DO
FOR J:=0 TO 10 DO
BEGIN
  X:=I*PI/5;Y:=J*PI/10;
  WRITELN(PANDQ,X:9:5,Y:9:5,REP(X,Y):13:6,IMP(X,Y):13:6)
END;

WRITELN(PANDQ);WRITELN(PANDQ);
FOR J:=0 TO 10 DO
BEGIN
  X:=0.0;Y:=J*PI/10;
  WRITELN(PANDQ,X:9:5,Y:9:5,REQ(Y):13:6,IMQ(Y):13:6)
END;

(* REAL AND IMAGINARY PARTS OF EAO
ARE OUTPUT TO EAO.DAT *)
REWRITE(EAO);

FOR I:=0 TO 10 DO FOR J:=0 TO 10 DO
BEGIN
  X:=I*PI/5;Y:=J*PI/10;
  WRITELN(EAO,X:9:5,Y:9:5,REEAO(X,Y):13:6,IMEAO(X,Y):13:6)
END
END.

```

PROGRAM 4.

(* F2 AND DERIVATIVES ARE
CALCULATED FROM EQUATIONS
4510.2,8 AND11 *)

```
VAR I,J,K,N,COUNT:INTEGER;
    X,Y,PI,EPS,KH,DELTA,ALPHA,KO,REQO,IMQO:REAL;
    REF2,IMF2:ARRAY [0..2] OF REAL;
    REP1,IMP1:ARRAY [0..10,0..10] OF REAL;
    REQ1,IMQ1:ARRAY [0..10] OF REAL;
    U1,V1,U1X,V1X,U1Y,V1Y:ARRAY [1..10,0..10,0..10] OF REAL;
    PANDQ,GFC,F2ETC:TEXT;
```

```
FUNCTION S(I:INTEGER):REAL;
BEGIN S:=SQRT(I*I-KH*KH) END;
```

```
FUNCTION REQ(Y:REAL):REAL;
BEGIN
    REQ:=REQ1[ROUND(10*Y/PI)]+REQO
END;
```

```
FUNCTION IMQ(Y:REAL):REAL;
BEGIN
    IMQ:=IMQ1[ROUND(10*Y/PI)]+IMQO
END;
```

```
FUNCTION REP(X,Y:REAL):REAL;
BEGIN
    REP:=REP1[ROUND(5*X/PI),ROUND(10*Y/PI)]
END;
```

```
FUNCTION IMP(X,Y:REAL):REAL;
BEGIN
    IMP:=IMP1[ROUND(5*X/PI),ROUND(10*Y/PI)]
END;
```

```
FUNCTION U(R:INTEGER;X,Y:REAL):REAL;
BEGIN
    U:=U1[R,ROUND(5*X/PI),ROUND(10*Y/PI)]
END;
```

```
FUNCTION V(R:INTEGER;X,Y:REAL):REAL;
BEGIN
    V:=V1[R,ROUND(5*X/PI),ROUND(10*Y/PI)]
END;
```

```
FUNCTION UY(R:INTEGER;X,Y:REAL):REAL;
BEGIN
    UY:=U1Y[R,ROUND(5*X/PI),ROUND(10*Y/PI)]
END;
```

```
FUNCTION VY(R:INTEGER;X,Y:REAL):REAL;
BEGIN
    VY:=V1Y[R,ROUND(5*X/PI),ROUND(10*Y/PI)]
END;
```

```
FUNCTION UX(R:INTEGER;X,Y:REAL):REAL;
BEGIN
    UX:=U1X[R,ROUND(5*X/PI),ROUND(10*Y/PI)]
END;
```

```

FUNCTION VX(R:INTEGER;X,Y:REAL):REAL;
BEGIN
  VX:=V1XR,ROUND(5*X/PI),ROUND(10*Y/PI))
END;

```

```

FUNCTION REG(X,Y,X0,Y0:REAL):REAL;
VAR R:INTEGER;Z:REAL;
BEGIN
  Z:=0;
  FOR R:=1 TO 10 DO
    Z:=Z+EPS*SIN(R*Y)*SIN(R*Y0)
      *(EXP(-S(R)*ABS(X-X0))
      -EXP(-S(R)*(X+X0)))/S(R)
      +U(R,X,Y)*SIN(R*Y0)/EXP(S(R)*X0);
  REG:=Z
END;

```

```

FUNCTION IMG(X,Y,X0,Y0:REAL):REAL;
VAR R:INTEGER;Z:REAL;
BEGIN
  Z:=0;
  FOR R:=1 TO 10 DO
    Z:=Z+V(R,X,Y)*SIN(R*Y0)/EXP(S(R)*X0);
  IMG:=Z
END;

```

```

FUNCTION REGY(X,Y,X0,Y0:REAL):REAL;
VAR R:INTEGER;Z:REAL;
BEGIN
  Z:=0;
  FOR R:=1 TO 10 DO
    Z:=Z+EPS*R*COS(R*Y)*SIN(R*Y0)
      *(EXP(-S(R)*ABS(X-X0))
      -EXP(-S(R)*(X+X0)))/S(R)
      +UY(R,X,Y)*SIN(R*Y0)/EXP(S(R)*X0);
  REGY:=Z
END;

```

```

FUNCTION IMGY(X,Y,X0,Y0:REAL):REAL;
VAR R:INTEGER;Z:REAL;
BEGIN
  Z:=0;
  FOR R:=1 TO 10 DO
    Z:=Z+VY(R,X,Y)*SIN(R*Y0)/EXP(S(R)*X0);
  IMGY:=Z
END;

```

```

FUNCTION REGX(X,Y,X0,Y0:REAL):REAL;
VAR R:INTEGER;Z,DO:REAL;
BEGIN
  IF X>X0 THEN DO:=-1;
  IF X<X0 THEN DO:=+1;
  IF ABS(X-X0)<1E-8 THEN DO:=0;
  Z:=0;
  FOR R:=1 TO 10 DO
    Z:=Z+DO*EPS*SIN(R*Y)*SIN(R*Y0)
      *(EXP(DO*S(R)*(X-X0))
      +DO*EXP(-S(R)*(X+X0))
      +UX(R,X,Y)*SIN(R*Y0)/EXP(S(R)*X0);

```

```
REGX:=Z
END;
```

```
FUNCTION IMGX(X,Y,X0,Y0:REAL):REAL;
VAR R:INTEGER;Z:REAL;
BEGIN
  Z:=0;
  FOR R:=1 TO 10 DO
    Z:=Z+VX(R,X,Y)*SIN(R*Y0)/EXP(S(R)*X0);
  IMGX:=Z
END;
```

```
FUNCTION F1(X,Y,X0,Y0:REAL):REAL;
BEGIN
  IF N=0 THEN
    F1:=REP(X0,Y0)*REG(X,Y,X0,Y0)
      -IMP(X0,Y0)*IMG(X,Y,X0,Y0);
  IF N=1 THEN
    F1:=REP(X0,Y0)*REGX(X,Y,X0,Y0)
      -IMP(X0,Y0)*IMGX(X,Y,X0,Y0);
  IF N=2 THEN
    F1:=REP(X0,Y0)*REGY(X,Y,X0,Y0)
      -IMP(X0,Y0)*IMGY(X,Y,X0,Y0)
END;
```

```
FUNCTION F2(X,Y,X0,Y0:REAL):REAL;
BEGIN
  IF N=0 THEN
    F2:=REQ(Y0)*REG(X,Y,X0,Y0)
      -IMQ(Y0)*IMG(X,Y,X0,Y0);
  IF N=1 THEN
    F2:=REQ(Y0)*REGX(X,Y,X0,Y0)
      -IMQ(Y0)*IMGX(X,Y,X0,Y0);
  IF N=2 THEN
    F2:=REQ(Y0)*REGY(X,Y,X0,Y0)
      -IMQ(Y0)*IMGY(X,Y,X0,Y0)
END;
```

```
FUNCTION F3(X,Y,X0,Y0:REAL):REAL;
BEGIN
  IF N=0 THEN
    F3:=REP(X0,Y0)*IMG(X,Y,X0,Y0)
      +IMP(X0,Y0)*REG(X,Y,X0,Y0);
  IF N=1 THEN
    F3:=REP(X0,Y0)*IMGX(X,Y,X0,Y0)
      +IMP(X0,Y0)*REGX(X,Y,X0,Y0);
  IF N=2 THEN
    F3:=REP(X0,Y0)*IMGY(X,Y,X0,Y0)
      +IMP(X0,Y0)*REGY(X,Y,X0,Y0)
END;
```

```
FUNCTION F4(X,Y,X0,Y0:REAL):REAL;
BEGIN
  IF N=0 THEN
    F4:=REQ(Y0)*IMG(X,Y,X0,Y0)
      +IMQ(Y0)*REG(X,Y,X0,Y0);
  IF N=1 THEN
    F4:=REQ(Y0)*IMGX(X,Y,X0,Y0)
      +IMQ(Y0)*REGX(X,Y,X0,Y0);
  IF N=2 THEN
    F4:=REQ(Y0)*IMGY(X,Y,X0,Y0)
      +IMQ(Y0)*REGY(X,Y,X0,Y0)
END;
```

```

      +IMQ(Y0)*REGY(X,Y,X0,Y0)
END:

FUNCTION G1(X0,Y0:REAL):REAL:
BEGIN
  G1:=F1(X,Y,X0,Y0)
END:

FUNCTION G2(X0,Y0:REAL):REAL:
BEGIN
  G2:=F2(X,Y,0,Y0)
END:

FUNCTION G3(X0,Y0:REAL):REAL:
BEGIN
  G3:=F3(X,Y,X0,Y0)
END:

FUNCTION G4(X0,Y0:REAL):REAL:
BEGIN
  G4:=F4(X,Y,0,Y0)
END:

(* SPACE INTEGRATION BY REPEATED
USE OF SIMPSON'S RULE *)
FUNCTION INT(FUNCTION F(X,Y:REAL):REAL:
            XMIN,XMAX,YMIN,YMAX:REAL):REAL:
VAR X1,Y1,HX,HY,SUM:REAL:
    I,J:INTEGER:
    F1:ARRAY [0..10,0..10] OF REAL:
    C:ARRAY [0..10] OF REAL:
BEGIN
  HX:=(XMAX-XMIN)/10;HY:=(YMAX-YMIN)/10;SUM:=0:
  FOR I:=1 TO 9 DO
    IF I MOD 2=0 THEN C[I]:=2
    ELSE C[I]:=4:
  C[0]:=1:C[10]:=1:

  FOR I:=0 TO 10 DO FOR J:=0 TO 10 DO
    BEGIN
      X1:=XMIN+I*HX:
      Y1:=YMIN+J*HY:
      F1[I,J]:=F(X1,Y1):
      SUM:=SUM+C[I]*C[J]*F1[I,J]
    END:
  INT:=HX*HY*SUM/9
END:

BEGIN
  (* INPUT FROM GFC.DAT *)
  RESET(GFC):

  FOR N:=1 TO 3 DO
    FOR J:=0 TO 10 DO
      FOR K:=0 TO 10 DO
        FOR I:=1 TO 10 DO
          BEGIN
            READ(GFC,X);READ(GFC,Y):
            IF N=1 THEN
              BEGIN READ(GFC,U1[I,J,K]);READ(GFC,V1[I,J,K]) END:

```

```

      IF N=2 THEN
      BEGIN READ(GFC,U1YCI,J,KJ);READ(GFC,V1YCI,J,KJ) END;
      IF N=3 THEN
      BEGIN READ(GFC,U1XCI,J,KJ);READ(GFC,V1XCI,J,KJ) END
END;

(* INPUT FROM PANDQ.DAT *)
RESET(PANDQ);

FOR I:=0 TO 10 DO FOR J:=0 TO 10 DO
BEGIN
  READ(PANDQ,X);READ(PANDQ,Y);
  READ(PANDQ,REP1CI,JJ);READ(PANDQ,IMP1CI,JJ)
END;

FOR J:=0 TO 10 DO
BEGIN
  READ(PANDQ,X);READ(PANDQ,Y);
  READ(PANDQ,REQ1CJJ);READ(PANDQ,IMQ1CJJ)
END;

PI:=4*ARCTAN(1);EPS:=-1/PI;DELTA:=1.229;
K0:=0.8602;ALPHA:=0.7;KH:=0.5;COUNT:=0;
REQ0:=0;IMQ0:=0;

(* OUTPUT ON F2ETC.DAT *)
REWRITE(F2ETC);
FOR N:=0 TO 2 DO
FOR I:=0 TO 10 DO
FOR J:=0 TO 10 DO
BEGIN
  X:=I*PI/5;Y:=J*PI/10;

  REF2CNJ:=INT(G1,0,2*PI,0,PI)
  +INT(G2,0,1,0,PI);

  IMF2CNJ:=INT(G3,0,2*PI,0,PI)
  +INT(G4,0,1,0,PI);

  IF COUNT MOD 11 =0 THEN WRITELN(F2ETC);
  IF COUNT MOD 121 =0 THEN WRITELN(F2ETC);
  COUNT:=COUNT+1;
  WRITELN(F2ETC,X:9:5,Y:9:5,REF2CNJ:13:6,IMF2CNJ:13:6)
END
END.

```

```

IF N=2 THEN
BEGIN READ(GFC,U1YCI,J,K);READ(GFC,V1YCI,J,K) END:
IF N=3 THEN
BEGIN READ(GFC,U1XCI,J,K);READ(GFC,V1XCI,J,K) END
END:

(* INPUT FROM PANDQ.DAT *)
RESET(PANDQ);

FOR I:=0 TO 10 DO FOR J:=0 TO 10 DO
BEGIN
READ(PANDQ,X);READ(PANDQ,Y);
READ(PANDQ,REP1CI,J);READ(PANDQ,IMP1CI,J)
END:

FOR J:=0 TO 10 DO
BEGIN
READ(PANDQ,X);READ(PANDQ,Y);
READ(PANDQ,REQ1CJ);READ(PANDQ,IMQ1CJ)
END:

PI:=4*ARCTAN(1);EPS:=-1/PI;DELTA:=1.229;
K0:=0.8602;ALPHA:=0.7;KH:=0.5;COUNT:=0;
REQ0:=0;IMQ0:=0;

(* OUTPUT ON F2ETC.DAT *)
REWRITE(F2ETC);
FOR N:=0 TO 2 DO
FOR I:=0 TO 10 DO
FOR J:=0 TO 10 DO
BEGIN
X:=I*PI/5;Y:=J*PI/10;

REF2CNJ:=INT(G1,0,2*PI,0,PI)
+INT(G2,0,1,0,PI);

IMF2CNJ:=INT(G3,0,2*PI,0,PI)
+INT(G4,0,1,0,PI);

IF COUNT MOD 11 =0 THEN WRITELN(F2ETC);
IF COUNT MOD 121 =0 THEN WRITELN(F2ETC);
COUNT:=COUNT+1;
WRITELN(F2ETC,X:9:5,Y:9:5,REF2CNJ:13:6,IMF2CNJ:13:6)
END
END.

```

PROGRAM 5.

(* A AND F1 ARE CALCULATED FROM
EQUATIONS 4511.3 AND 7 *)

VAR REF21, IMF21, REF2X1, IMF2X1, REF2Y1, IMF2Y1,
REEA01, IMEA01: ARRAY [0..11, 0..11] OF REAL;
I, J: INTEGER;
X, Y, PI, ALPHA, KO, DELTA, REBETA1, IMBETA1: REAL;
EAO, F2ETC, AANDF1: TEXT;

FUNCTION INT(FUNCTION F(X: REAL): REAL; XMIN, XMAX: REAL): REAL;
VAR X1, HX, SUM: REAL; I: INTEGER;
C, F1: ARRAY [0..100] OF REAL;

BEGIN
HX := (XMAX - XMIN) / 100; SUM := 0;
FOR I := 1 TO 99 DO
IF I MOD 2 = 0 THEN C[I] := 2
ELSE C[I] := 4;
C[0] := 1; C[100] := 1;

FOR I := 0 TO 100 DO
BEGIN
X1 := XMIN + I * HX;
F1[I] := F(X1);
SUM := SUM + C[I] * F1[I]
END;
INT := HX * SUM / 3
END;

FUNCTION REF2(X, Y: REAL): REAL;
VAR I, J: INTEGER; X1, X2, Y1, Y2: REAL;
BEGIN
I := TRUNC(5 * X / PI); J := TRUNC(10 * Y / PI);
X1 := 5 * X / PI - I; Y1 := 10 * Y / PI - J;
X2 := 1 - X1; Y2 := 1 - Y1;

REF2 := X2 * Y2 * REF21[I, J]
+ X1 * Y1 * REF21[I + 1, J + 1]
+ X1 * Y2 * REF21[I + 1, J]
+ X2 * Y1 * REF21[I, J + 1]
END;

FUNCTION IMF2(X, Y: REAL): REAL;
VAR I, J: INTEGER; X1, X2, Y1, Y2: REAL;
BEGIN
I := TRUNC(5 * X / PI); J := TRUNC(10 * Y / PI);
X1 := 5 * X / PI - I; Y1 := 10 * Y / PI - J;
X2 := 1 - X1; Y2 := 1 - Y1;

IMF2 := X2 * Y2 * IMF21[I, J]
+ X1 * Y1 * IMF21[I + 1, J + 1]
+ X1 * Y2 * IMF21[I + 1, J]
+ X2 * Y1 * IMF21[I, J + 1]
END;

FUNCTION REF2X(X, Y: REAL): REAL;
VAR I, J: INTEGER; X1, X2, Y1, Y2: REAL;
BEGIN
I := TRUNC(5 * X / PI); J := TRUNC(10 * Y / PI);
X1 := 5 * X / PI - I; Y1 := 10 * Y / PI - J;

```

X2:=1-X1;Y2:=1-Y1;

REF2X:=X2*Y2*REF2X1[I,J]
      +X1*Y1*REF2X1[I+1,J+1]
      +X1*Y2*REF2X1[I+1,J]
      +X2*Y1*REF2X1[I,J+1]
END;

FUNCTION IMF2X(X,Y:REAL):REAL;
VAR I,J:INTEGER;X1,X2,Y1,Y2:REAL;
BEGIN
  I:=TRUNC(5*X/PI);J:=TRUNC(10*Y/PI);
  X1:=5*X/PI -I;Y1:=10*Y/PI-J;
  X2:=1-X1;Y2:=1-Y1;

  IMF2X:=X2*Y2*IMF2X1[I,J]
        +X1*Y1*IMF2X1[I+1,J+1]
        +X1*Y2*IMF2X1[I+1,J]
        +X2*Y1*IMF2X1[I,J+1]
END;

FUNCTION REF2Y(X,Y:REAL):REAL;
VAR I,J:INTEGER;X1,X2,Y1,Y2:REAL;
BEGIN
  I:=TRUNC(5*X/PI);J:=TRUNC(10*Y/PI);
  X1:=5*X/PI -I;Y1:=10*Y/PI-J;
  X2:=1-X1;Y2:=1-Y1;

  REF2Y:=X2*Y2*REF2Y1[I,J]
        +X1*Y1*REF2Y1[I+1,J+1]
        +X1*Y2*REF2Y1[I+1,J]
        +X2*Y1*REF2Y1[I,J+1]
END;

FUNCTION IMF2Y(X,Y:REAL):REAL;
VAR I,J:INTEGER;X1,X2,Y1,Y2:REAL;
BEGIN
  I:=TRUNC(5*X/PI);J:=TRUNC(10*Y/PI);
  X1:=5*X/PI -I;Y1:=10*Y/PI-J;
  X2:=1-X1;Y2:=1-Y1;

  IMF2Y:=X2*Y2*IMF2Y1[I,J]
        +X1*Y1*IMF2Y1[I+1,J+1]
        +X1*Y2*IMF2Y1[I+1,J]
        +X2*Y1*IMF2Y1[I,J+1]
END;

FUNCTION REEA0(X,Y:REAL):REAL;
VAR I,J:INTEGER;X1,X2,Y1,Y2:REAL;
BEGIN
  I:=TRUNC(5*X/PI);J:=TRUNC(10*Y/PI);
  X1:=5*X/PI -I;Y1:=10*Y/PI-J;
  X2:=1-X1;Y2:=1-Y1;

  REEA0:=X2*Y2*REEA01[I,J]
        +X1*Y1*REEA01[I+1,J+1]
        +X1*Y2*REEA01[I+1,J]
        +X2*Y1*REEA01[I,J+1]
END;

FUNCTION IMEA0(X,Y:REAL):REAL;

```

```

VAR I,J:INTEGER;X1,X2,Y1,Y2:REAL;
BEGIN
  I:=TRUNC(5*X/PI);J:=TRUNC(10*Y/PI);
  X1:=5*X/PI -I;Y1:=10*Y/PI-J;
  X2:=1-X1;Y2:=1-Y1;

  IMEA0:=X2*Y2*IMEA01[I,J]
        +X1*Y1*IMEA01[I+1,J+1]
        +X1*Y2*IMEA01[I+1,J]
        +X2*Y1*IMEA01[I,J+1]
END;

FUNCTION RERHO(X,Y:REAL):REAL;
BEGIN
  RERHO:=ALPHA*REF2X(X,Y)
        -K0*IMF2Y(X,Y)
        -K0*IMEA0(X,Y)
END;

FUNCTION IMRHO(X,Y:REAL):REAL;
BEGIN
  IMRHO:=ALPHA*IMF2X(X,Y)
        +K0*REF2Y(X,Y)
        +K0*REEA0(X,Y)
END;

FUNCTION F1(X:REAL):REAL;
BEGIN
  F1:=(RERHO(X,Y)*SIN(K0*X)
        -IMRHO(X,Y)*COS(K0*X))/(2*K0)
END;

FUNCTION F2(X:REAL):REAL;
BEGIN
  F2:=(RERHO(X,Y)*COS(K0*X)
        +IMRHO(X,Y)*SIN(K0*X))/(2*K0)
END;

FUNCTION F3(X:REAL):REAL;
BEGIN
  F3:=(RERHO(X,Y)*SIN(K0*X)
        +IMRHO(X,Y)*COS(K0*X))/(2*K0)
END;

FUNCTION F4(X:REAL):REAL;
BEGIN
  F4:=(-RERHO(X,Y)*COS(K0*X)
        +IMRHO(X,Y)*SIN(K0*X))/(2*K0)
END;

FUNCTION RERHO1(X,Y:REAL):REAL;
BEGIN
  RERHO1:=INT(F1,X,2*PI)-IMBETA1*EXP(ALPHA*(Y-PI/2))
END;

FUNCTION IMRHO1(X,Y:REAL):REAL;
BEGIN
  IMRHO1:=INT(F2,X,2*PI)+REBETA1*EXP(ALPHA*(Y-PI/2))
END;

FUNCTION RERHO2(X,Y:REAL):REAL;

```

```

3EGIN
  RERHO2:=-INT(F3,0,X)
            -IMF2(0,Y)/DELTA +RERHO1(0,Y)
END;

FUNCTION IMRHO2(X,Y:REAL):REAL;
3EGIN
  IMRHO2:=-INT(F4,0,X)
            +REF2(0,Y)/DELTA +IMRHO1(0,Y)
END;

FUNCTION REA(X,Y:REAL):REAL;
3EGIN
  REA:=(RERHO1(X,Y)-RERHO2(X,Y))*COS(K0*X)
        +(IMRHO2(X,Y)-IMRHO1(X,Y))*SIN(K0*X)
END;

FUNCTION IMA(X,Y:REAL):REAL;
3EGIN
  IMA:=(IMRHO1(X,Y)+IMRHO2(X,Y))*COS(K0*X)
        +(RERHO1(X,Y)-RERHO2(X,Y))*SIN(K0*X)
END;

FUNCTION REAX(X,Y:REAL):REAL;
3EGIN
  REAX:=-K0*(RERHO1(X,Y)+RERHO2(X,Y))*SIN(K0*X)
        +K0*(IMRHO2(X,Y)-IMRHO1(X,Y))*COS(K0*X)
END;

FUNCTION IMAX(X,Y:REAL):REAL;
3EGIN
  IMAX:=K0*(RERHO1(X,Y)-RERHO2(X,Y))*COS(K0*X)
        -K0*(IMRHO1(X,Y)+IMRHO2(X,Y))*SIN(K0*X)
END;

FUNCTION REF1(X,Y:REAL):REAL;
3EGIN
  REF1:=(-IMAX(X,Y)+ALPHA*IMF2(X,Y))/K0
END;

FUNCTION IMF1(X,Y:REAL):REAL;
3EGIN
  IMF1:=(REAX(X,Y)-ALPHA*REF2(X,Y))/K0
END;

3EGIN
  ALPHA:=0.7;K0:=0.8602;PI:=4*ARCTAN(1);DELTA:=1.229;
  IMBETA1:=0.6; REBETA1:=0.4;

  RESET(F2ETC);

  FOR I:=0 TO 10 DO FOR J:=0 TO 10 DO
  BEGIN
    READ(F2ETC,X);READ(F2ETC,Y);
    READ(F2ETC,REF21(I,J));READ(F2ETC,IMF21(I,J))
  END;

  FOR I:=0 TO 10 DO FOR J:=0 TO 10 DO
  BEGIN
    READ(F2ETC,X);READ(F2ETC,Y);
    READ(F2ETC,REF2X1(I,J));READ(F2ETC,IMF2X1(I,J))
  END;

```

```

END;

FOR I:=0 TO 10 DO FOR J:=0 TO 10 DO
BEGIN
  READ(F2ETC,X);READ(F2ETC,Y);
  READ(F2ETC,REF2Y1CI,J);READ(F2ETC,IMF2Y1CI,J)
END;

RESET(EA0);

FOR I:=0 TO 10 DO FOR J:=0 TO 10 DO
BEGIN
  READ(EA0,X);READ(EA0,Y);
  READ(EA0,REEA01CI,J);READ(EA0,IMEA01CI,J)
END;
FOR I:=0 TO 10 DO
BEGIN
  Y:=I*PI/10;
  X:=RERHO2(2*PI,Y)*EXP(ALPHA*(Y-PI/2));
  WRITE(X:9:5,' ');
  X:=IMRHO2(2*PI,Y)*EXP(ALPHA*(Y-PI/2));
  WRITE(X:9:5);
  X:=RERHO1(2*PI,Y)*EXP(-ALPHA*(Y-PI/2));
  WRITE(' ',X:9:5);
  X:=IMRHO1(2*PI,Y)*EXP(-ALPHA*(Y-PI/2));
  WRITELN(' ',X:9:5)
END;

REWRITE(AANDF1);

FOR I:=0 TO 10 DO FOR J:=0 TO 10 DO
BEGIN
  X:=I*PI/5;Y:=J*PI/10;
  WRITELN(AANDF1,X:9:5,Y:9:5,
    REA(X,Y):13:6,IMAX(X,Y):13:6,
    REF1(X,Y):13:6,IMF1(X,Y):13:6)
END
END.

```

PROGRAM 6.

(* CORANGE LINES ARE CALCULATED FOR THE
CORRECTED AMPLITUDE $A=A_0+EPS*A_1$ WHERE EPS
IS THE SQUARE ROOT OF THE ROSSBY NUMBER.

A0 IS DETERMINED FROM THE EQUATIONS
AND COEFFICIENTS OF TAYLOR, 1921;
NOTATION AS IN SECTION 453 .

A1 IS OBTAINED FROM THE
OUTPUT OF PROGRAM 5 *)

TYPE MATRIX=ARRAY [0..11,0..11] OF REAL;

VAR ALPHA,K,K0,X1,PI,EPS,
XMIN,XMAX,YMIN,YMAX,X,Y,C1:REAL;
I,J,COUNT,NZ:INTEGER;
A,B,C,D,P,Q:ARRAY [1..10] OF REAL;
Z:ARRAY [0..100] OF REAL;
REA11,IMA11,REF1,IMF1:MATRIX;
AANDF1,CORNGO:TEXT;

FUNCTION S(M:INTEGER):REAL;
BEGIN S:=SQRT(M*M-K*K) END;

FUNCTION COSH(X:REAL):REAL;
BEGIN
COSH:=(EXP(X)+EXP(-X))/2
END;

FUNCTION SINH(X:REAL):REAL;
BEGIN
SINH:=(EXP(X)-EXP(-X))/2
END;

FUNCTION REAO(X,Y:REAL):REAL;
VAR Z,XBAR,YBAR:REAL;M:INTEGER;
BEGIN
XBAR:=X+X1;YBAR:=Y-PI/2;Z:=0;
FOR M:=1 TO 10 DO
Z:=Z+P[M]*SIN(M*YBAR)/EXP(S(M)*X);
REAO:=-PI*SINH(ALPHA*YBAR)*SIN(K0*XBAR)
/(4*ALPHA) -Z
END;

FUNCTION IMAO(X,Y:REAL):REAL;
VAR Z,XBAR,YBAR:REAL;M:INTEGER;
BEGIN
XBAR:=X+X1;YBAR:=Y-PI/2;Z:=0;
FOR M:=1 TO 10 DO
Z:=Z+Q[M]*COS(M*YBAR)/EXP(S(M)*X);
IMAO:=PI*COSH(ALPHA*YBAR)*COS(K0*XBAR)
/(4*ALPHA) -Z
END;

FUNCTION INTERP(F:MATRIX;X,Y:REAL):REAL;
VAR I,J:INTEGER;X1,X2,Y1,Y2:REAL;
BEGIN
I:=TRUNC(5*X/PI);J:=TRUNC(10*Y/PI);
X1:=5*X/PI -I;Y1:=10*Y/PI -J;

```

X2:=1-X1;Y2:=1-Y1;

INTERP:=X2*Y2*F[I,J]
      +X1*Y1*F[I+1,J+1]
      +X1*Y2*F[I+1,J]
      +X2*Y1*F[I,J+1]

END;

FUNCTION REA1(X,Y:REAL):REAL;
BEGIN
  REA1:=INTERP(REA11,X,Y)
END;

FUNCTION IMA1(X,Y:REAL):REAL;
BEGIN
  IMA1:=INTERP(IMA11,X,Y)
END;

FUNCTION F(X,Y:REAL):REAL;
BEGIN
  F:=(REA0(X,Y)+EPS*REA1(X,Y))**2
    +(IMA0(X,Y)+EPS*IMA1(X,Y))**2
    -C1*C1
END;

FUNCTION G(X:REAL):REAL;
BEGIN
  G:=F(X,Y)
END;

FUNCTION H(Y:REAL):REAL;
BEGIN H:=F(X,Y) END;

(*ZEROS OF A FUNCTION ARE FOUND
BY A SIGN CHANGE SEARCH*)
PROCEDURE ZEROS(FUNCTION F(X:REAL):REAL;XMIN,XMAX:REAL);
VAR X:ARRAY [0..100] OF REAL;
    X1,X2,X3:REAL;
    I,J,COUNT:INTEGER;
BEGIN

  FOR I:=0 TO 100 DO
  BEGIN
    XCI:=XMIN+I*(XMAX-XMIN)/100;
    ZCI:=0
  END;

  J:=0;NZ:=0;COUNT:=0;

  FOR I:=0 TO 99 DO
  BEGIN
    IF ABS(F(XCI))<1E-3 THEN
    BEGIN J:=J+1;ZCJ:=XCI;NZ:=NZ+1 END
    ELSE IF F(XCI)*F(XCI+1)<0 THEN
    BEGIN
      X1:=XCI;X2:=XCI+1;
      REPEAT
        COUNT:=COUNT+1;
        X3:=(X1+X2)/2;
        IF F(X1)*F(X3)<0 THEN X2:=X3

```

```

        ELSE X1:=X3
        UNTIL (ABS(F(X3))<1E-3)
        OR (COUNT=10);
        IF ABS(F(X3))<1E-3 THEN
        BEGIN
            J:=J+1;ZCJ:=X3;NZ:=NZ+1
        END
    END
END
END:

BEGIN
    ALPHA:=0.7;K:=0.5;K0:=0.8602;
    PI:=4*ARCTAN(1);X1:=0.427;

    AC1:=0.765;AC2:=-0.427;AC3:=-0.009;
    AC4:=0.100;AC5:=0.0012;AC6:=-0.0425;
    AC7:=-0.0003;AC8:=0.0245;AC9:=0.0001;
    AC10:=-0.0147;

    BC1:=-1.100;BC2:=0.066;BC3:=0.132;
    BC4:=-0.004;BC5:=-0.050;BC6:=0.001;
    BC7:=0.027;BC8:=-0.0002;BC9:=-0.017;
    BC10:=0.0001;

    CC1:=1.892;CC2:=0.0;CC3:=-0.138;
    CC4:=0.0;CC5:=0.510;CC6:=0.0;
    CC7:=-0.027;CC8:=0.0;CC9:=0.017;
    CC10:=0.0;

    DC1:=0.0;DC2:=-0.495;DC3:=0.0;
    DC4:=0.103;DC5:=0.0;DC6:=-0.043;
    DC7:=0.0;DC8:=0.024;DC9:=0.0;
    DC10:=-0.015;

    FOR I:=1 TO 10 DO
    BEGIN
        PEI:=(S(I)*BCI+I*CCI)/K0;
        OEI:=(I*DCI-S(I)*ACI)/K0
    END;

    RESET(AANDP1);

    FOR I:=0 TO 10 DO FOR J:=0 TO 10 DO
    BEGIN
        READ(AANDP1,X);READ(AANDP1,Y);
        READ(AANDP1,REAL1(I,J));READ(AANDP1,IMA1(I,J));
        READ(AANDP1,REF1(I,J));READ(AANDP1,IMP1(I,J))
    END;

    XMIN:=0;XMAX:=2*PI;
    YMIN:=0;YMAX:=PI;

    C1:=0.2;COUNT:=0;EPS:=-0.10;

    REWRITE(CORNGO);

    WRITELN(CORNGO);WRITELN(CORNGO);
    WRITELN(CORNGO,
    * *,XMIN:9:6,* *,XMAX:9:6,* *,YMIN:9:6,* *,YMAX:9:6,* *);

```

```

WRITELN(CORNGO);

REPEAT
  FOR I:=0 TO 50 DO
    BEGIN
      Y:=YMIN+I*(YMAX-YMIN)/50;
      ZEROS(G,XMIN,XMAX);
      FOR J:=1 TO NZ DO
        BEGIN
          WRITE(CORNGO,' ',ZCJJ:9:6,' ',Y:9:6,' ');
          COUNT:=COUNT+1;
          IF COUNT MOD 3=0 THEN WRITELN(CORNGO)
        END
      END;

      WRITELN(CORNGO);WRITELN(CORNGO);
      FOR I:=0 TO 50 DO
        BEGIN
          X:=XMIN+I*(XMAX-XMIN)/50;
          ZEROS(H,YMIN,YMAX);
          FOR J:=1 TO NZ DO
            BEGIN
              WRITE(CORNGO,' ',X:9:6,' ',ZCJJ:9:6,' ');
              COUNT:=COUNT+1;
              IF COUNT MOD 3=0 THEN WRITELN(CORNGO)
            END
          END;
          C1:=C1+0.2;
          UNTIL ROUND(10*C1)=14;

      WRITELN(CORNGO);WRITELN(CORNGO);WRITELN(CORNGO,' -9999 ')
    END.

```

PROGRAM 7.

(* PLOTS A DATA FILE OF
COORDINATE PAIRS *)

TYPE VECTOR=ARRAY [1..2000] OF REAL;
STRING=PACKED ARRAY [1..10] OF CHAR;

VAR XMIN,XMAX,YMIN,YMAX,XL,YL,X1,Y1:REAL;
X,Y,AX,AY:VECTOR;
I,J,COUNT,NX,NY,NXC,NYC:INTEGER;
XC,YC:STRING;

PROCEDURE JBAXES(CX:VECTOR;NX:INTEGER;
XL:REAL;XC:STRING;NXC:INTEGER;
AY:VECTOR;NY:INTEGER;YL:REAL;
YC:STRING;NYC:INTEGER);EXTERN;

PROCEDURE MARKPT(X,Y:REAL;I:INTEGER);EXTERN;

PROCEDURE BREAK;EXTERN;

PROCEDURE JOINPT(X,Y:REAL);EXTERN;

PROCEDURE ENDPLT;EXTERN;

BEGIN

READ(XMIN);READ(XMAX);READ(YMIN);READ(YMAX);
XC1]:=XMIN;XC2]:=XMAX;YC1]:=YMIN;YC2]:=YMAX;
COUNT:=2;I:=3;XC1]:=0;
WHILE XC1]<>-9999 DO

BEGIN

READ(XC1]);

IF XC1]<>-9999 THEN

BEGIN

READ(YC1]);COUNT:=COUNT+1;I:=I+1

END

END;

XL:=15.0;YL:=7.5;NXC:=0;NYC:=0;

JBAXES(X,COUNT,XL,XC,NXC,Y,COUNT,YL,YC,NYC);

BREAK;JOINPT(XMIN,YMAX);JOINPT(XMAX,YMAX);

J:=1;

FOR I:=1 TO COUNT DO

MARKPT(XC1],YC1],J);ENDPLT

END.

BIBLIOGRAPHY

- ALLEN, J.R.L., 1968, Current ripples, North-Holland.
- BATCHELOR, G.K., 1967, An introduction to fluid dynamics, Cambridge University Press.
- BERGSTROM, R.W. and COGLEY, A.C., 1976, Viscous boundary layers in rotating fluids driven by periodic flows, J. Atmosph. Sci., 33, 1234-1247.
- BOWEN, D.Q., 1978, Quaternary Geology, Pergamon Press.
- BRADSHAW, P., 1975, An introduction to turbulence and its measurement, Pergamon Press.
- BROWN, P.J., 1973, Kelvin-wave reflection in a semi-infinite canal, J. Mar. Res., 31, 1-10.
- BROWN, T., 1978, Tidal models with applications to the North Sea, Ph.D. thesis, C.N.A.A.
- BUCHWALD, V.T., 1968, The diffraction of Kelvin waves at a corner, J. Fluid Mech., 31, 193-205.
- CASTON, V.N.D. and STRIDE, A.H., 1973, Influence of older relief on the location of sand waves in a part of the southern North Sea, Estuarine and Coastal Marine Science, 1, 379-383.
- COPSON, E.T., 1935, An introduction to the theory of functions of a complex variable, Oxford University Press.
- CREASE, J., 1958, The propagation of long waves into a semi-infinite channel in a rotating system, J. Fluid Mech., 4, 306-320.

- DAVIES, A.M. and FURNES, G.K., 1980, Observed and computed M2 tidal currents in the North Sea, *J. Phys. Oceanogr.*, 10, 237-257.
- DAVIS, H.T., 1936, The theory of linear operators, Principia Press.
- DEFANT, A., 1961, Physical oceanography, Volume 2, Pergamon Press.
- DURANCE, J.A. and JOHNSON, J.A., 1970, East coast ocean currents, *J. Fluid Mech.*, 44, 161-172.
- EVANS, G., 1979, Quaternary transgressions and regressions, *J. Geol. Soc. Lond.*, 136, 125-132.
- FLATHER, R.A., 1976, A tidal model of the north west European continental shelf, *Mem. Soc. Roy. Sci. Liege*, 10, 131-164.
- GILL, A.E., 1976, Adjustment under gravity of a rotating channel, *J. Fluid Mech.*, 77, 603-621.
- GODIN, G., 1965 (a), Some remarks on the tidal motion in a narrow rectangular sea of constant depth, *Deep Sea Research*, 12, 461-468.
- GODIN, G., 1965 (b), The M2 tide in the Labrador Sea, Davis Strait and Baffin Bay, *Deep Sea Research*, 12, 469-477.
- HAGEMAN, B.P., 1969, Development of the western part of the Netherlands during the Holocene, *Geol. Mijnbouw*, 48, 373-388.

HEAPS, N.S., 1973, Three-dimensional numerical model of the Irish Sea, *Geophys. J. R. Astr. Soc.*, 35, 99-120.

HENDERSHOTT, M. and MUNK, W., 1970. Tides, *Ann. Rev. Fluid Mech.*, 2, 205-224.

HENDERSHOTT, M.C. and SPERANZA, A., 1971. Co-oscillating tides in long, narrow bays; the Taylor problem revisited, *Deep-Sea Res.*, 18, 459-480.

HUNT, J.N. and JOHNS, B., 1963, Currents induced by tides and gravity waves, *Tellus*, 15, 343-351.

JANOWITZ, G.S., 1972, The effect of finite vertical Ekman number on the coastal boundary layers of a lake. *Tellus*, 24, 414-420.

JELGERSMA, S., 1961, Holocene sea level changes in the Netherlands, *Mendelingen van de Geologische Stichting (C)*, 6.

JOHNS, B., 1965, Mass transport in rotatory tidal currents, *PAGEOPH*, 60, 107-116.

KRAAV, V.K., 1969, Computation of the semidiurnal tide and turbulence parameters in the North Sea. *Oceanology*, 9, 332-341.

KRAUSS, W., 1973, Methods and results of theoretical oceanography, Volume 1, Gebruder Borntraeger.

KREISS, H., 1957, Some remarks about nonlinear oscillations in tidal channels, *Tellus*, 9, 53-68.

LAMB, H., 1932, Hydrodynamics, 6th Edition, Cambridge University Press.

LAMOURE, J. and MEI, C.C., 1977, Effects of horizontally two-dimensional bodies on the mass transport near the sea bottom, J. Fluid Mech., 83, 415-431..

LESLIE, D.C., 1973, Developments in the theory of turbulence, Clarendon.

LONGUET-HIGGINS, M.S., 1953, Mass transport in water waves, Phil. Trans. Roy. Soc. Lond. (A), 245, 535-581.

MORSE, P.M. and FESHBACH, H., 1953, Methods of theoretical physics, Mc-Graw Hill.

MUIR WOOD, A.M., 1969, Coastal hydraulics. Macmillan.

NAYFEH, A.H., 1973, Perturbation methods, Wiley-Interscience.

NAYFEH, A.H., 1981, Introduction to perturbation techniques, Wiley-Interscience.

NIHOUL, J.C.J. and RONDAY, F.C., 1976, Hydrodynamic models of the North Sea; a comparative assessment, Mem.Soc. Roy. Sci. Liege (6), 10, 61-96.

NIO, S.D., 1976, Marine transgressions as a factor in the formation of sandwave complexes, Geol. Mijnbouw, 55, 18-40.

NODA, H., 1969, A study of mass transport in boundary layers in standing waves, Coastal Engineering in Japan, 12, 57-68.

- OFF, T., 1963. Rhythmic linear sand bodies caused by tidal currents, Am. Assoc. Petroleum Geologists Bull., 47, 324-341.
- OWEN, A., 1980, A three-dimensional model of the Bristol Channel, J. Phys. Oceanogr., 10, 1290-1302.
- POND, S. and PICKARD, G.L., 1978, Introductory dynamic oceanography, Pergamon Press.
- PROUDMAN J. and DOODSON, A.T., 1924, The principal constituent of the tides of the North Sea, Phil. Trans. Roy. Soc. Lond. (A), 224, 185-219.
- REINECKER, M.M. and TEUBNER, M.D., 1980, A note on frictional effects in Taylor's problem, J. Mar. Res., 38, 183-191.
- ROBINSON I.S., 1981, Tidal vorticity and residual circulation, Deep-Sea Research, 28, 195-212.
- SCHLICHTING, H., 1968, Boundary-layer theory, 6th edition, Mc-Graw Hill.
- SHIH-ZAO, F., 1977, A three-dimensional non-linear model of tides, Scientia Sinica, 20, 436-446.
- STOKER, J.J., 1957, Water waves, Interscience.
- TAYLOR, G.I., 1921, Tidal oscillations in gulfs and rectangular basins, Proc. Lond. Math. Soc. (2), 20, 148-181.
- WILLIAMS, W.E., 1980, Partial differential equations, Oxford University Press.
- YALIN, M.S., 1977, Mechanics of sediment transport, 2nd edition, Pergamon Press.

Attention is drawn to the fact that the copyright of this thesis rests with its author.

This copy of the thesis has been supplied on condition that anyone who consults it is understood to recognise that its copyright rests with its author and that no quotation from the thesis and no information derived from it may be published without the author's prior written consent.

III

D57626'85

END